UNIVERSITÀ
DEGLI STUDI
DI PADOVA

UNIVERSITÀ DEGLI STUDI DI PADOVA

Dipartimento di *Biomedicina Comparata e Alimentazione*

SCUOLA DI DOTTORATO DI RICERCA IN SCIENZE VETERINARIE

XXVII CICLO

THE PROGRESSION OF THE TUBULOINTERSTITIAL DAMAGE IN CANINE RENAL DISEASES

Direttore della Scuola: Ch.mo Prof. Gianfranco Gabai

Supervisore: Ch.mo Prof. Luca Aresu

Dottorando : Silvia Lucia Benali

“Sei cambiato, Bilbo Baggins.

Non sei lo stesso hobbit che ha lasciato la Contea.”

J.R.R. Tolkien, Lo Hobbit

CONTENTS

SUMMARY

Kidney lesions can primarily involve the glomeruli, tubulointerstitium, or renal vessels. However, regardless of the initiating site of injury, all compartments often eventually become affected. Tubulointerstitial damage (TID) plays a central role in the progression of renal diseases, leading to an irreversible decline in renal function and ultimately resulting in end-stage renal disease (ESRD). TID is characterized by loss of renal tubules, increased number of interstitial myofibroblasts, and accumulation of extracellular matrix (ECM) in the interstitium usually with chronic inflammatory cell infiltrate.

This project aimed at investigating different aspects of the progression of chronic TID in canine renal diseases.

The first part of the project consisted in a morphological study describing the progression of renal lesions in canine Leishmaniosis possibly representing a model of TID progression in infectious immune-mediated glomerulonephritis. Renal biopsies taken at the beginning and after a 60-day period specific leishmanicidal treatment were evaluated. Progression of the TID was overall mild but present in half of the dogs especially those that had severe TID already at the first biopsy. The results further confirmed that the progression of the chronic TID is independent from the persistence of the causative agent. Moreover, elimination of the etiological agent, by means of the leishmanicidal treatment is not responsible for a significant improvement of renal lesions when these are severe and include irreversible changes like the presence of obsolescent glomeruli andd fibrosis. In contrast the positive effect of the treatment seems to occur in case of mild TID and is possibly related to the reduction of the inflammatory component.

The second part of the project focused on the role of tubular epithelial cells (TECs) in the progression of chronic TID. Morphological diagnosis, severity of inflammation, interstitial fibrosis, HLA-DR expression by TECs and clinicopathological variables were compared in renal biopsies from dogs with spontaneous kidney diseases of varying severities and etiologies. Fibrosis, HLA-DR expression, serum creatinine concentration (SCr), and urine protein-to-creatinine ratio (UPC) were all increased in dogs with primary glomerular disease compared with dogs with acute tubular necrosis. HLA-DR expression by TECs was positively correlated to fibrosis, inflammation, UPC, and SCr. The study provided evidence of the capacity of TECs of acting as non-professional antigen presenting cells (APCs) in chronic

TID, identifying a potential causative effect of the proteinuria. Moreover, this expression of TECs seems to precede and partially overlap with the process of epithelial-to-mesenchymal transition (EMT) and potentially represents a phase of the EMT process itself.

The last part of the project investigated and described the progression of TID in a canine model of CKD and was conducted in partnership with the Texas A&M University (College Station, TX, USA). The included dogs were members of a single family affected by a X-linked hereditary nephropathy (XLHN) caused by a mutation in the gene encoding the α5 chain of type IV collagen, which is a crucial component of normal glomerular basement membranes (GBM). The salient clinical and pathological features of the nephropathy that occurs in male dogs with XLHN include juvenile onset of proteinuria and renal failure rapidly progressive to ESRD. Aims of the study were to examine the evolution of renal injury and the expression of selected molecules potentially involved in the progression of chronic TID. Affected dogs were characterized by progressive loss of glomeruli mostly undergoing cystic glomerular atrophy and less commonly global glomerulosclerosis. Primary lesions into the glomerulus were mesangial matrix expansion and hypercellularity. The tubulointerstitial lesions included changes typical of chronic TID, like tubular necrosis and atrophy, interstitial fibrosis and inflammation. The obtained results suggested that two different phases of the disease can be identified. The first was classified as an “early” phase (4 months of age), characterized by minimal or absence of histopathological lesions but evident proteinuria that is characterized by TGFβ, CTGF, and PDGFRα overexpression, likely produced by podocytes and TECs in response to the glomerular damage and intratubular proteinuria. The second “advanced” phase (after 6 months of age) was characterized by prominent glomerular and tubulointerstitial changes associated with an upregulation of clusterin and TIMP1 by TECs.

The obtained results significantly improved the understanding of the progression of chronic TID in canine renal diseases pointing out the importance of proteinuria and possibly other molecular changes that precede the morphological changes. More data are needed to further understand the mechanisms responsible for the initiation ad promotion of the secondary TID and the major cellular and molecular players involved in order to identify early and specific markers of renal damage, improve the time of the diagnosis and eventually new targets for therapy.

RIASSUNTO

Un danno renale primario può coinvolgere uno dei comparti del tessuto renale: glomerulare, tubulointerstiziale o vascolare. Tuttavia, indipendentemente dalla struttura anatomica primariamente colpita, tutte le componenti del tessuto renale possono venire secondariamente coinvolte. Il danno tubulointerstiziale cronico svolge un ruolo centrale nella progressione del danno renale e nell'irreversibile declino della funzionalità renale risultante nella Malattia Renale Cronica. Morfologicamente il danno tubulointerstiziale cronico è caratterizzato da perdita del parenchima funzionale, in cui si osserva marcata atrofia tubulare ed espansione dell'interstizio dovuto ad aumento del numero di fibroblasti e accumulo di matrice extracellulare. Spesso in associazione si rileva infiltrato infiammatorio cronico di entità variabile.

Il progetto di dottorato è stato suddiviso in tre parti e ha avuto come obiettivo lo studio della progressione del danno tubulo-interstiziale cronico nelle patologie renali del cane.

In una prima fase si è analizzata l'evoluzione delle lesioni renali in soggetti con glomerulonefrite immunomediata associata all'infezione da *Leishmania spp*. Lo studio si è svolto su 14 cani *Leishmania*-positivi sottoposti ad un trattamento leishmanicida specifico della durata di 60 giorni e in cui si è ottenuta una duplice biopsia renale, pre-trattamento e post-trattamento. Complessivamente si è osservata lieve progressione delle lesioni renali in metà dei soggetti, particolarmente in quei pazienti caratterizzati da prominente danno tubulo-interstiziale già alla valutazione della biopsia pretrattamento. I risultati ottenuti forniscono ulteriore supporto alla tesi secondo cui la progressione del danno tubulo-interstiziale cronico è indipendente dalla persistenza dell'agente causale. Inoltre l'eliminazione dell'agente eziologico, conseguente al trattamento leishmanicida, non sembra essere responsabile di un significativo miglioramento delle lesioni e funzionalità renale soprattutto in caso di lesioni in stadio avanzato e quindi croniche e di gravi come nel caso di glomerulosclerosi globale e fibrosi interstiziale. Al contrario un'efficacia del trattamento farmacologico si è evidenziato in presenza di un danno tubulo-interstiziale lieve ed è apparentemente imputabile ad una riduzione della componente infiammatoria.

Nella seconda fase del progetto, lo studio è stato focalizzato ad esplorare il ruolo delle cellule epiteliali tubulari nella progressione del danno tubulointerstiziale cronico.

Lo studio è stato svolto su biopsie renali di cane affetti da patologie di diversa natura e gravità ricercando una correlazione tra le lesioni istopatologiche e la funzionalità renale, nonché la capacità delle cellule tubulari epiteliali di agire come cellule presentanti l'antigene. Si è potuto evidenziare che cani affetti da glomerulopatie primarie presentavano più comunemente un danno tubulointerstiziale cronico con fibrosi interstiziale e innalzamento dei parametri di creatinemia e proteinuria, così come si osservava l'espressione *ex novo* di HLA-DR da parte delle cellule epiteliali tubulari. Ulteriormente si è osservata una correlazione positiva tra l'espressione di HLA-DR nelle cellule epiteliali, il grado di fibrosi, d'infiammazione, e i valori di proteinuria e creatinemia.

Lo studio ha evidenziato la capacità delle cellule epiteliali tubulari di agire come cellule presentanti l'antigene nel danno tubulo-interstiziale cronico. Si è inoltre identificata nella proteinuria un possibile agente causale nell'indurre questa capacità. Infine questa parte dello studio ha messo in luce che l'espressione di HLA-DR nelle cellule epiteliali tubulari sembra precedere e parzialmente sovrapporsi con il fenomeno di transizione epitelio-mesenchimale delle cellule epiteliali e potrebbe rappresentarne una fase iniziale.

La terza parte del progetto ha descritto la progressione del danno tubulointerstiziale cronico in un modello canino di Malattia Renale Cronica ed è stato svolto in collaborazione con la Texas A&M University (College Station, TX, USA).

Lo studio è stato svolto su cani con nefropatia ereditaria legata al cromosoma X e mantenuti in condizioni sperimentali presso la Texas A&M University (College Station – Texas – USA). Tale nefropatia è dovuta ad una mutazione del gene codificante per la catena α5 del collagene di tipo IV, che rappresenta uno dei principali componenti della membrana basale glomerulare. Le caratteristiche cliniche e patologiche della malattia renale in cani affetti da nefropatia ereditaria consistono nell'insorgenza precoce di proteinuria ed insufficienza renale, rapidamente progressive a Malattia Renale Cronica. Obiettivi del lavoro sono stati quelli di esaminare l'evoluzione del danno renale da un punto di vista morfologico, clinico patologico e tramite lo studio dell'espressione genica e proteica di fattori potenzialmente coinvolti nella progressione del danno. I soggetti patologici presentavano una progressiva aumento del numero di glomeruli atrofici cistici o, meno frequentemente globalmente sclerotici. Le lesioni primarie osservate a livello glomerulare consistevano in espansione del mesangio ed ipercellulatià mesangiale. Il tubulointerstizio era caratterizzato da lesioni croniche ed aspecifiche come la necrosi ed atrofia tubulare, la fibrosi interstiziale e l'infiltrato infiammatorio

cronico. I risultati ottenuti suggeriscono che si possano distinguere due fasi della malattia renale nella nefropatia ereditaria studiata. Un fase “precoce” (4 mesi di età) in cui si sono osservate da lesioni morfologiche minime o assenti ma con proteinuria conclamata. Da un punto di vista molecolare in questa fase si è evidenziata una sovra-espressione di TGFβ, CTGF, and PDGFRα probabilmente prodotti da podociti e cellule epiteliali tubulari in risposta al danno glomerulare e alla proteinuria. Una seconda fase “avanzata” (dopo i 6 mesi di età) sarebbe invece caratterizzata da lesioni glomerulari e tubulointerstiziali conclamate e da una up-regulation di clusterina e TIMP1 ad opera delle cellule epiteliali tubulari.

I risultati ottenuti forniscono nuove informazioni e aumentano la conoscenza dei meccanismi di progressione del danno tubulointerstiziale cronico nelle malattie renali del cane. Dal lavoro effettuato emerge che l’insorgenza di proteinuria e l’alterata espressione di alcune molecole sembra precedere la presenza di lesioni morfologiche. Ulteriori studi sono necessari per approfondire la nostra conoscenza dei meccanismi di iniziazione e promozione del danno tubulointerstiziale cronico, delle componenti cellulari e molecolari coinvolte con l’obiettivo di identificare marcatori di danno renale precoci e specifici e possibili target terapeutici per la gestione del paziente con insufficienza renale.

ABBREVIATIONS

AFOG: acid fuchsine orange G

AMYL: amyloidosis

ANOVA: One-way analysis of variance

ATN: acute tubular necrosis

BM: basement membrane

bp: base pair

BPM7: bone morphogenic protein 7

CDA: canonical discriminant analysis

CGS: chronic glomerulosclerosis

CIF: cortical interstitial fibrosis

CKD: chronic kidney disease

CLUST: clusterin

CTGF: connective tissue growth factor

DAB: diaminobenzidine

EC: endothelial cells

ECAD: E-cadherin

ECM: extracellular matrix

EGFR: epidermal growth factor receptor

ESK: end stage kidney

ESRD: end stage renal disease

GBM: glomerular basement membrane

GLM: generalized linear model

GN: glomerulonephritis

HCL: Hierarchical clustering

HE: hematoxylin and eosin

HGF: hepatocyte growth factor

HLA: human leukocytes antigen

IL-4: interleukin 4

MC: mesangial cells

MeGN: mesangioproliferative GN

MHC: major histocompatibility complex

MMPs: matrix metalloproteinases

MPGN: membranoproliferative GN

NAV: Navasota

NCAD: N-cadherin

P: podocytes

PAS: periodic acid–Schiff

PCA: principal component analysis

PDGF: platelet-derived growth factor

qRT-PCR = quantitative real time polymerase chain reaction

RQ: Relative Quantification

SCr: serum creatinine concentration

TBP: TATA-binding protein

TECs: tubular epithelial cells

TEM: transmission electron microscopy

TGFR2: TGF beta receptor 2

TGFβ: transforming growth factor beta

TID: tubulointerstitial damage

TIMP: tissue inhibitor of metalloproteinases

TNFα: tumor necrosis factor alpha

UPC: urinary protein and creatinine ratio

VEGF: vascular endothelial growth factor

VEGFR: VEGF receptor

XLHN: X-linked Hereditary Nephropathy

βCAT: βcatenin

INTRODUCTION

CHRONIC KIDNEY DISEASE

Chronic kidney disease (CKD) is the final common pathway resulting from persistent renal injury. Glomerular diseases are the most common causes of CKD in dogs and are important causes of morbidity and mortality in this species (Polzin and Cowgill, 2013). Other less frequent causes (e.g., renal dysplasia, pyelonephritis) have also been reported. Recently published data on the prevalence of different categories of pathologic diagnoses identified in dogs with suspected glomerular disease (Schneider et al., 2013), indicate that immune-complex glomerulonephritides are the largest single category of canine glomerular diseases (about 48% of cases). However, all other diagnostic categories taken together accounted for about half (52%) of all cases, although no other category (e.g., primary glomerulosclerosis, amyloidosis, etc.) alone accounted for more than about 20% of all cases (Schneider et al., 2013). Recently, many advances in the diagnosis of renal biopsies have been achieved in veterinary medicine through the greater use of diagnostic modalities such as optical microscopy, transmission electron microscopy (TEM) and immunofluorescence, which are routinely used in human nephropathology, and more detailed data are expected to be forthcoming (Aresu et al. 2008a; Cianciolo et al., 2013; James et al., 2013). However, in dogs it is well known that most chronic nephropathies share common pathogenic mechanisms that contribute to disease progression, regardless of the original cause of disease, and that renal fibrosis is an inevitable and consequential feature of all kinds of progressive CKD.

THE CHRONIC TUBULOINTERSTITIAL DAMAGE IN CANINE RENAL DISEASES

The tubulointerstitial compartment of renal tissue consists of tubular and vascular structures that are embedded in and supported by a moderately cellular connective tissue matrix (interstitium). Interstitial cells are an heterogeneous population including fibroblasts, dendritic, inflammatory and hematopoietic progenitor cells, that are primarily involved in the fibrogenic process. The entire tubulointerstitial compartment accounts for more than 80% of the total kidney volume, and involvement of each of the cell types has been correlated to CKD in various ways (Eddy, 2005a). In general, the typical features of chronic tubulointerstitial damage (TID) are the presence of interstitial inflammation and fibrosis associated with the

loss of tubules and peritubular capillaries (Eddy, 2005b). Fibrosis is mostly due to an imbalance between the production and degradation of extracellular matrix (ECM), leading to excessive accumulation and deposition of collagenous ECM. Increased internal renal pressure and external compression by the interstitium are also possible causes of tubular atrophy and dilatation. Multiple phases of the fibrotic process can be distinguished and considered in chronologic order, but each phase is part of an overall attempt by the kidney to repair its injury and recover from the damage (Eddy, 2000). The first to occur is the inflammatory phase, wherein lymphocytes, mostly T-lymphocytes, monocytes and plasma cells are distributed in the interstitial compartment and accumulate progressively (Aresu et al., 2012). Subsequently, resident kidney cells are activated, leading to the production and secretion of pro-inflammatory cytokines (Eddy, 2000). Interstitial inflammatory cells are found in all forms of canine glomerular diseases and an association between inflammatory index (number of inflammatory cells per optical microscopy field) and interstitial fibrosis has been found in multiple recent studies (Aresu et al., 2012; Benali et al., 2013). The next phase of the fibrotic process partially overlaps the inflammatory phase and is mainly characterized by the proliferation of fibroblasts and deposition and collection of ECM (Eddy, 2005b). Resident interstitial fibroblasts are known to be the primary source of ECM (Nahas, 2003). Fibroblasts become activated due to stimulation by cytokines, including Transforming Growth Factor beta (TGFβ) and members of the Platelet-derived Growth Factor (PDGF) family. Fibroblasts are able to synthesize many of the constituents of the ECM, such as fibronectin and types I, III, and V collagen. They are also a major source of ECM-degrading proteases such as matrix metalloproteinases (MMPs), underscoring their crucial role in maintaining ECM homeostasis via regulation of turnover (Aresu et al., 2011a). The possible bone marrow origin of some fibroblasts and the concept of fibroblast stem cells have raised several hypotheses and novel therapeutic possibilities, but their exact contribution remains to be determined (Eddy, 2005a). Correlated with the accumulation of ECM, an increased number of atrophic tubules are found in the interstitium. The morphology of the tubules is characterized by thickening or wrinkling of the basement membrane. Atrophy begins with loss of the brush border and basal interdigitating cell processes and continues with transformation of the complex proximal tubular epithelium into a simple flat epithelium. From a physiological perspective the tubule is no longer able to perform its normal secretion and reabsorption functions, one manifestation of which is the development of proteinuria (Roura et al., 2013).

Figure 1. Features of the tubulointerstitial damage secondary to a primary glomerular disease

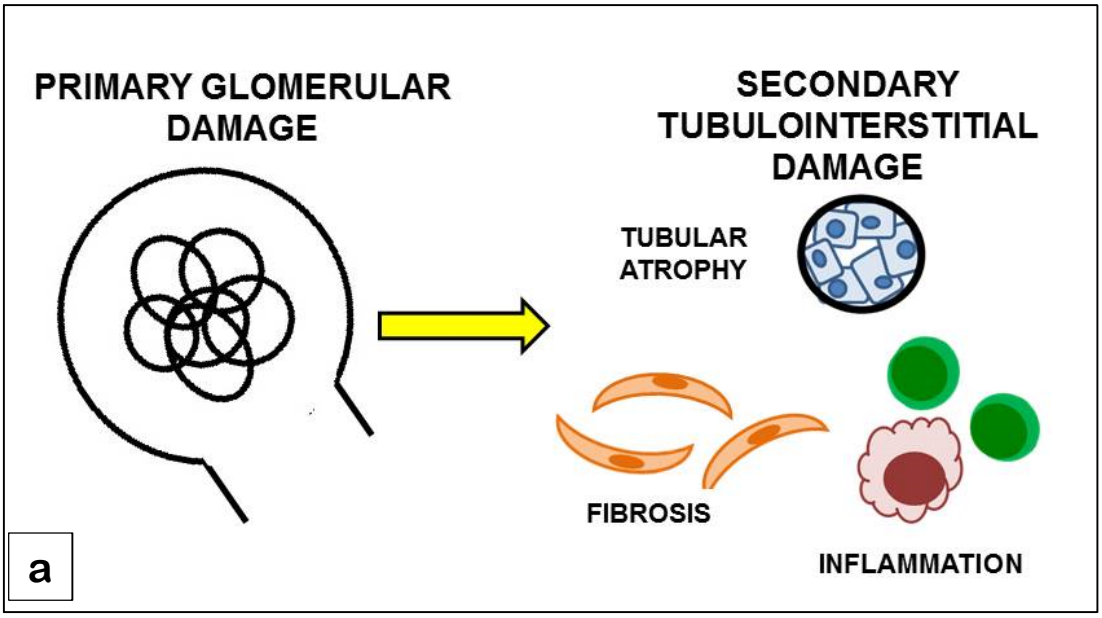

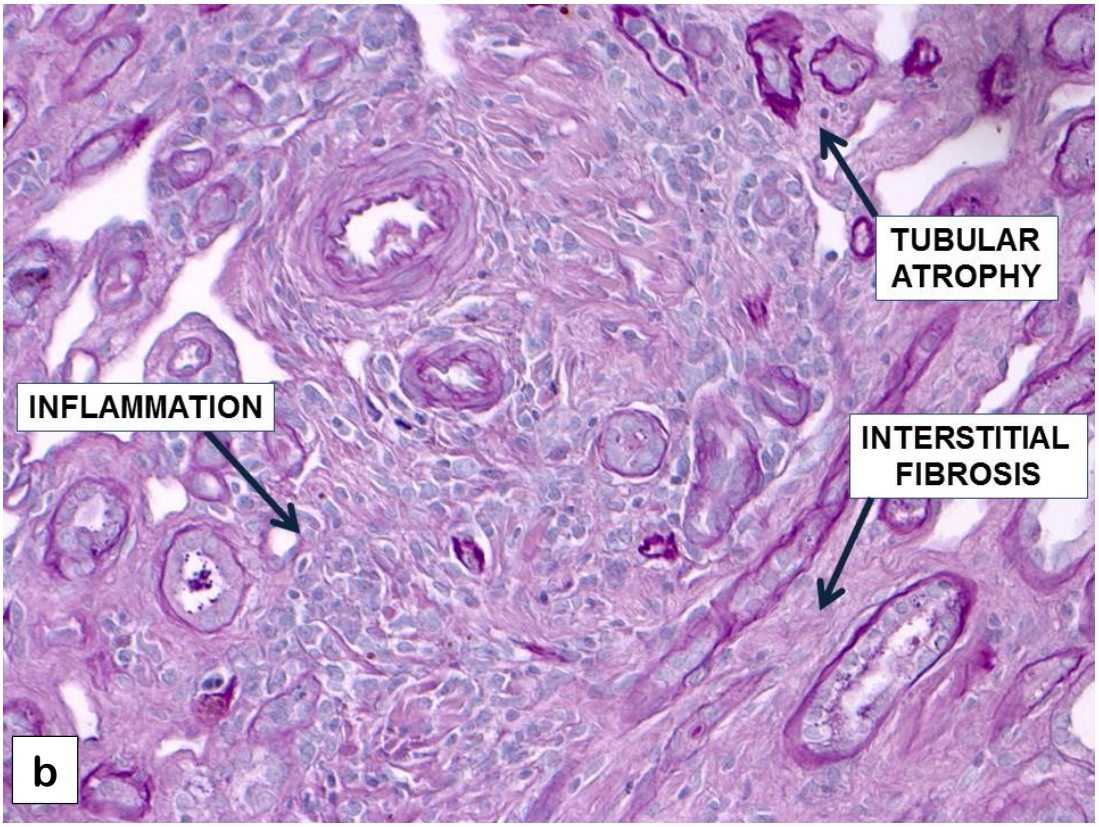

a) schematic view; b) Jone's Methanamine silver stain 200x

OBJECTIVES

Chronic TID plays a central role in the progression of different canine renal diseases, leading to an irreversible decline in organ function and ultimately resulting in ESRD. The main goal of this project is to investigate the mechanisms involved in the initiation and promotion of the TID in different canine renal diseases. In this contest, the project aims to define and classify the steps that are associated with the progression of the TID. The principal cellular and molecular mechanisms are studied through the use of morphological analysis, immunohistochemistry and molecular biology techniques.

For this purpose the project is divided in three parts:

- In the first part the progression of chronic TID is investigated in a canine model of infectious immune-mediated glomerulonephritis
- The second part of the study is focused on the role of the tubular epithelial cells (TECs) and specifically explores the capacity of TECs of acting as non-professional antigen presenting cells (APCs)
- In the third part of the project, the progression of TID is studied using a previously well-established canine model of hereditary nephropathy focusing on the potential role of different molecules reported to be involved in the mechanisms of fibrosis.

PART 1

THE PROGRESSION OF TUBULOINTERSTITIAL DAMAGE IN CANINE RENAL DISEASES: A MODEL OF IMMUNE-MEDIATED GLOMERULONEPHRITIS

Adapted from: Aresu L, Benali S, Ferro S, Vittone V, Gallo E, Brovida C, Castagnaro M. "*Light and electron microscopic analysis of consecutive renal biopsy specimens from leishmania-seropositive dogs*". Vet Pathol. 2013 Sep;50(5):753-60.

BACKGROUND

Canine leishmaniasis due to *Leishmania infantum* is a major cause of renal disease in Italy (Zatelli et al., 2003). The renal damage in canine visceral leishmaniasis is thought to be a multifactorial process that is caused by immune complex deposition; however, a recent study has also highlighted the role of T lymphocytes and adhesion molecules (Costa et al., 2010). Immune complex deposition can be the consequence of persistent antigenemia and circulating immune complexes; the process typically triggers the activation of the complement system and causes acute injury to the glomerular capillaries and mesangium. The severity of the TID is probably linked to the progression of the disease (Ruggenenti and Remuzzi, 2000; Strutz and Neilson 2003). In dogs with nephropathy from naturally acquired visceral leishmaniasis, diffuse membranoproliferative and mesangioproliferative glomerulonephritis appear to be the most common histologic patterns (Binhazim et al., 1992; Koutinas et al., 1994; Costa et al., 2003; Zatelli et al., 2003; Aresu et al., 2007; Poli et al., 1991). No data explored the progression of renal lesions in *Leishmania spp.* infection in dogs.

AIM

The objective of this study was to analyze the histopathological and ultrastructural changes in 15 symptomatic dogs that were serologically positive for *Leishmania spp*.; these dogs were biopsied at diagnosis and again at the end of treatment with a specific anti-Leishmania pharmacological agent. Immunohistochemistry was also performed to characterize the interstitial inflammatory infiltrate.

MATERIALS AND METHODS

Case Selection

Fifteen dogs, seropositive for Leishmania spp., were selected from a canine shelter. The selected dogs had a serum titer > 1:160 by indirect fluorescent antibody test and had *Leishmania* amastigotes in fine-needle aspirate samples of sternebral bone marrow (Maia et al., 2008). The dogs were treated with a leishmanicidal pharmacologic compound without supportive therapy for chronic renal failure. The study was performed in accordance with an approved Institutional Animal Care and Use Committee protocol.

Sample Collection

A percutaneous ultrasound-guided biopsy specimen was collected from the caudal pole of the left kidney at diagnosis (T0) using a Tru-cut disposable biopsy needle. A second biopsy was performed on the caudal pole of the right kidney 60 days later (T1). All biopsy specimens were divided for light and electron microscopy. Blood and urine samples were also obtained at T0 and T1.

Light Microscopy

For histopathology, renal tissue was fixed in 10% neutral buffered formalin, processed routinely, and embedded in paraffin. Serial 3 μm sections were stained with hematoxylin and eosin (HE), Masson's trichrome, periodic acid–Schiff (PAS), acid fuchsine orange G (AFOG) and Jones' methenamine silver. Histologic sections were evaluated and scored (Table 1) independently by 2 pathologists without knowledge of the clinical data; any inter-observer discrepancy in grading was resolved by arbitration.

The histologic diagnoses were categorized according to the World Health Organization classification of human glomerular diseases. A diagnosis of immune-mediated glomerulonephritis was corroborated by the finding of characteristic electron-dense deposits ultrastructurally. Renal lesions classified as mesangioproliferative glomerulonephritis had increased mesangial cells and matrix with no involvement of the capillary lumen, and immune deposits were found in the mesangium at electron microscopy. Chronic glomerulosclerosis was characterized by increased mesangial matrix with or without hypercellularity and absence of immune deposits. End-stage kidney was characterized by severe glomerular damage with

obsolescence of > 40% of the glomeruli, severe tubular atrophy and fibrosis, and few electron-dense deposits in the basement membrane and in the mesangium. In membranoproliferative glomerulonephritis, glomeruli had increased mesangial matrix and cellularity and thickened glomerular capillary walls with immune complexes in the basement membrane and mesangium, cellular interposition, and new basement membrane formation.

Electron Microscopy

For transmission electron microscopy (TEM), the tissue was post-fixed in osmium (2% in distilled water) for 1.5 hours, dehydrated in graded acetone, and embedded in Epon. Semithin sections were stained with azure-methylene-blue. Ultrathin sections were contrasted with uranyl acetate and lead citrate and examined with a Philips EM 420 transmission electron microscope.

Immunohistochemistry (IHC)

For IHC, serial paraffin sections were cut at 4 μm thickness on surface-coated slides (Superfrost Plus). Slides were incubated at 37°C for 30 minutes before immunohistochemistry, which was performed with an automatic immunostainer (Ventana Benchmark XT, Roche-Diagnostics, Monza, Italy). The immunostainer uses a kit with a secondary antibody with a horse radish peroxidase–conjugated polymer to enhance the signal (ultraViews Universal DAB, Ventana Medical System Inc.). All reagents are dispensed automatically except for the primary antibody, dispensed by hand. Antibodies against CD3 (clone F7.2.38, Dako Italia Milano-Italy) and CD79acy (clone HM57, Dako Italia Milano-Italy) were used to detect T lymphocytes and B lymphocytes, respectively; incubation time was 20 minutes at 37° C. For negative controls, the primary antibody was replaced by antibody diluent; sections of hyperplastic lymph node were used as positive controls.

Clinical Chemistry

Total urinary protein and urinary creatinine were quantified by Pyrogallol red direct colorimetric method (Sentinel Diagnostics, CH) and Jaffe´ enzymatic colorimetric method (Sentinel Diagnostics–CH, Hitachi 911, Roche), respectively. Samples with very high urinary protein were diluted with sterile saline (1:3 or 1:10). For measurement of urinary creatinine, all samples were diluted 1:10, as recommended by the manufacturer.

Table 1. Histologic scoring of renal biopsy specimens

Histologic parameter and definition	Severity	Score
Glomerular compartment		
Endocapillary hypercellularity Increased numeber endothelial cells with luminal effacement	Absent to rare	0
	1-2 capillary profiles in few glomeruli	1
	1-2 capillary profiles in most glomeruli	2
	Many capillary profiles in most glomeruli	3
Mesangial hypercellularity Increased number mesangial cells, including macrophages	Absent to rare	0
	Segmental in few glomeruli	1
	Segmental to global in few glomeruli	2
	Segmental to global in most glomeruli	3
Immune deposits	Absent	0
	Rare	1
	In few glomeruli	2
	In most glomeruli	3
Increased mesangial matrix	Absent	0
	Segmental in few glomeruli	1
	Segmental to global in most glomeruli with obliteration of few capillary loops	2
	Global in most glomeruli with obliteration of many capillary loops	3
Capillary thickening	Absent	0
	Rare	1
	Mild in most capillary loops	2
	Moderate in most capillary loops	3
Tubulo-interstitial compartment		
Interstitial fibrosis	<10% of the section	0
	10-30% of the section	1
	31-50% of the section	2
	>50% of the section	3
Interstitial inflammation	Absent or rare scattered leukocytes	0
	Focal to multifocal mild inflammation	1
	Multifocal moderate inflammation	2
	Multifocal severe inflammation	3

RESULTS

The median age at T0 was 4.5 years (range, 2.6–7.7 years). Renal biopsy specimens varied from 10 to 17 mm long x 2 mm thick; each histologic section contained an average of 19 glomeruli (range, 15–37). At T0 biopsy, a wide spectrum of glomerular lesions was evident. Membranoproliferative and mesangioproliferative glomerulonephritis were observed in 6 dogs, chronic glomerulosclerosis in 5, end-stage kidney in 3, and no lesions in 1 case. Biopsy specimens were evaluated by electron microscopy in all dogs; the most striking glomerular lesion in 9 dogs was the presence of electron-dense deposits in various sites. Seven dogs had a multifocal and moderate distribution of lymphocytes and plasma cells in the renal interstitium. The mean inflammation score for all dogs was 1.9 (range, 0–3). At T1, progression of the glomerular lesions was minimal in most dogs. Interstitial fibrosis was stable or increased; the mean interstitial inflammation score (1.8; range, 0–3) was not significantly different. Histological evaluation and scoring at T0 and T1 are summarized in Table 2.

Normal Dog

At T0, dog No. 14 was considered within normal limits, with only a few glomeruli having minimal and segmental increase in mesangial cellularity and matrix. At electron microscopy, mild and multifocal foot-process effacement was presented. Neither interstitial fibrosis nor inflammation (except for rare CD3 lymphocytes) was evident. At T1, glomerular and tubulointerstitial scores were similar to those for the T0 biopsy specimen, as were the electron microscopic results.

Mesangioproliferative Glomerulonephritis

The diagnosis for dog Nos. 1, 2, and 15 was mesangioproliferative glomerulonephritis. The glomeruli had a moderate increase in mesangial matrix and mesangial hypercellularity (Fig. 2a). Most podocytes were hypertrophied with karyomegaly and 1 or more large cytoplasmic vesicles. With Jones' methenamine silver stain, multiple mesangial holes (2 mm in diameter) were observed. Overall, the glomerular basement membrane (GBM) had normal thickness. Two dogs lacked tubulointerstitial inflammation; one dog had multifocal moderate lymphoplasmacytic infiltrate. Fibrosis was absent in dog 15 and scored as 1 in dog Nos. 1 and 2. Ultrastructural electron-dense deposits were in the mesangium and in the subepithelial surface of the GBM overlying the mesangium (paramesangium) (Fig. 2b). At T1, segmental

endocapillary hypercellularity (absent at T0) was observed in few glomeruli. Ultrastructurally, the GMB was segmentally thickened due to mesangial cell interposition, and mesangial immune complex deposits had a similar distribution to that at T0. Tubulointerstitial changes were mild, and in dog No. 1, no leukocytes were detected. At T1, mesangial and paramesangial deposits were still present.

Chronic Glomerulosclerosis

At T0, 5 dogs were diagnosed with chronic glomerulosclerosis and lacked immune complex deposits. Three dogs had mild glomerular lesions with diffuse, mild to moderate expansion of the mesangium and minimal segmental mesangial hypercellularity (6 mesangial cell nuclei per mesangial area) and rare obsolescent glomeruli (Fig 3a and 3b). Electron microscopy confirmed the histologic lesions, and no electron-dense deposits were detected at T0 (Fig. 3c). Multifocal foot-process effacement was also observed. No tubulointerstitial inflammation was evident except for rare CD3 lymphocytes, which were not associated with tubular damage. At T1, glomerular and tubulointerstitial scores were similar to those at T0. Electron-dense deposits were detected in only 1 dog, in the mesangium, so the diagnosis for dog No. 12 was changed to mesangioproliferative glomerulonephritis. Dog Nos. 3 and 7 had more severe glomerular lesions. Global and diffuse glomerular lesions, with increased mesangial matrix and endocapillary and mesangial hypercellularity, were scored as 2 or 3 in the absence of GBM thickening or immune complex deposits. Many cystic atrophic or obsolescent glomeruli were observed. Electron microscopy confirmed the histologic lesions with multifocal expansion of mesangium and mesangial hypercellularity. Electron-dense deposits were not detected. Multifocal foot-process effacement was observed. These results were similar at T1. Interstitial damage included moderate multifocal fibrosis and variable degree of inflammation. At T1, glomerular lesions were moderate; the tubulointerstitium had reduced inflammation, but the fibrosis score remained mild to moderate.

End-Stage Kidney

Three dogs had the most severe and chronic lesions, in both the glomerular and tubulointerstitial compartments. The glomerular tufts were irregular in shape, and the Bowman's capsules were markedly thickened. More than 40% of the glomeruli were obsolescent; many were cystic and atrophic (Fig 4a and Fig 4b). Synechiae and GBM

hyalinosis were segmentally present. The GBMs, where identifiable, were minimally to mildly thickened. Podocytes were diffusely hypertrophic; some contained protein resorption droplets and large cytoplasmic vacuoles. Ultrastructural lesions at T0 and T1 included multifocally increased mesangial matrix and cellularity (possibly including macrophages) with electrondense deposits. The deposits were predominantly in the paramesangial regions. In addition, multifocal mesangial cell interpositioning was observed in the GBM. Interstitial damage was characterized by severe, multifocal fibrosis (Fig 4c and Fig 4d). However, the inflammation score for these dogs was low (mean score, 1.3), whereas the mean score for fibrosis was 2.6. At T1, the severity
of fibrosis had increased.

Membranoproliferative Glomerulonephritis

In dog Nos. 6, 9, and 13, the diagnosis was membranoproliferative glomerulonephritis, with severe and global hypercellularity, and a lobulated appearance of the glomerular tufts. The hypercellularity was mainly mesangial, with lesser contributions from hypertrophic podocytes and an increased number of endothelial cells (Fig. 5a). The GBMs were moderately and globally thickened with multifocal membrane duplication, which indicated mesangial cell interpositioning. The immune complex deposits in the capillary wall were accentuated with AFOG stain (Fig. 5b,5c). Electron-dense deposits were common in the mesangium and in the GBM at T0 and T1 (Fig. 5d), specifically, in the subepithelial, subendothelial, and intramembranous regions, often in association with interpositioned mesangial cells. All dogs had severe multifocal to confluent visceral epithelial cell foot-process fusion (Fig. 5d). Tubulointerstitial lesions were mild and mainly inflammatory, with lymphoplasmacytic infiltration in all cases. Only dog No. 9 had interstitial fibrosis, scored as 1. Dog No. 13 died during the study period, so a T1 biopsy specimen could not be obtained. Other dogs at T1 had an increased number of immune complex deposits by light microscopy. Three parameters, increased mesangial matrix and mesangial and endocapillary hypercellularity, were scored 2 or 3 for global and diffuse glomerular involvement. The T1 tubulointerstitial inflammation score was reduced, but fibrosis score was increased in comparison to that at T0.

Immunohistochemistry

At both T0 and T1, the immunohistochemical analyses demonstrated that CD79a and CD3 cells were equally distributed in the dogs. The majority of the CD79a cells were plasma cells. The CD3 lymphocytes were the most numerous lymphoid cell adjacent to tubules that were atrophied or contained luminal protein. The predominant leukocyte in areas of interstitial fibrosis was also the CD3 lymphocyte.

Clinical Chemistry

At T0, 13 dogs (Nos. 1–7, 9–13, and 15) were proteinuric (urine protein: creatinine ratio > 0.3). The diagnosis for these dogs was membranoproliferative glomerulonephritis (n= 3), mesangioproliferative glomerulonephritis (n= 3), chronic glomerulosclerosis (n= 4), and end-stage kidney disease (n= 3). All the dogs, except dogs Nos. 10, 12, and 14, had increased serum creatinine (> 88.4 mmol/L). Clinical chemistry data are summarized in Table 3.

Table 2: Light microscopy examination of renal biopsy of 15 Leishmaniotic dogs: scoresheet of parameters of glomerular and tubulo-interstitial damage and morphological diagnosis

Dog No	GLOMERULI								TUBULOINTERSTITIUM							
	Endocapillary hypercellularity[a]		Mesangial hypercellularity[a]		Mesangial expansion[a]		Immuno-deposits[a]		Capillary thickening[a]		Inflammation[a]		Fibrosis[a]		Diagnosis[b]	
	T0	**T1**	**T0**	**T1**	**T0**	**T1**	**T0**	**T1**	**T0**	**T1**	**T0**	**T1**	**T0**	**T1**	**T0**	**T1**
1	0	1	2	2	2	1	1	1	0	0	2	0	1	1	MeGN	MeGN
2	0	1	2	2	1	2	1	1	0	1	0	1	1	1	MeGN	MeGN
3	2	1	2	1	3	1	0	0	0	0	1	0	2	1	CGS	CGS
4	2	2	3	2	3	3	2	2	1	2	2	2	1	2	ESK	ESK
5	2	2	3	2	3	3	1	2	0	0	1	1	2	3	ESK	ESK
6	1	2	3	3	2	2	1	2	1	1	1	0	0	1	MPGN	MPGN
7	2	1	3	1	2	1	0	0	0	0	3	1	2	2	CGS	CGS
8	0	0	2	1	1	1	0	0	0	0	0	0	0	0	CGS	CGS
9	2	2	2	1	1	2	2	3	1	1	2	0	1	2	MPGN	MPGN
10	1	1	1	2	1	1	0	0	0	1	0	0	0	0	CGS	CGS
11	3	2	3	3	3	3	3	2	2	2	2	3	1	3	ESK	ESK
12	1	1	2	2	1	2	0	1	1	0	0	0	0	0	CGS	MeGN[c]
13[d]	2		2		2		2		1		2		0		MPGN	
14	0	0	1	1	1	1	0	0	0	0	0	0	0	0	Normal	Normal
15	0	1	1	2	1	2	1	2	0	1	0	1	0	1	MeGN	MeGN

a: parameters considered at light microscopy semi-quantitatively scored from 0 to 3; b: morphological diagnosis: MeGN (mesangioproliferative glomerulonephritis), MPGN (membranoproliferative glomerulonephritis type I), CGS (chronic glomerulosclerosis), ESK (end stage kidney); c: at T1 immunodeposits were evident in the mesangium and the diagnosis changed in mesangioproliferative glomerulonephritis; d: dog died in the period between the two sampling thus no comparison is available; T0: evaluation at first biopsy; T1: evaluation at second biopsy (after 60days)

Table 3. Urine protein-creatinine ratio (UPC) and serum creatinine (SCr) in 15 leishmaniotic dogs at time of first renal biopsy (T0)

Diagnosis[a] *(dog No.)*	*UPC*[b]	*SCr*
	T0[d]	**T0**[d]
Normal (dog 14)	0.11	46.8
MeGN (dog 1)	0.88	140.5
MeGN (dog 2)	0.73	115.8
MeGN (dog 15)	0.93	131.7
MPGN (dog 6)	1.05	111.4
MPGN (dog 9)	1.13	110.5
MPGN (dog 13)[e]	1.29	118.4
CGS (dog 3)	1.06	118.4
CGS (dog 7)	1.79	1.28
CGS (dog 8)	0.06	113.1
CGS (dog 10)	0.48	78.7
CGS (dog 12)	0.75	55.7
ESK (dog 11)	3.54	92.8
ESK (dog 4)	3.25	127.3
ESK (dog 5)	2.35	178.6

[a]:morphological diagnosis: MeGN (mesangioproliferative glomerulonephritis), MPGN (membranoproliferative glomerulonephritis type I), CGN (chronic glomerulonephritis), ESK (end stage kidney); [b]: urine protein-creatinine ratio (normality range: 0-0.3).; [c]: serum creatinine µmol/L (normality range 0-176.8 µmol/L); [d]: T0: evaluation at first sampling; e: dog died in the period between the two sampling thus no comparison is available

Figure 2: Mesangioproliferative glomerulonephritis

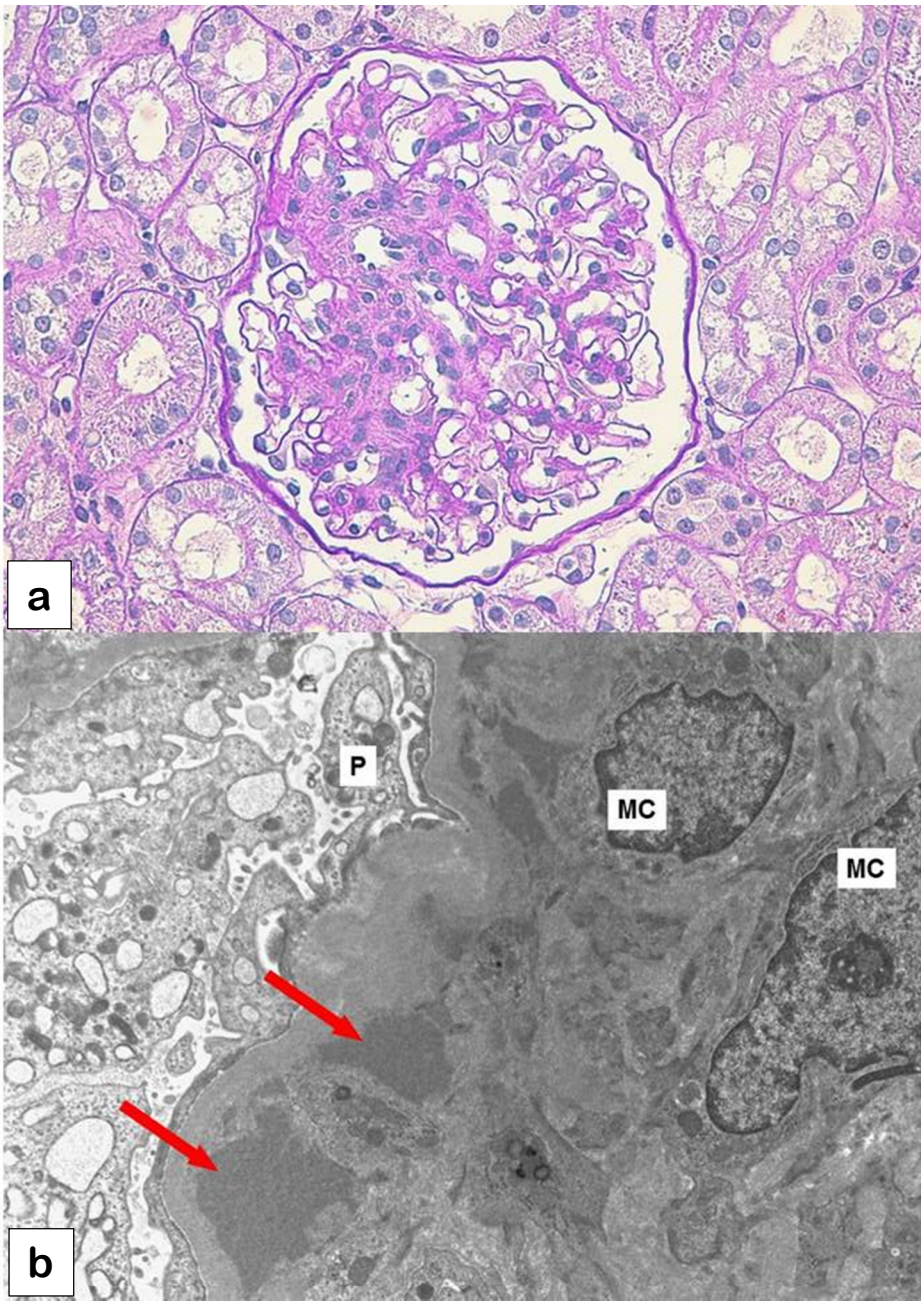

a) Glomerulus with moderate mesangial expansion and mesangial hypercellulatiry. PAS 400x; b) Renal glomerulus, paramesangial and mesangial area. Within the mesangium there are multiple variably sized irregular electron-dense deposits consistent with immune-complex deposits (red arrows). Foot processes of podocytes are swollen and fused. P: podocytes, MC: mesangial cells. Transmission electron microscopy (TEM).

Figure 3: Chronic glomerulosclerosis

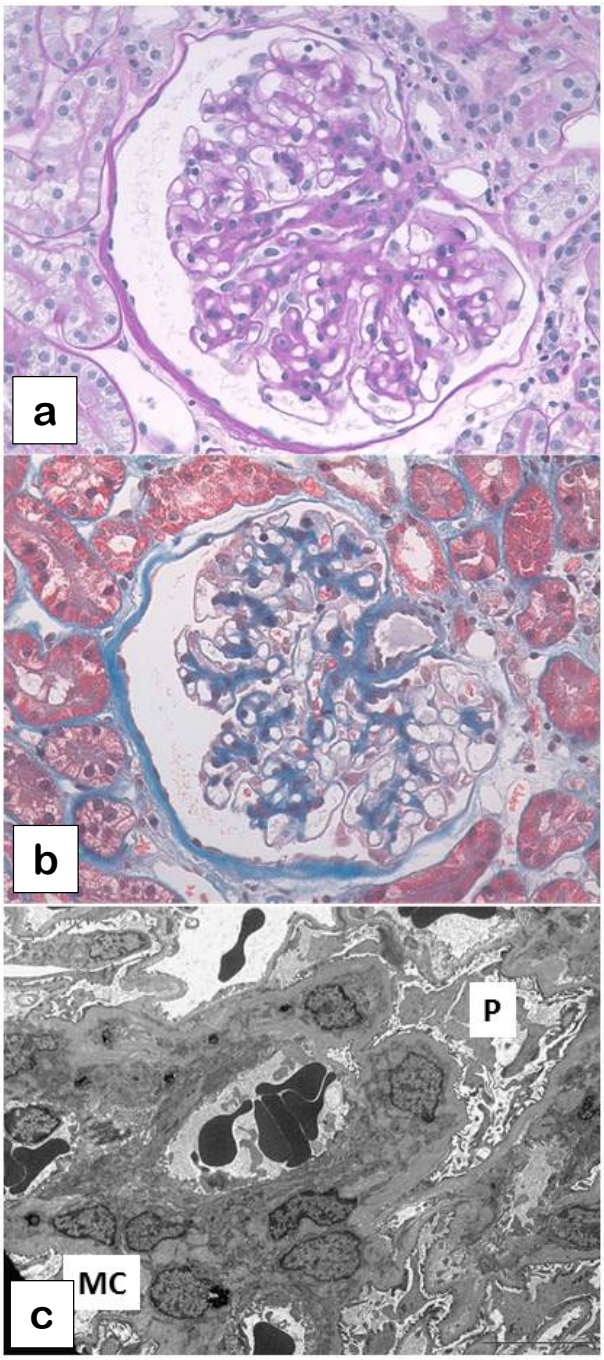

a-b) Glomerulus with mild-moderate mesangial expansion and mesangial hypercellularity and absence of immune deposits. PAS and Masson's Trichrome 400x. c) Renal glomerulus. Within the mesangium there is moderate mesangial hypercellularity associate with mesangial expansion. Foot processes of podocytes are swollen and fused. P: podocytes, MC: mesangial cells. TEM.

Figure 4 : End Stage Kidney

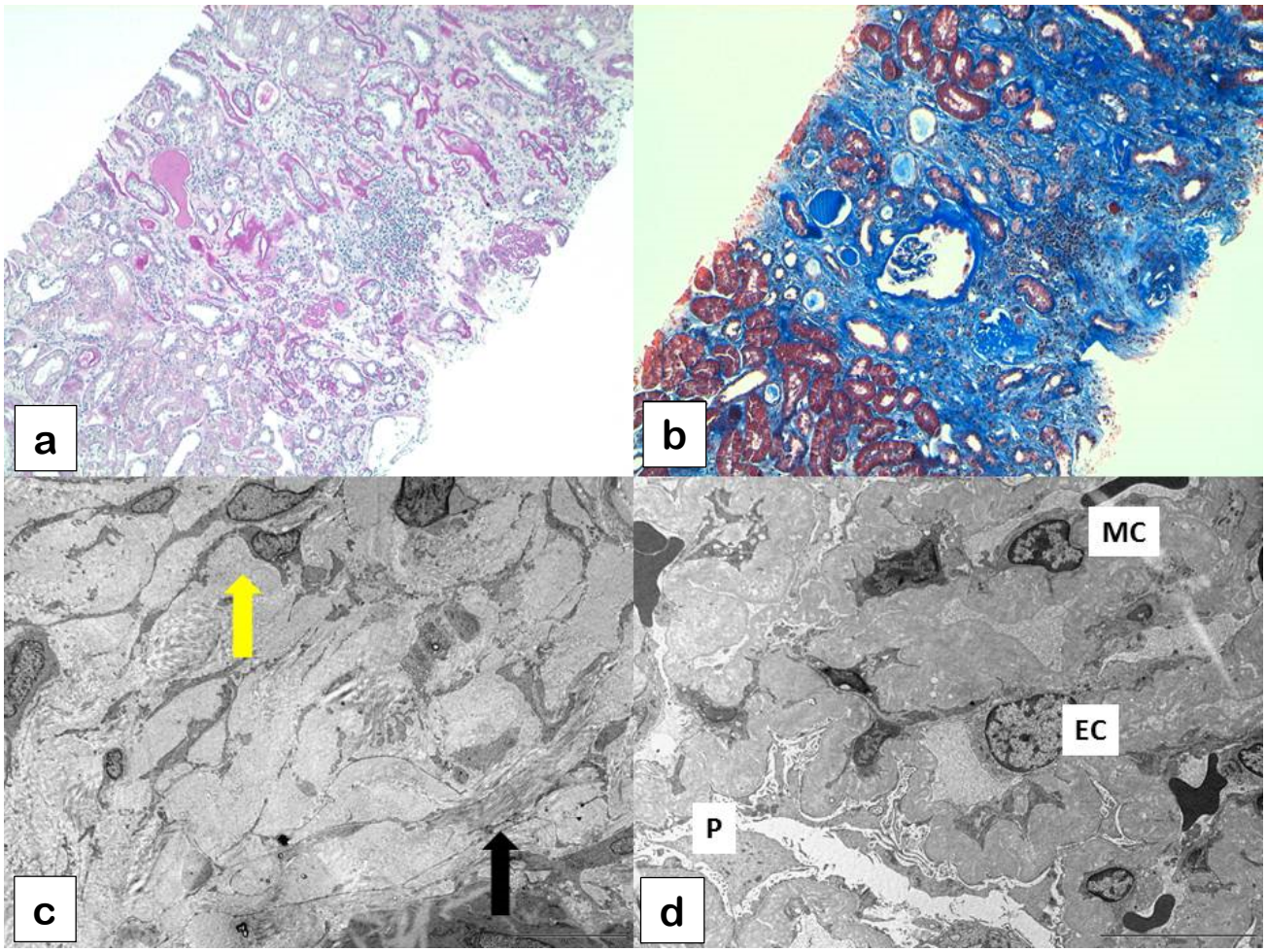

a-b) Renal tissue with severe lesions, in both the glomerular and tubulointerstitial compartments. Most glomeruli are obsolescent or cystic and atrophic. The interstitium is severely expanded by fibrosis and marked lymphoplasmacytic infiltrate associated with multifocal atrophic tubules. PAS and Masson's Trichrome 200x; c) Interstitium severely expanded by collagen deposition (black arrow) and with increased number of fibroblasts (yellow arrow). TEM; d) Glomerulus. Severe expansion of the mesangium and thickening of basement membrane with partial collapse of capillary loops. The foot processes of podocytes are swollen and occasionally fused. P: podocytes; EC: endothelial cells; MC: mesangial cells. TEM

Figure 5: Membranoproliferative glomerulonephritis

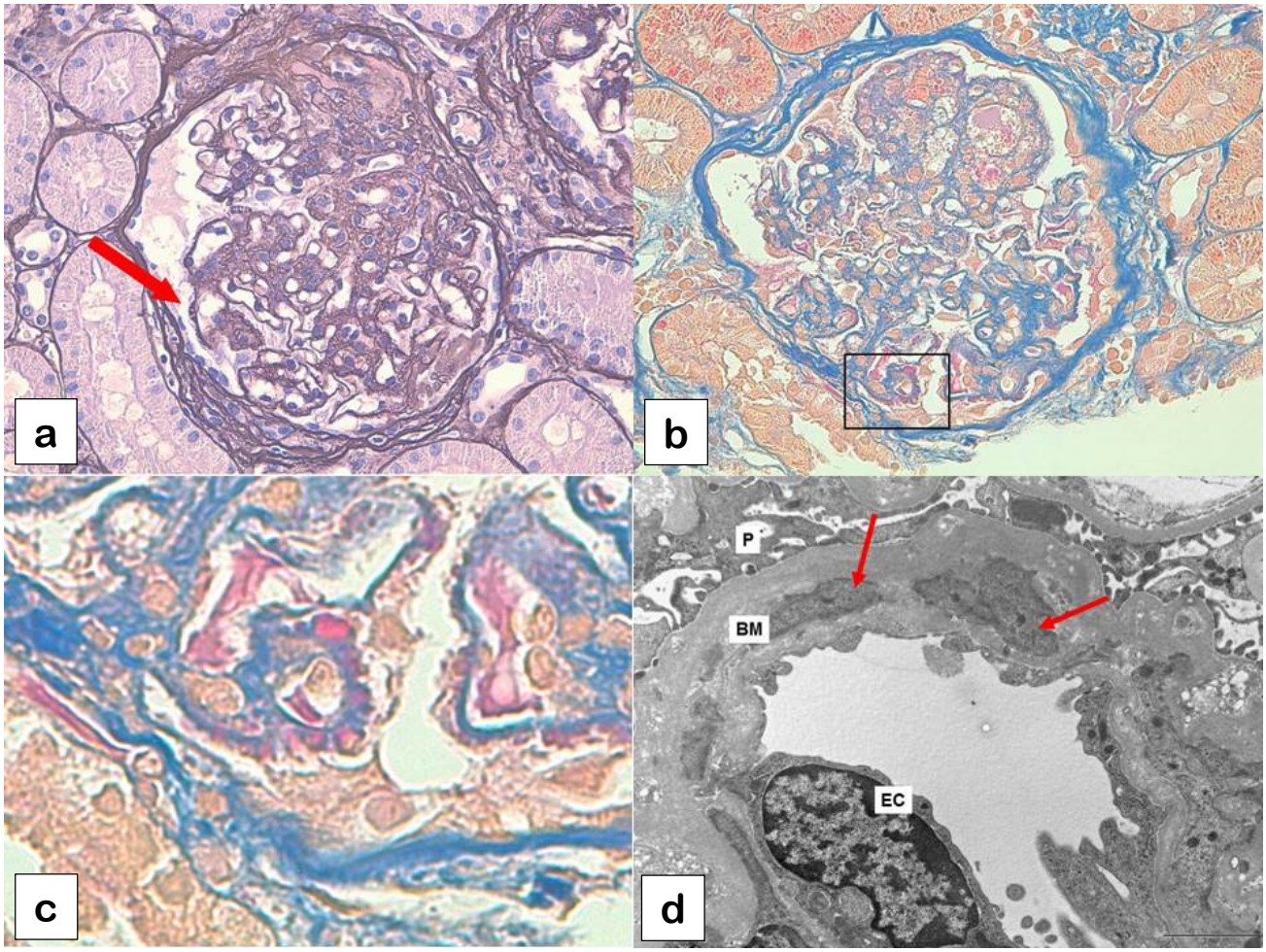

a) Glomerulus with moderate mesangial expansion and mesangial hypercellulatiry and multifocal thickening of the basement membrane (red arrow). Jone's methanamine silver 400x; b) Glomerulus with diffuse red deposits on the subepithelial side of the basement membrane and in the mesangium. Acid fuchsine orange G (AFOG) 400x; c) detail of figure b) showing the capillary loop expanded by multiple granular deposits. AFOG; d) Renal glomerulus, capillary loop. The glomerular basement membrane is diffusely thickened and characterized by the presence of multiple variably sized irregular electron-dense deposits consistent with immune-complex deposits (red arrows). Foot processes of podocytes are swollen and occasionally fused. P: podocytes; EC: endothelial cells; BM: basement membrane. TEM

DISCUSSION

Visceral leishmaniasis is a frequent cause of renal damage that evolves into progressive CKD in dogs (Zatelli et al., 2003). Membranoproliferative and mesangioproliferative glomerulonephritis are the most frequently reported lesions in affected dogs (Costa et al., 2003; Koutinas et al., 1994); this trend is substantiated in the present study.

The pathogenesis of the renal damage in Leishmania infection is not well defined; both a type III hypersensitivity mechanism and the involvement of $CD4^+$ T cells have been proposed. The glomerular proliferation pattern has also been attributed to an inhibition of mesangial cells apoptosis and the migration of inflammatory cells into the glomerular tuft (Costa et al., 2010). In the current study, immune complex deposits were detected within the GBM and in the mesangium by electron microscopy, supporting a role of type III hypersensitivity in the renal damage during Leishmania infection. To our knowledge, sequential biopsy has not been used to evaluate histologic and ultrastructural progression of renal lesions in Leishmania-infected dogs. The 15 dogs had various types of renal damage at T0, with a minimal progression of the glomerular lesions between the 2 sampling times in most dogs. However, in 1 dog, the finding of mesangial immune complex deposits at T1 prompted a change in diagnosis from chronic glomerulosclerosis to mesangioproliferative glomerulonephritis. This change could have been the result of progression of an early lesion with rare and small deposits that were not detected at the first biopsy. In contrast, greater change was detected in the tubulointerstitial compartment between the 2 samplings, with a reduction of the inflammation score in most dogs at T1. This could have been the result of the leishmanicidal treatment, which could have eliminated most parasites, thereby reducing the circulating antigens and, consequently, the immune-mediated glomerular damage.

Inflammation is part of an active process that might be reversible with the correct therapy. Inflammatory cells are also known to contributed to fibrosis through the secretion of various cytokines. Both $CD4^+$ and $CD8^+$ T cells are the most important inducers of tubulointerstitial fibrosis; these cells promote the proliferation of fibroblasts and the production of the ECM mainly by stimulating the production of TGFβ, IL-4, TNFα, and other fibroblast-stimulating factors (Strutz and Neilson., 2003). Although T lymphocytes were not detected in glomeruli in the current study, Costa et al. demonstrated the correlation of $CD4^+$T cells with

the presence of Leishmania antigens in the pathogenesis of canine glomerulonephritis (Costa et al., 2000; Costa et al., 2010). $CD4^{+}$T cells may stimulate B cells to produce antibodies against circulating antigens, leading to the formation of large immune complexes that precipitate in the mesangium and GBM, and trigger the complement cascade (Kurtz et al., 2007).

In contrast to inflammation, fibrosis is considered an irreversible replacement of destroyed parenchyma by connective tissue (Scholondorff, 2008) and is the most common pathogenic mechanism in the chronic failure of parenchymal organs, such as liver, kidney, and lungs. In chronic glomerulosclerosis with mild glomerular lesions, fibrosis was absent at T0 and T1. The absence of detectable glomerular immune complex deposits and the minimal interstitial fibrosis could be key factors in the slow progression of the TID. Immune complex deposits in the glomerular capillary wall and in the mesangium promote inflammation, first in the glomeruli, then extending into the interstitium. The presence of the deposits alters the slit diaphragm with the consequent leakage of proteins into the urinary space. The resultant hemodynamic changes contribute to the reduction in glomerular filtration rate and expansion of mesangial matrix (Meyrier et al., 1998). A progression of the fibrosis was observed in dogs with moderate to severe glomerular damage and in which the tubulointerstitial involvement was already evident at T0. Previous studies have also shown that, regardless of the glomerular lesions, most renal diseases that progress to chronic renal failure involve the interstitium and the tubules (Aresu et al., 2007; Polzin et al., 2005; Ruggenenti and Remuzzi, 2000; Strutz and Neilson, 2003). The mild progression of the TID in this study may reflect the short (a 60-day) interval between T0 and T1; a longer interval between biopsy samplings might uncover more significant changes.

Dog Nos. 4, 5, and 11 had the most severe lesions. The main finding in these dogs was ischemic glomerular obsolescence (probably secondary to hypertension). In these 3 dogs, the T0 diagnosis was end-stage kidney disease; a more specific diagnosis could not be made due to the severity of the lesions. At the second biopsy, the severity of the fibrosis, and the number of obsolescent glomeruli and cystic atrophied glomeruli, had increased. The prognosis in such dogs is usually poor due to the severity and presumed irreversibility of the renal lesions.

In conclusion, the progression of renal lesions is described in dogs naturally infected by *Leishmania spp*. Despite the primary location of the lesions in the glomeruli, by the time

damage is moderate, tubulointerstitial involvement is also evident. The lesions did progress between the first and second biopsies; however, a longer period between biopsies might allow detection of more severe changes. A specific anti-Leishmania treatment could reduce the tubulointerstitial inflammatory response, especially in the absence of glomerular immune complex deposits. In contrast, anti-Leishmania treatment may be less effective for glomerulonephritis and renal interstitial fibrosis. Thus, supportive treatment for chronic renal failure is recommended for the dogs with visceral leishmaniasis.

PART 2

THE PROGRESSION OF TUBULOINTERSTITIAL DAMAGE IN CANINE RENAL DISEASES: THE ROLE OF TUBULAR EPITHELIAL CELLS

Adapted from: Benali SL, Lees GE, Nabity MB, Mantovani R, Bonsembiante F, Aresu L. "*De novo expression of human leukocyte antigen-DR (HLA-DR) and loss of beta-catenin expression in tubular epithelial cells: a possible event in epithelial-mesenchymal transition in canine renal diseases*". Vet J. 2013 Oct;198(1):229-34.

Presented at the annual meeting of the European Society of Veterinary Pathology, London (UK), September 2013.

BACKGROUND

The tubular portion of the nephron is divided into several tracts: 1.the proximal tubule, 2.the loop of Henle, 3. the distal tubule, and 4. the collecting duct. The proximal and distal tubules are mainly located into the cortex whether the loop of Henle and the collecting ducts are found in the medulla. Generally, renal biopsies submitted to the nephropathology diagnostic services are tru-cut samples that include only cortex (Lees et al., 2011) and for this reason most of the examined tubules correspond to proximal and distal tubules and we will referred to these portions hereafter. Tubules are lined by monolayered cubical epithelial cells with extensive lateral and basal interdigitations and molecular junctions on the lateral and basal surfaces that interconnect the neighboring cells one to the other and with the basement membrane. Moreover proximal TECs have another significant morphologic adaptation: the apical brush border which is fundamental for the reabsorption of nutrients (e.g. ions, amino acids, glucose, etc.) from the ultrafiltrate. On the other hand, the distal tubule is involved in maintaining the acid-base balance modulating the ions and urea concentrations. In addition, TECs are believed to actively participate in the mechanisms of renal inflammation and fibrosis in chronic TID. Several evidences in both human and veterinary medicine reported the capacity of TECs of acting as non-professional antigen presenting cells (APCs) and undergoing Epithelial-Mesenchymal Transition (EMT).

TUBULAR EPITHELIAL CELLS AS NON PROFESSIONAL ANTIGEN PRESENTING CELLS (APCS)

Class II major histocompatibility complex (MHC) molecules are heterodimeric transmembrane proteins that are responsible for activation of antigen-specific T helper (Th) lymphocytes during antigen processing by various antigen-presenting cells (APCs) (Frei et al., 2010). The cells recognize antigens as peptide fragments that have been processed by the APCs, bound to MHC molecules, and transported to the surface of the APCs where they are available for recognition. Class II MHC are constitutively expressed on classic APCs such as macrophages, dendritic cells, and B cells (Kelley and Singer, 1993). Other cell types (i.e. intestinal epithelial cells, endothelial cells, chondrocytes, and thyroid epithelial cells) have been shown to function in a limited context as APCs (Wuthrich et al., 1989; German et al.,

1998; Roda et al, 2010). Their efficiency is considered low and they are referred to as non-professional APCs.

The role of epithelial cells as non-professional APCs have been extensively investigated in intestinal epithelial cells both in human and veterinary medicine (Roda et al., 2010; German et al., 1998). Intestinal epithelial cells within the mucosal immune system are able to directly process and present antigens to lymphocytes by a highly polarized system with apical antigen sorting, processing and exclusively basolateral presentation activating T lymphocytes (Roda et al. 2010). Similarly TECs show several features that strongly suggest that they may function as APCs. Studies on animal models of renal injury have demonstrated not only that TECs express MHC molecules but also costimulatory molecules, that are a requirement for actually activating lymphocytes. Finally *in vivo* and *in vitro* studies shown the actual capacity of TECs to process and present foreign antigens (Cheng et al., 1989; Wutrich et al., 1989; Hagerty and Allen, 1992).

To the best of the author's knowledge only one study described the expression of class II MHC in TECs in dogs (Vilafranca, 1995). In its study the author described the expression of class II MHC molecules by interstitial dendritic cells in normal renal tissue. In cases of tubulointerstitial nephritis, however, the expression was extended to other renal elements such as the TECs. These results suggest that also in the dog the TECs can behave as non-professional APCs.

EPITHELIAL-MESENCHYMAL TRANSITION

Epithelial-Mesenchymal Transition (EMT) is defined as the phenotypic conversion of epithelial cells into cells with a mesenchymal phenotype (Kalluri and Weinberg, 2009). This represents a simplistic definition of a more complex process that occurs in both physiological and pathological biological settings. However, the key points of the transition include four events: (1) loss of epithelial adhesion properties; (2) *de novo* expression of mesenchymal markers; (3) disruption of basement membrane (BM); and (4) enhanced cell migration and invasion (Liu, 2010; Zeisberg and Duffield, 2010).

EMT in renal fibrosis was first demonstrated by Strutz (Strutz et al., 1995) more than a decade ago, whether the mechanisms of EMT in canine renal fibrosis have been studied only recently (Yamate, et al. 2005; Aresu et al., 2007b; Benali et al., 2014). In the study of Aresu

and colleagues, the phenotype of TECs was studied in relation to the severity of tubulointerstitial lesions, and cytokeratin and vimentin were used as epithelial and mesenchymal markers, respectively. The study showed the progressive loss of cytokeratin expression by TECs in association with increasing expression of vimentin, suggesting the presence of a transition to a mesenchymal phenotype. Moreover this phenotypic conversion were positively correlated with the degree of fibrosis.

As mentioned previously, EMT is a multistep process in which the down-regulation of junctional complexes is one of the key events. In dogs with different types of spontaneous glomerular diseases, a strong correlation between the severity of TID and the down-regulation of E-cadherin and βcatenin was observed. Additionally, the loss of adhesion junction molecules was detected in association with the acquisition of mesenchymal markers expression by TECs (Aresu et al., 2008b). The splitting or rupture of the tubular BM is considered one of the fundamental steps of EMT. Many factors seem to be involved in the degradation or disruption of the BM and main actors seem to be represented by MMPs (Cheng and Lovett, 2003; Liu, 2004; Cheng et al., 2006, Aresu et al., 2011). Supportive evidence was obtained by identifying MMP2 protein located within the segments of tubular BM splitting. Finding MMP2 in the tubular BM suggested an active role of this enzyme in the degradation of collagen type-IV structure, leading to basement membrane damage but without disruption (Aresu et al., 2011).

Figure 6. Epithelial Mesenchymal Transition (EMT) in tubular epithelial cells (TECs)

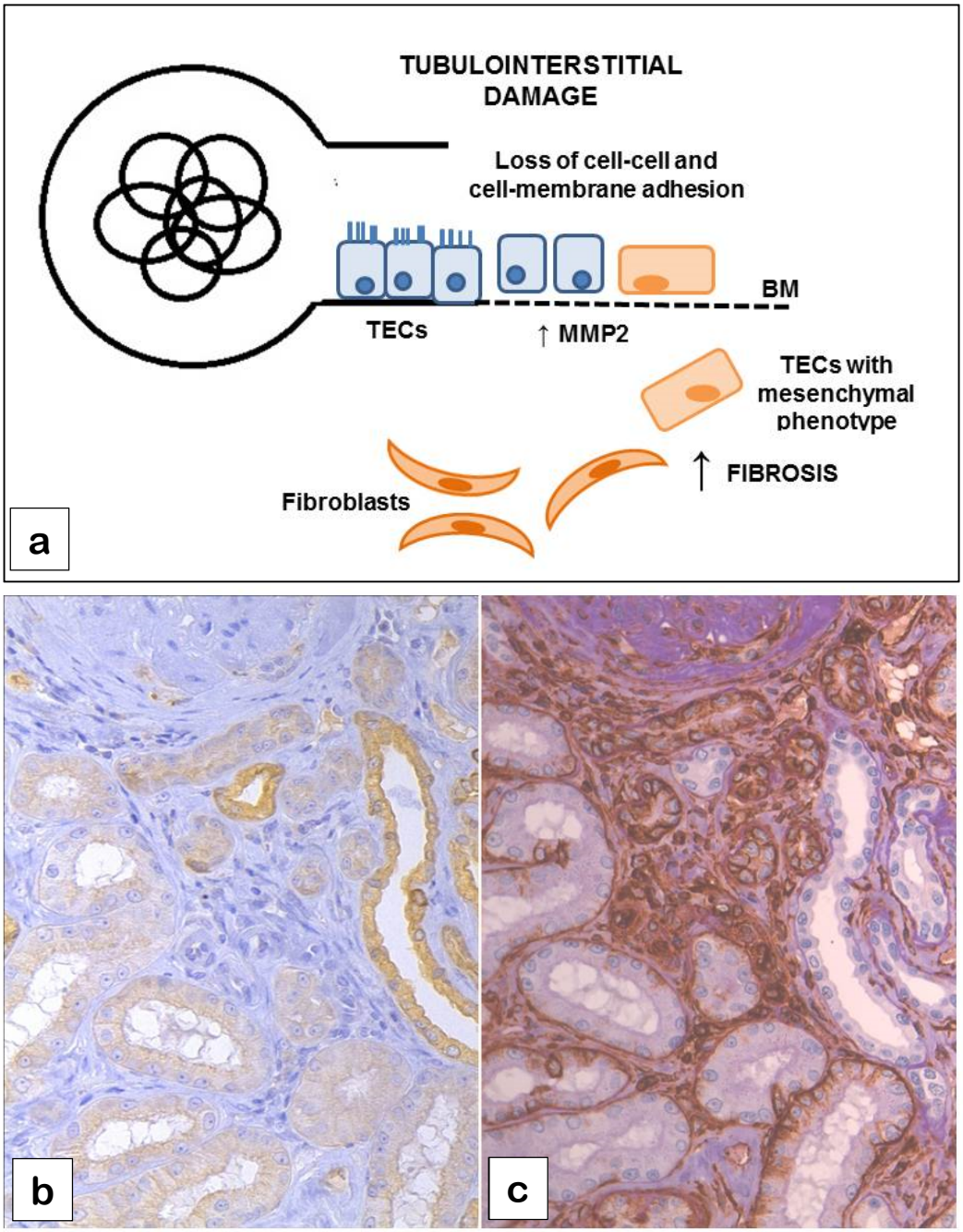

a) schematic view of EMT. TECs: tubular epithelial cells; MMPS: matrix metalloproteinases 2; BM: basement membrane. b) Citokeratin positive immunostaing in TECs of normal tubules, loss of immunolabelling in tubules associated with fibrosis and inflammation. Immunohistochemistry (IHC) Meyer's hematoxylin counterstain, 400x. c) *de novo* vimentin expression by TECs in association with interstitial fibrosis and inflammation. IHC PAS counterstain, 400x.

AIM

The aim of the second part of the study was two-fold: 1) to explore and describe the capacity of TECs to express HLA-DR in dogs with naturally-occurring renal disease due to various causes; 2) to assess the relationship between βcatenin and HLA-DR expression by TECs as assessed by immunohistochemistry (IHC) and the severity of chronic TID.

MATERIALS AND METHODS

Case selection and clinical chemistry

Canine renal biopsies (n= 28) were selected from routine diagnostic cases submitted to the Histopathology Service, Department of Comparative Biomedicine and Food Science, University of Padova between January 2009 and December 2011. All biopsies had a minimum of 12 evaluable glomeruli in 10 serial histological sections (3 μm in thickness) and were composed of only cortex. Five renal biopsies from dogs with no signs or history of renal disease were used as controls. Serum Creatinine concentration (SCr) and urine protein–creatinine ratio (UPC) were provided by the referring clinicians at the time of renal biopsy submission. Proteinuria was defined as UPC > 0.5 and azotaemia by SCr > 123.8lmol/L.

Classification of renal biopsies

Renal biopsies were evaluated by light microscopy and electron microscopy as previously described. Based on biopsy findings, each case was assigned to one of five diagnostic categories as follows: (1) acute tubular necrosis (ATN), (2) amyloidosis (AMYL), (3) chronic glomerulosclerosis (CGS), (4) membranoproliferative glomerulonephritis (MPGN), and (5) mesangioproliferative glomerulonephritis (MeGN). ATN was characterized by primary damage to proximal tubules, which showed degeneration and necrosis of epithelial cells. Multifocally, the injured tubules contained sloughed tubular epithelial cytoplasm, pyknotic nuclear debris and mineralization. AMYL was characterized by glomeruli with diffuse and global mesangial expansion by an amorphous congophilic material consistent with amyloid. CGS was characterized by glomeruli with moderate to severe global mesangial matrix increase, with or without hypercellularity, and absence of immune deposits. MPGN was characterized by glomeruli that exhibited increased mesangial matrix and cellularity, thickening of glomerular capillary walls with endothelial hypertrophy, and immune deposits in

the capillary wall and mesangium. MeGN was characterized by glomeruli with mesangial hypercellularity and increased mesangial matrix with no involvement of the capillary lumen, together with immune deposits in the mesangium as demonstrated on ultrastructural examination.

Histological indices of interstitial inflammation and fibrosis

Interstitial inflammation was evaluated using HE-stained sections. The inflammation index was determined by counting the number of inflammatory cell nuclei (lymphocytes, plasma cells and neutrophils) in 10 randomly selected microscopic fields of renal cortex with a 20x objective. The index for each case was expressed as the average number of inflammatory cells per field.

Interstitial fibrosis was evaluated using Masson's Trichrome-stained sections. Interstitial fibrosis was evaluated in the cortex and severity of cortical interstitial fibrosis (CIF) was graded by examining 20 randomly selected fields with a 20x objective. A semi-quantitative assessment of the extent of fibrosis for each field was done as follows: grade 0: normal tubulointerstitium; grade 1: <25%; grade 2: 26–50%; grade 3: >51% (Aresu et al., 2007). The final score for each biopsy was the total of the scores for each field ranging from 0 to 60 (Nabity et al., 2012).

Immunohistochemistry (IHC)

For IHC, serial paraffin sections (3μm) were placed on surface-coated slides (Superfrost Plus). The details of the immunohistochemal performance are described in Part 1. A mouse monoclonal antibody against the a-chain of human HLA-DR (Clone TAL.1B5, Dako, dilution 1:50) was used. Human class II genes are encoded by genes in the HLA-D region, which includes three subregions called DQ, DP, and DR. The HLA-DR subregions are highly conserved in nearly all mammals, including the dog (Yuhki et al., 2007). Cross-reactivity with canine tissue was also confirmed by previous studies (Darbès et al., 1997; German et al., 1998). A mouse monoclonal antibody against human βcatenin (clone 14, Transduction Laboratories, dilution 1:100) was used to detect βcatenin expression and cross-reactivity of this antibody has previously been tested (Aresu et al., 2008b). Tissues were incubated with the primary antibody for 32 min at room temperature for HLA-DR and for 24 min at 42°C for βcatenin. Slides were counterstained with Mayer's haematoxylin. Interstitial dendritic cells and

epithelial cells in normal renal tissue were used as positive controls for HLA-DR and βcatenin, respectively. Negative controls were performed by replacing the primary antibody with antibody diluent. Quantification of HLA-DR and βcatenin expression was assessed by counting the number of positively labelled and non-stained TECs in 10 randomly selected fields with a 40x objective. Expression of HLA-DR and βcatenin was determined by calculating the percentage of positively labelled cells among the total as follows: [positive-labeled cells/ (positive-labeled cells plus non-stained TECs) x 100].

Double immunolabeling for HLA-DR and vimentin (V9 clone, monoclonal mouse, Dako) was performed on selected representative cases. Tissues were incubated with HLA-DR as described above, followed by incubation with vimentin (diluted 1:150 and incubated 20 min at RT). Peroxidase activity was demonstrated using ultraViews universal diaminobenzidine (DAB, Ventana Medical System, brown to black chromogen reaction) for vimentin. For HLA-DR detection, ultraView universal alkaline phosphatase red detection kit was used (Ventana Medical System, red chromogen reaction). Slides were counterstained with PAS to highlight tubular basement membranes.

Statistical analysis

One-way analysis of variance (ANOVA) using the GLM procedure of the SAS Institute was carried out to assess relationships between renal disease diagnostic categories, magnitudes of azotaemia and proteinuria, and histologic indices of interstitial inflammation and fibrosis. Effects of different disease categories (ATN, AMYL, CGS, MPGN, MeGN, and NORMAL) on CIF grade, inflammation index, SCr, and UPC were examined. The degrees of freedom of the different disease categories were decomposed by a multiple comparisons test using the Bonferroni adjustment method (SAS Institute) to analyze the relative significance of each disease category within each analyzed variable. Correlation and linear regression analyses were carried out with the CORR and REG procedures of SAS, respectively (SAS Institute), comparing HLA-DR with CIF grade, inflammation index, SCr, UPC, and βcatenin expression. Correlation and linear regression analysis were also carried out for CIF grade, inflammation score, SCr, and UPC in relation to βcatenin expression (i.e., using βcatenin expression as a dependent variable). Lastly, correlation and linear regression analysis were also conducted for inflammation score, SCr, and UPC in relation to CIF grade (i.e., using CIF grade as a dependent variable).

RESULTS

Dogs, diagnostic categories, and clinical chemistry findings

A total of 33 canine renal biopsies were examined (28 affected dogs, 5 controls). The 28 dogs with renal disease were composed of 12 females, 15 males, and 1 unspecified. These dogs ranged in age from 1 to 13 years with a median of 6 years, and Boxer was the most represented breed (6/28 dogs).

Primary glomerular lesions were diagnosed in 21 biopsies: 9 CGS, 7 MPGN, 3 MeGN and 2 AMYL. In seven dogs the histological diagnosis was primary ATN. The controls dogs were 4 month-old Beagles, 3 males and 2 females. All but one of the affected dogs were azotemic (SCr > 123.8lmol/L) and all but two were proteinuric (UPC > 0.5). Clinical data are shown in Table 4.

Histological indices of interstitial inflammation and fibrosis

Inflammation was present in all dogs with renal disease. In dogs with acute tubular damage, the infiltrate was mild and multifocal, mainly composed of lymphocytes and rare neutrophils. In dogs with glomerular disease, the inflammation index was greater and mainly composed of lymphocytes and plasma cells (Table 4 and Fig. 7). In dogs with ATN, the amount of fibrosis was significantly lower compared with the other disease categories ($P < 0.01$) (Fig. 7). The inflammation index, UPC and SCr were significantly and progressively increased in samples with moderate (grade 2) and severe grade 3) CIF grade (Fig. 6). In contrast no differences were detected in the aforementioned parameters between normal renal tissue and samples with CIF grade classified as 1 (Fig. 8). Independently of the histological diagnosis, the CIF grade was associated with the inflammation index ($r = 0.986$), UPC ($r = 0.914$), and SCr ($r = 0.904$) ($P < 0.05$) (Fig. 9).

Expression of HLA-DR and βcatenin in TECs

In control dogs, the expression of HLA-DR was restricted to the cytoplasm of dendritic cells within the renal interstitium (Fig. 10a). In all control dogs and one dog with minimal tubulointerstitial involvement, TECs were negative for HLA-DR staining (Fig. 10a). HLA-DR labelling was present in TECs in all other dogs (Fig. 10b). The intensity of immunostaining was moderate to strong and homogenous in the cytoplasm. Scattered lymphocytes and macrophages were also positive for HLA-DR. The number of HLA-DR positive TECs was

significantly increased in biopsies with higher severity of CIF and higher inflammation index, and was highly correlated with UPC (Table 5 and Fig. 11). Multifocally, TECs showed more intense immunoreactivity for HLA-DR when adjacent to inflammatory cells (Fig. 10c).

Uniform membranous and cytoplasmatic βcatenin staining was observed in TECs in control dogs. A reduction of βcatenin expression was observed in the different renal diseases (Table 5). The number of βcatenin positive TECs was negatively correlated with the severity of inflammation (r=-0.981), CIF grade (r=-0.984), and with UPC (r=-0.906) and SCr (r=-0.901). Moreover, HLA-DR and βcatenin expression by TECs were negatively correlated (Fig. 12).

Evaluation of double immunostaining for HLA-DR and vimentin showed four different patterns: (1) tubules with a mixture of cells positive for either HLA-DR or vimentin, (2) tubules with onlyvimentin-positive cells, (3) tubules with only HLA-DR positive cells, and (4) tubules with co-localization of both markers in the same cell (Fig. 10d). In control biopsies, TECs were not immunolabelled by either marker.

Table 4. Comparison of clinical and histopathological variables according to diagnostic categories

Diagnostic Categories[a]	Normal	ATN	AMYL	MPGN	MeGN	CGS
Number of dogs	5	7	2	7	3	9
sCr[b]						
Mean	0.8	1.6	11.7	7.8	9.6	5.8
Median	0.9	1.5	11.7	8.7	11.4	7.0
Min - Max	0.7-1.1	1.1 - 2.1	11.4 -12.1	3.4 - 10.4	5.3 - 12.6	1.5 - 8.4
UPC[c]						
Mean	0.24	1.45	3.6	3.6	4.8	2.5
Median	0.2	0.7	3.6	3.0	5.9	2.2
Min – Max	0.2-0.3	0.3-1.2	3.1-4.1	1.8-6.5	1.9-6.7	1.0-4.1
Inflammation Index[d]						
Mean	0	5.41	77.1	39.4	54.1	34.3
Median	0	5.1	77.1	35.5	65.4	33.1
Min - Max	0	3.5-8.9	75.3-78.8	20.5-80.9	22.3-74.7	3.2-75.7
CIF score[e]						
Mean	5.6	11.6	50.5	32.3	40.0	31.2
Median	5.0	11.0	50.5	30.0	46.0	34.0
Min-Max	12-53	8-55	8-15	22-52	51-52	5-7

[a] ATN: acute tubular necrosis; AMYL: amyloidosis; MPGN membranoproliferative glomerulonephritis, MeGN: mesangioproliferative glomerulonephritis; CGS: chronic glomerulosclerosis; [b] sCr: serum creatinine (mg/dL); [c] UPC: urine protein-creatinine ratio; [d] Inflammation index: average number of inflammatory cells per in 10 fields (200x); [e] CIF score: chronic interstitial fibrosis.

Figure 7. Chronic tubulointerstitial damage evaluation and morphological diagnosis

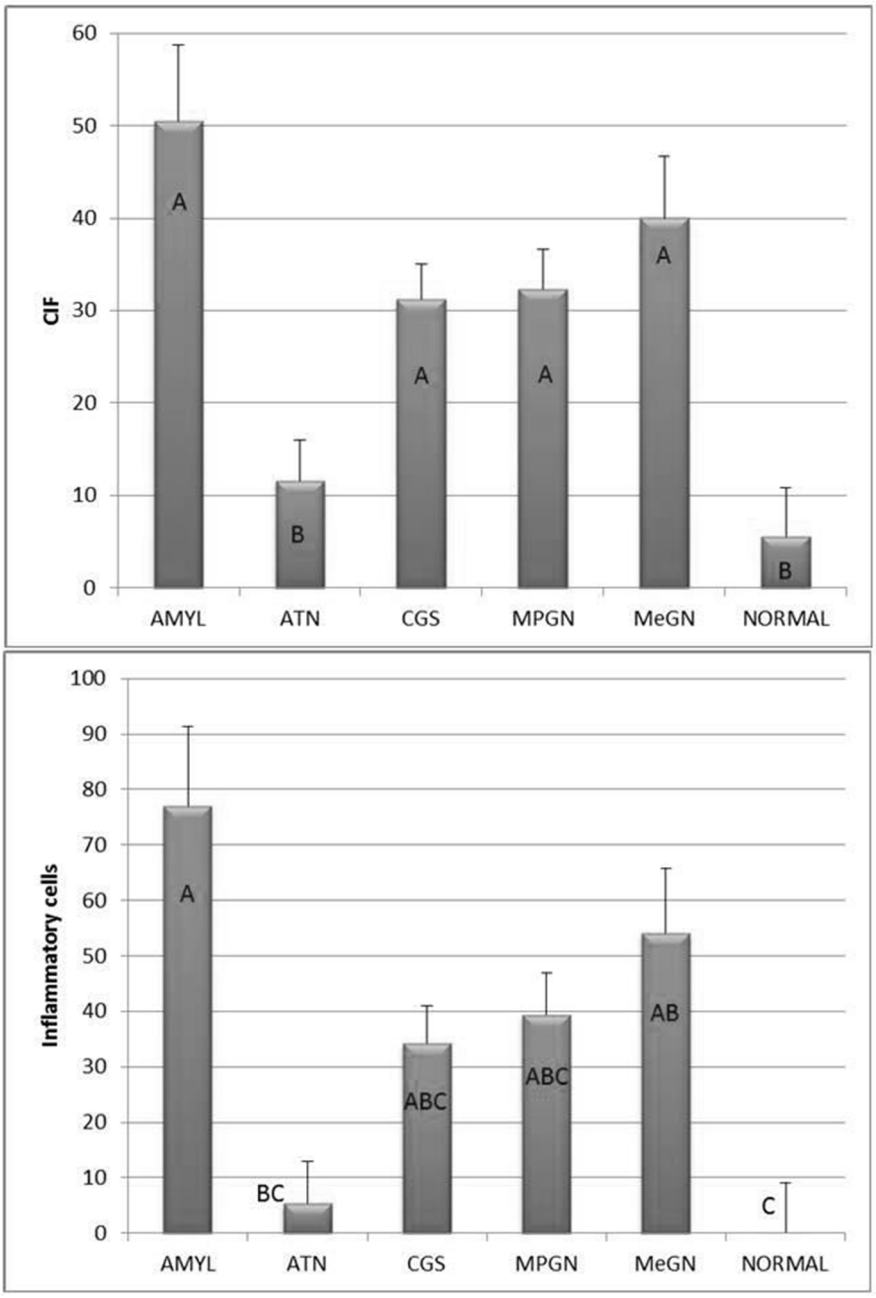

AMYL: amyloidosis; ATN: acute tubular necrosis; CIF: cortical interstitial fibrosis; CGS: chronic glomerulosclerosis; MPGN: membranoproliferative glomerulonephritis; MeGN: mesangioproliferative glomerulonephritis.

Figure 8. Inflammatory cell count, proteinuria and serum creatinine values according to the cortical interstitial fibrosis grade

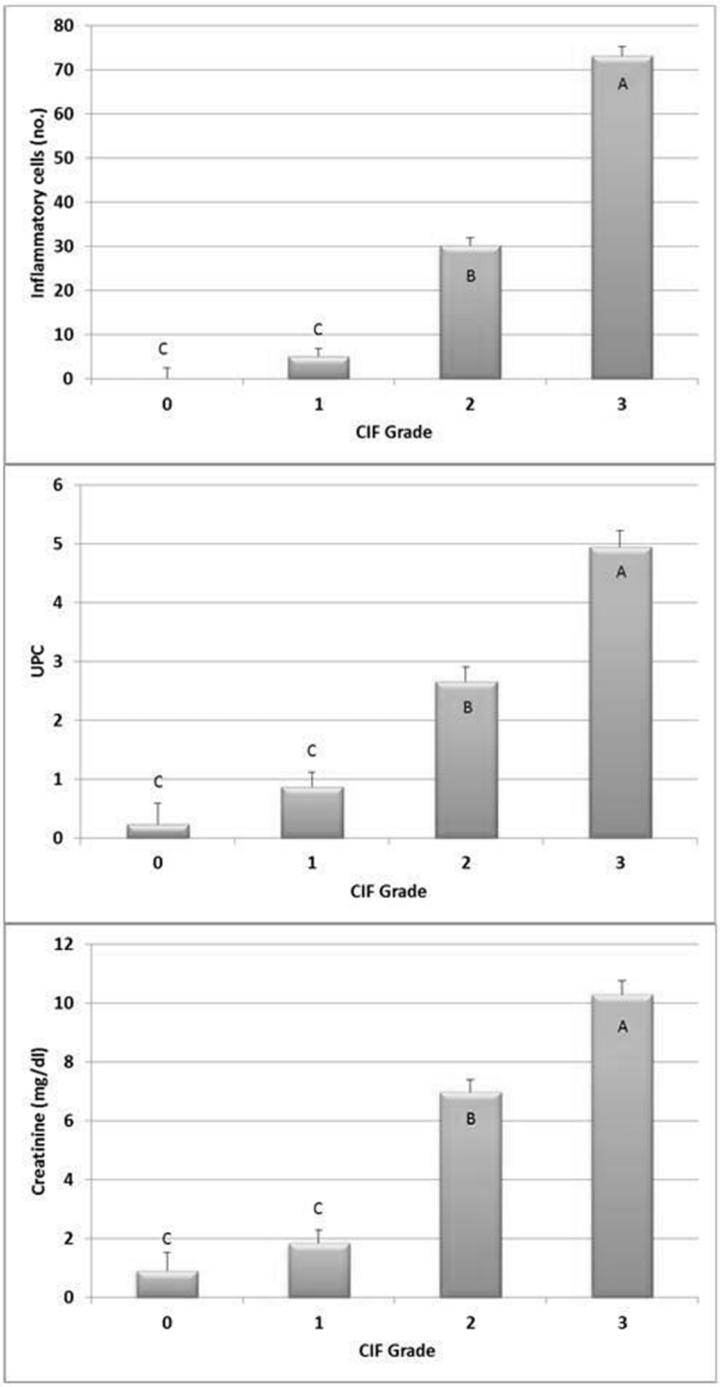

CIF: cortical interstitial fibrosis; UPC: urinary protein and creatinine ratio

Figure 9. Correlations between CIF grade and inflammatory cells count, proteinuria and serum creatinine

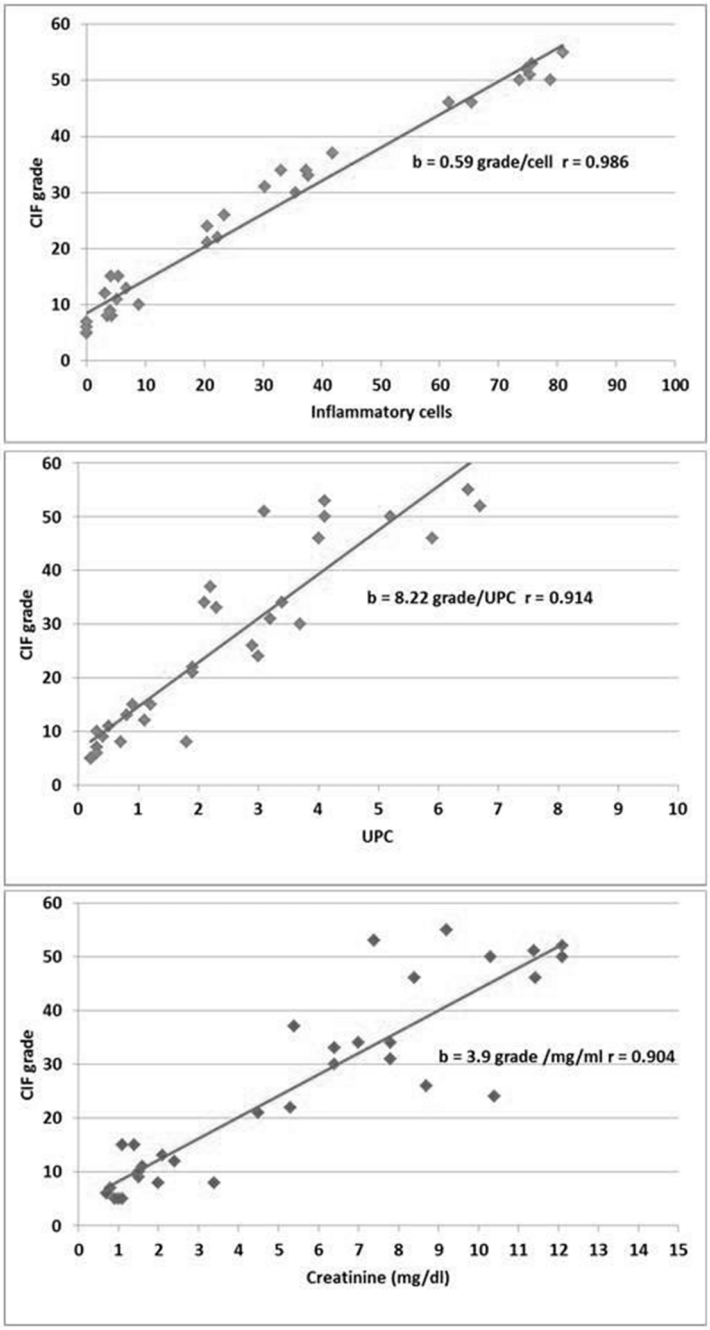

CIF: cortical interstitial fibrosis; UPC: urinary protein and creatinine ratio

Table 5. Comparison of immunohistochemical results according to diagnostic categories

Diagnostic Category[a]	**Normal**	**ATN**	**AMYL**	**MPGN**	**MeGN**	**CGS**
Number of dogs	5	7	2	7	3	9
HLA-DR expression in TECs (% positive-labeled cells)[b]						
Mean	0	4	64	41	5	33
Median	0	5	64	34	6	39
Min - Max	0	0-8	64-64	4-84	28-64	0-62
β-Catenin expression in TECs (% positive-labeled cells)[b]						
Mean	97	90	30	59	48	62
Median	97	90	30	62	39	61
Min - Max	96-99	87-92	29-31	21-74	35-68	28-92

[a] ATN: acute tubular necrosis; AMYL: amyloidosis; MPGN membranoproliferative glomerulonephritis, MeGN: mesangioproliferative glomerulonephritis; CGS: chronic glomerulosclerosis; [b] TECs: tubular epithelial cells

Figure 10. Immunohistochemistry for Human Leukocytes Antigen (HLA) in canine renal tissue

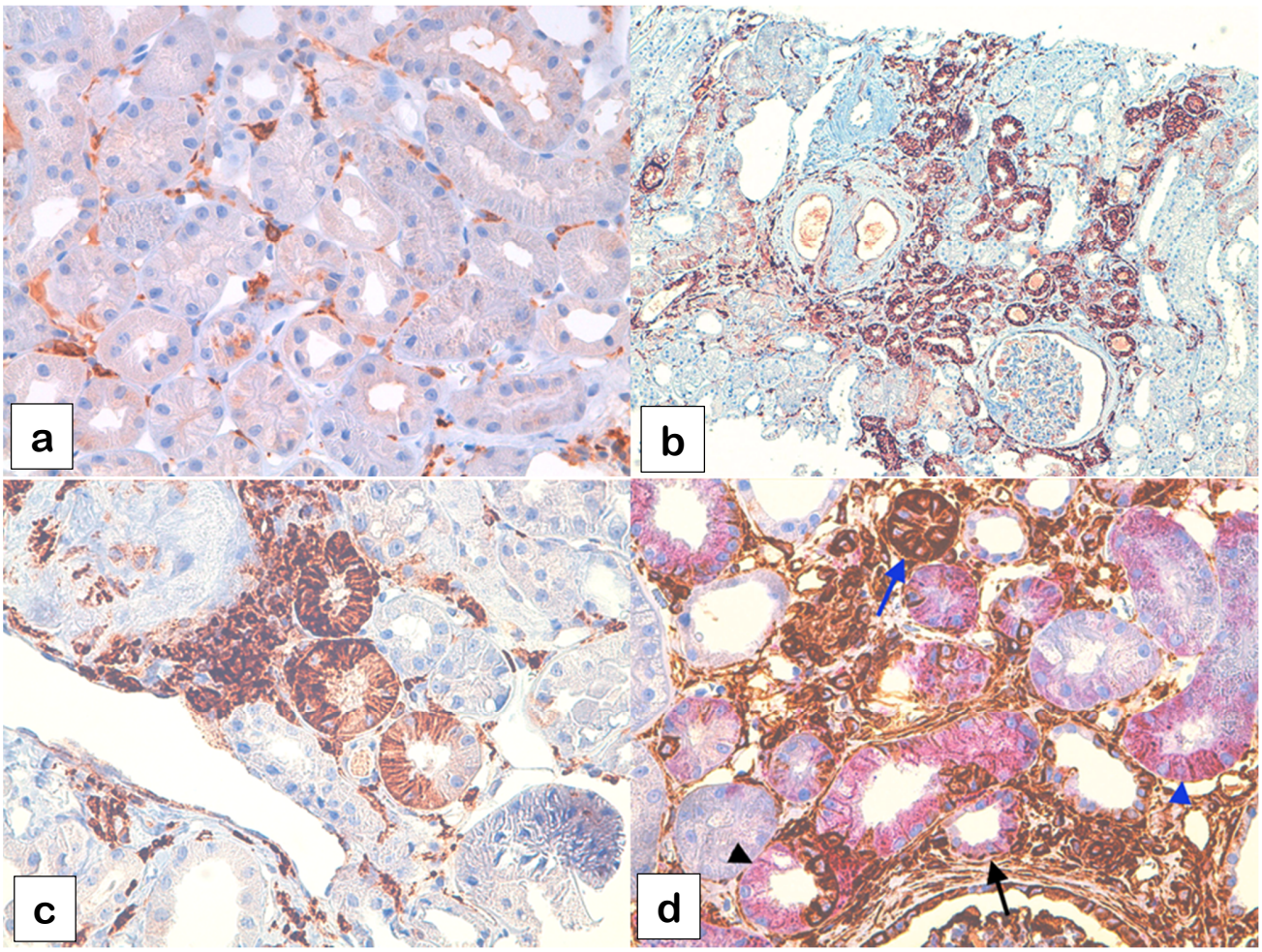

a) Dog, renal biopsy, control. Diffuse cytoplasmatic HLA-DR expression is evident in interstitial dendritic cells. Immunohistochemical staining for HLA-DR, haematoxylin counterstain (400x); b) Dog, renal biopsy, membranoproliferative glomerulonephritis. HLA-DR expression is detectable multifocally in the cytoplasm of proximal tubular epithelial cells. Immunohistochemical staining for HLA-DR, haematoxylin counterstain (200x); c) Dog, renal biopsy, membranoproliferative glomerulonephritis. HLA-DR expression is diffusely detectable in lymphocytes and tubules adjacent to inflammation. Immunohistochemical staining for HLA-DR, haematoxylin counterstain (400x); d) Dog, renal biopsy, chronic glomerulosclerosis. Different pattern are present. (1) HLA-DR and vimentin expression in a single tubule (black arrow-head). (2) HLA- DR and vimentin co-localization in the cytoplasm of epithelial tubular cells (black arrow). (3) Diffuse vimentin expression in a tubule (blue arrow). (4) Diffuse HLA-DR expression in a tubule (blue arrow-head). Double immunostaining for HLA-DR (red signal) and vimentin (brown signal), PAS counterstain (400x).

Figure 11. Correlations between HLA-DR expression grade and cortical interstitial fibrosis, inflammatory cells count, proteinuria and serum creatinine.

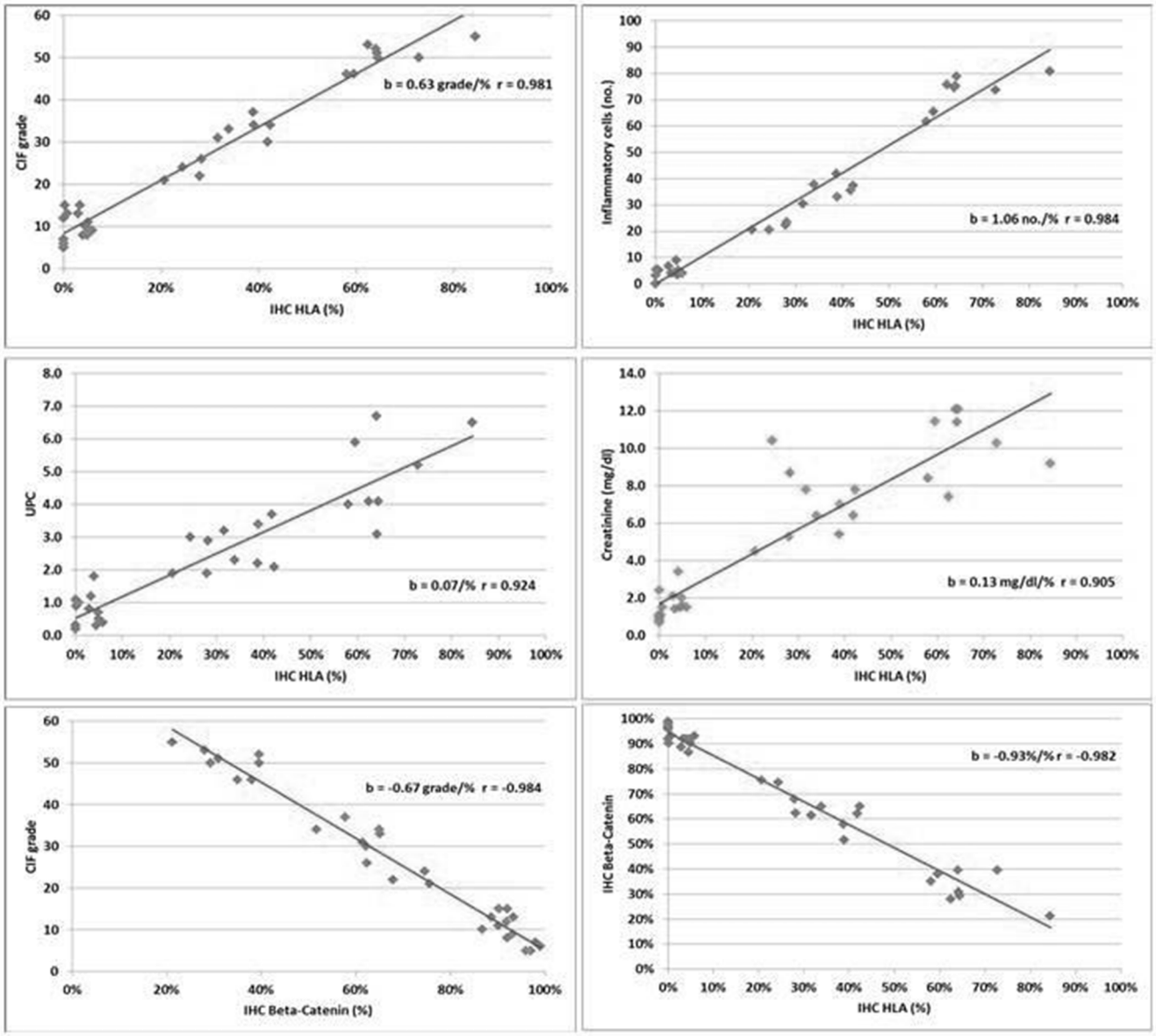

CIF: cortical interstitial fibrosis; UPC: urinary protein and creatinine ratio; IHC HLA (%): percentage of HLA-DR positive immunolabelled tubular epithelial cells (TECs)

Figure 12. Correlations between βcatenin expression and cortical interstitial fibrosis, inflammatory cells count, proteinuria, serum creatinine and HLA-DR expression.

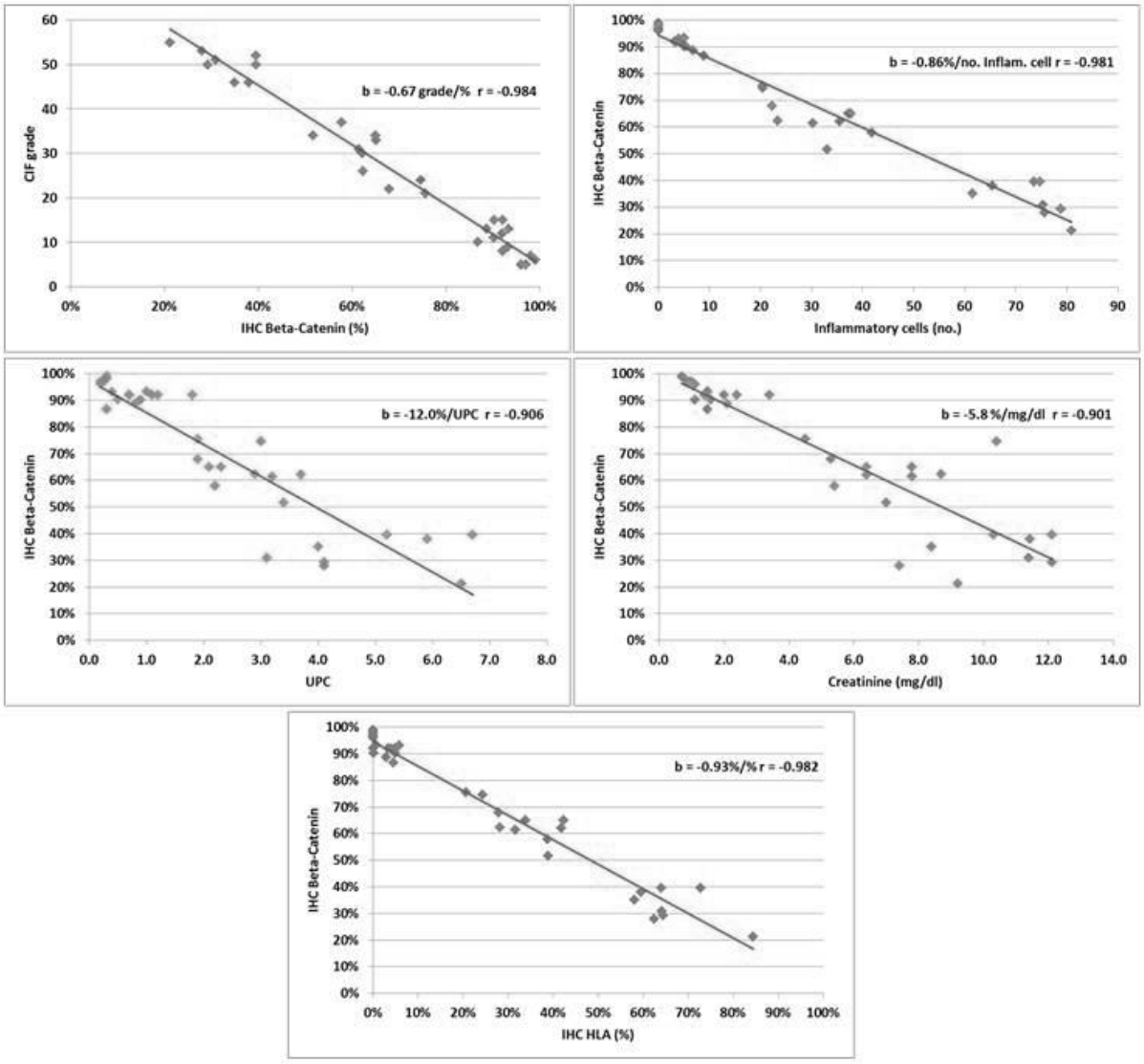

CIF: cortical interstitial fibrosis; UPC: urinary protein and creatinine ratio; IHC HLA (%): percentage of HLA-DR positive immunolabelled tubular epithelial cells (TECs); IHC beta-catenin (%):percentage of βcatenin positive immunolabelled TECs

DISCUSSION

The present study investigated the immunohistochemical expression of HLA-DR and βcatenin in renal biopsies from dogs with various kidney diseases. Association of expression of these markers with clinicopathological data, as well as with measures of interstitial inflammation and fibrosis was examined. The inflammation index and CIF grade were significantly increased in dogs with primary glomerular diseases compared to dogs with primary acute tubular injury. No differences were evident for CIF grade and inflammation index among the CGS, MPGN, and MeGN disease categories.

Acute tubular damage is frequently characterized by degeneration and necrosis of tubules with no involvement of the interstitium, while glomerular diseases are associated with a variable increase in ECM, fibroblasts, and inflammatory cells in the interstitium at the time of biopsy. One possible explanation for the lack of tubulointerstitial changes in the ATN cases may be the rapid clinical onset of the disease in these dogs, since all ATN dogs were biopsied within a few days of the initial injury.

With primary glomerular diseases, compensatory mechanisms such as glomerular hypertrophy and hyperfiltration are described to maintain kidney function for some time during the development of the primary process; therefore, secondary tubulointerstitial lesions may already be chronic and advanced by the time clinical signs become evident (Finco et al., 1999). UPC and SCr were positively correlated with the severity of CIF and inflammation. However, these parameters were normal or only slightly increased in dogs with mild CIF and inflammation, supporting their insensitivity for detecting early renal disease. This finding supports the need for additional more sensitive biomarkers of early damage in canine renal disease as pointed out in recent studies (Meyer et al., 2010; Smets et al., 2010; Slocum et al., 2012; Nabity et al., 2012).

The main objectives of this part of the study were to investigate the possible role of TECs as APCs and secondary to examine whether HLA-DR expression by TECs may be part of EMT. As expected, HLA-DR was expressed by interstitial dendritic cells, while TECs were negative in the control kidneys. In contrast, *de novo* expression of HLA-DR in the cytoplasm of TECs was found in the diseased kidneys and this expression was correlated with the CIF grade, UPC, and inflammation index. This result suggests a possible progressive transition of

TECs to APCs. Particularly interesting is the positive correlation between the magnitude of the proteinuria and the expression of HLA-DR by TECs.

The role of proteinuria in the pathogenesis of CKD is still uncertain, but several studies in humans and experimental animal models report a direct link between the degree of proteinuria and the progression of the TID (Strutz, 2009; Erkan, 2013).

Different studies have shown that proteinuria might be a cause rather than merely a consequence of the progression of the TID specifically interacting with TECs. As aforementioned, one of the functions of proximal TECs is the reuptake of nutrients and proteins (e.g. albumin) filtered by the glomerulus in primary glomerular diseases. The proteins absorbed at the luminal membrane are endocytosed and concentrated within vesicles at the apical border of tubular cells. Though this is a physiological function of the proximal tubule, an increased uptake of albumin and albumin-bound lipids by proximal tubules has been shown to correlate with the pathogenesis of CKD: an overload of high molecular weight proteins causes a toxic effect on TECs leading to apoptosis, as well as to the production of pro-inflammatory, pro-fibrogenic growth factors and cytokines (Abbate et al., 1998; Abbate et al., 2006; Christensen and Verroust, 2008; Erkan, 2013).

Our results show a possible involvement of TECs in exposing the protein antigens with subsequently presentation of class II MHC, which may then exacerbate or perpetuate interstitial inflammation, particularly in glomerular diseases. Vilafranca and colleagues were the first to identify expression of the class II MHC by TECs in dogs with interstitial nephritis, suggesting that these cells were capable of acting as non-professional APCs. In our study, we analyzed a set of renal biopsies from dogs with a variety of glomerular and tubular diseases and found a close correlation between the expression of HLA-DR in TECs and degree of proteinuria. Further evidence of the actual capacity of TECs of acting as APCs is confirmed by the more intense immunostaining found in TECs adjacent to lymphocytes suggesting a direct interaction with inflammatory cells and a possible pro-inflammatory role for the TECs. The hypothesis supported by these observations is that tubular protein overload initiates and contributes to the progression of renal damage by invoking interstitial inflammatory cell accumulation and subsequently fibrosis in renal interstitium. Based on the results of the present study, canine TECs could also be considered as non-professional APCs.

Figure 13. Schematic view of the possible "activation" of TECs acting in response to proteinuria and acting as non-professional APCs with recruitment of inflammatory cells.

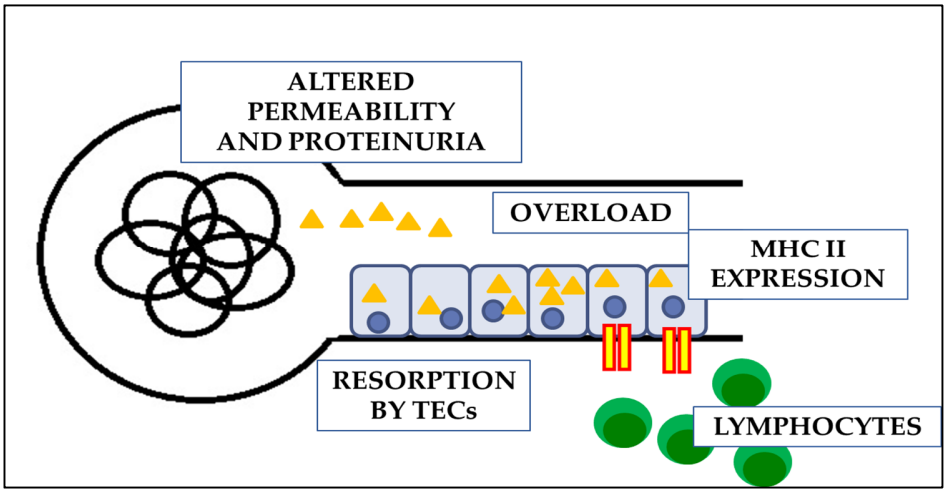

βcatenin was found diffusely expressed within the cytoplasm and on the cellular membrane virtually of all TECs in control kidneys, and progressive loss of staining correlated with worsening of the CIF grade and higher inflammation index. βcatenin plays an essential role in maintaining the structural integrity and polarity of epithelial cells, and its decreased expression may reduce adherens junction formation and lead to epithelial transdifferentiation. In fact, in the early phase of EMT, the expression of protein constituents of the tight junctions is decreased in epithelial cells. Subsequently, epithelial cells lose their intercellular contacts and polarity and undergo cytoskeleton reshaping by expressing proteins specific to mesenchymal cells, such as vimentin. In contrast to observations in human kidneys, the EMT of TECs in dogs seems to be characterized by *de novo* expression of vimentin rather than smooth muscle actin (Aresu et al., 2007b). The negative correlation between expression of HLA-DR and βcatenin by TECs observed in this study suggests the possibility of a previously unrecognized phase in the EMT process.

To further investigate this observation, a double IHC protocol for vimentin and HLA-DR was used. The findings showed several different patterns of expression that may be consistent with the following three phase hypothesis: (1) when TECs express only HLA-DR, they act as APCs, presumably preceding the mesenchymal phase of EMT; (2) when TECs express both markers, a transition from one phase to another is occurring; (3) when TECs express only vimentin, the complete EMT process has occurred.

Summarizing this part of the study confirms the progressive decrease in βcatenin expression in TECs during TID associated with fibrosis and inflammation. *De novo* expression of HLA-DR in TECs could contribute to the recruitment of inflammatory cells and vimentin expression by TECs may be considered as a step during EMT.

PART 3

THE PROGRESSION OF TUBULOINTERSTITIAL DAMAGE IN CANINE RENAL DISEASES: A MODEL OF CANINE CKD

submitted

Presented at the Annual Meeting of the Associazione Italiana Patologi Veterinari (AIPVet) Pisa, June 16-18, 2014 (preliminary results); and at the Annual Meeting of American College of Veterinary Pathology (ACVP), Atlanta (GE, USA) November 8-12, 2014.

BACKGROUND

CKD is the final common pathway resulting from persistent renal injury. As previously demonstrated though the potential causes of glomerular disease in dog are numerous, a uniform process of progressive TID downstream of the primary glomerular injury is common (Part 1 and Part 2).

The third part of the study was performed on a spontaneously occurring canine model of CKD. Navasota dogs (abbreviated NAV) belong to a family of mixed-breed dogs developing a form of canine X-linked hereditary nephropathy (XLHN) that was described for the first time in 1999 (Lees et al. 1999). The XLHN occurring in NAV dogs is an inherited glomerular nephropathy caused by mutations in type IV collagen gene (Lees et al., 1999). In affected males the gene encoding for the α5 chain of collagen protein has a 10-bp deletion in exon 9 causing a frame-shift that results in a premature stop codon in exon 10 (Cox et al. 2003). The inability to synthetize α5 chain of collagen prevents the formation of type IV collagen, a principal component of the GBM. The abnormal composition of the GBM results in altered ultrafiltration and juvenile onset of proteinuria typically occurring between 2 and 6 months of age in affected males and rapidly progressive to ESRD by 6 to 15 months of age (Lees et al., 1999, reviewed in Kashtan 2002 and Lees 2013).

Histopathological lesions occurring in advanced stages of XLHN are typical of chronic glomerular disease with secondary involvement of the tubulointerstitium and include non-specific changes such as global glomerulosclerosis, tubular dilation, interstitial fibrosis and inflammation (Lees, 2013; Nabity et al 2012; Lees et al., 1999). Nevertheless, early microscopic changes in NAV dogs and their evolution during the course of disease have been partially described (Nabity et al. 2012). The first part of this study was focused on the description of renal morphology and function in early stages of the disease and to characterize the evolution of lesions over time.

Investigating the mechanisms responsible for canine XLHN during its initial phases and progression can be highly beneficial in designing new strategies for the diagnosis and treatment of chronic nephropathies. The second part of this study, therefore, explored the expression of genes potentially involved in the pathogenesis of XHLN. The set of examined genes included molecules reported to be involved in different ways to the extent chronic renal damage. TGFβ and the Connective tissue growth factor (CTGF) are profibrotic molecules

whose expression and activity are strictly correlated. Indeed, the two molecules are reported to reciprocally enhance their expression in a positive feedback manner (Weier et al., 2008; Wang et al., 2011). Similarly members of the PDGF family and the Epidermal Growth Factor Receptors are reported to be increased in advanced stages of TID and increasing fibrosis in humans (Bonner, 2004; Zeng et al., 2009). A second group of molecules included anti-fibrotic factors: the Hepatocyte growth factor (HGF) and Bone morphogenetic protein-7 (BMP-7) that are considered nephroprotective by inhibiting the TGFβ pathway (Nishinakamura and Sakaguchi, 2014; Lopez-Fernandez et al., 2012; Zeisberg et al., 2006). A third group of genes included several MMPs and their inhibitors (tissue inhibitor of MMPs type 1 and 2 named TIMP1 and TIMP2 respectively). A fourth group of genes included adhesion molecules typical of TECs that were investigated to explore the mechanisms of EMT in XLHN. These included βcatenin, N-cadherin and E-cadherin (Aresu et al 2008). A last molecule investigated was Clusterin, a glycoprotein found upregulated in several renal diseases in humans (Jones and Jamary, 2002; Fuchs and Hewitt, 2011). Published data suggest that it may have an important role in the pathogenesis of renal injury and has become a molecule of interest as potential biomarker of renal damage in both human and veterinary medicine (Jones and Jamary, 2002; Garcia-Martinez et al., 2012).

Selected markers with significantly increased or decreased mRNA expression in affected dogs were further investigated at the protein level using IHC.

AIM

Aims of the study were: 1) to describe the evolution of renal lesions in dogs with XLHN; 2) to explore the gene and protein expression of selected molecules potentially involved in the progression of TID in dogs and 3) to evaluate changes in their expression in different phases of the disease and correlated them to the renal lesions in XLHN.

MATERIALS AND METHODS

Dogs

Dogs were from a colony at Texas A&M University referred to as the Navasota kindred, which is on a mixed background, in which a missense mutation in the gene encoding the α5 chain of type IV collagen causes XLHN. Affected males (n=10) were monitored to a standardized end point of serum creatinine (SCr) >5.0 mg/dL (upper reference limit ≤ 1.2 mg/dL) or onset of uremic signs (anorexia and vomiting on 2 consecutive days), whereupon each dog was euthanized. Randomly selected unaffected males (n=5) evaluated under the same protocol served as age-matched controls. All studies of these dogs were approved by the Texas A&M University Institutional Animal Care and Use Committee.

Tissue samples

Samples of kidney were collected at established time-points: 4 (T0), 6 (T1) and 9 (T2) months of age. Most were collected using an ultrasound-guided needle biopsy technique (Groman et al., 2004), unless the dog reached the study end-point at or prior to the time points, in which case samples were obtained immediately post-euthanasia. At each time-point, renal cortex was fixed in 10% buffered formalin and embedded in paraffin within 24 hours. Samples were also placed in RNA-later (Applied Biosystems, Foster City, CA) , flash frozen, and then stored at -80°C.

Renal histopathological evaluation

Three-micrometer thick sections were cut from 2 levels of each biopsy 100 µm apart in order to represent different planes within the biopsy. Sections stained with HE, Masson's trichrome, and PAS were evaluated. The interstitium, tubules, and glomeruli were evaluated as follows and scored according to a grading system (full scoresheet in Table 6a and 6b).

(1) In each PAS-stained section, the number of glomeruli demonstrating obsolescence and cystic glomerular atrophy was counted, and other glomerular features (Table 6) were scored.

(2) Twenty 400X fields of tubulointerstitium were evaluated in HE, PAS and Masson's Trichrome-stained sections.

Clinical Chemistry

Blood and voided, midstream urine were collected in association with the renal biopsy. SCr concentration was measured (Vitros 250, Ortho-Clinical Diagnostics Inc., Rochester, NY, USA). Urine specific gravity was measured with a refractometer. Urine was centrifuged (500 x g for 5 minutes) and the supernatant was removed for urine protein and creatinine determination (Vitros 250, Ortho-Clinical Diagnostics Inc., Rochester, NY, USA). In addition, urine albumin concentration was determined by ELISA as previously described (Pressler et al., 2002).

Gene expression

Total RNA was isolated using the RNeasy Mini Kit (Qiagen, Valencia, California, USA) according to the manufacturer's instructions. The total RNA concentration and quality were evaluated with a NanoDrop ND-1000 spectrophotometer (NanoDrop Technologies, Wilmington, Delaware, USA) and by denaturing gel electrophoresis. First-strand cDNA was synthesized from 2μg of total RNA in a final volume of 20 μl using the High Capacity cDNA Reverse Transcription Kit (Applied Biosystems, Foster City, California, USA) according to the manufacturer's protocol and stored at -20°C until use. The cDNA was used as a template for the quantification of 21 genes by quantitative real-time reverse transcriptase polymerase chain reaction (qRT-PCR) in a Light Cycler 480 Instrument (Roche Diagnostics, Basel, Switzerland). The amplification protocol consisted of an initial step of 2 min at 50°C and 2 min at 95°C followed by 45 cycles of 10 s at 95°C and 30 s at 60°C. The qRT-PCR reaction consisted of 5 μl Platinum SYBR Green qPCR SuperMix-UDG (Invitrogen, Life Technologies, Carlsbad, California, USA), 0.3 μl forward and reverse primers (10 μM) (the primer combination and final concentrations were optimized during assay setup) and 2.5 μl cDNA (diluted 1:100). The primers, shown in Table 7, were designed using Primer Express 2.0 (Applied Biosystems, Life Technologies, Carlsbad, CA). Calibration curves using a 7-fold serial dilution (1:2) of a cDNA pool revealed PCR efficiencies near 2.0 and error values < 0.2. Seven candidate genes (beta-actin, GADPH, TATA-binding protein, HPRT, 1RPL32, 2RPL32) were selected based on existing literature (Peters et al., 2007; Brinkhof et al., 2006) and tested as reference genes. TATA-binding protein (TBP) was chosen as a reference gene for the absence of statistically significant differences in its expression profile between the healthy and pathologic samples. Moreover its amplification efficiency was approximately equal to

those of the target genes. The ΔΔCt method (Livak and Schmittgen, 2001) was used for the relative quantification of mRNA, ultimately expressed as Relative Quantification (RQ).
RQ values were analyzed by using Multid-Genex software (Bergkvist et al, 2010). Hierarchical clustering (HCL) and principal component analysis (PCA) were performed, adopting the following settings: mean center scaling, Complete linkage, and Euclidean for the evaluation of all samples, and Ward's algorithm and Manhattan distance for the evaluation of T0 samples.

Immunohistochemistry (IHC)

Protein expression of selected growth factors was investigated by immunohistochemistry in affected and control dogs. The details of the immunohistochemal performance are described in Part 1. Antibodies and protocol details are listed in Table 8. The immunohistochemical evaluation consisted in a qualitative assessment of cell types and location (cytoplasmic/membranous or nuclear) of the immunostaining. Tissues known to express the molecules were used as positive controls. Negative controls were performed by replacing the primary antibody with antibody diluent.

Statistical Analysis

Data were analyzed statistically using a commercially available statistical package (SAS 9.1, SAS Institute). Normal distribution was confirmed by Shapiro-Wilk test and the equality of variance by Levene's test. A linear repeated mixed model was used to analyze morphological and clinicopathologic parameters and gene expression over time with the group (renal disease vs control dogs) as fixed effect; time and animal effects were included as repeated and random effect respectively. Interaction between group and time was inserted in the models and the Bonferroni post-hoc pair wise comparison test was used if statistically differences were detected.

Stepwise forward canonical discriminant analysis (CDA) was performed time by time on data expressing morphological and clinicopathologic parameters, in order to characterize the experimental group (renal disease vs control dogs). The rank correlation by means of the Spearman's Rho coefficient were used to assess the degree of association between all the variables included in the study and between genes expression variables. $P < 0.05$ was considered statistically significant.

Table 6a. Histologic scoring of renal biopsy specimens: glomerular evaluation

Histologic parameter and definition	Severity	Score
Glomerular compartment		
Endocapillary hypercellularity Increased number endothelial cells with luminal effacement	Absent to rare	0
	1-2 capillary profiles in few glomeruli	1
	1-2 capillary profiles in most glomeruli	2
	Many capillary profiles in most glomeruli	3
Mesangial hypercellularity Increased number mesangial cells, including macrophages	Absent to rare	0
	Segmental in few glomeruli	1
	Segmental to global in few glomeruli	2
	Segmental to global in most glomeruli	3
Immune deposits	Absent	0
	Rare	1
	In few glomeruli	2
	In most glomeruli	3
Increased mesangial matrix	Absent	0
	Segmental in few glomeruli	1
	Segmental to global in most glomeruli with obliteration of few capillary loops	2
	Global in most glomeruli with obliteration of manu capillary loops	3
Capillary thickening	Absent	0
	Rare	1
	Mild in most capillary loops	2
	Moderate in most capillary loops	3

Table 6b. Histologic scoring of renal biopsy specimens: tubulo-interstitial evaluation

Histologic parameter and definition	Severity	Score
Tubulo-interstitial compartment		
Tubular Dilation	Absent to rare	0
	Mild: scattered dilated tubules (<2 tubules/field)	1
	Moderate: many dilated tubules	2
	Severe: most tubules are dilated	3
Brush borders	Absent to rare	0
	Mild: scattered tubules retain their brush borders (<2 tubules/field)	1
	Moderate: many tubules retain their brush borders	2
	Severe: most tubules retain their brush borders	3
Epithelial cell microvacuolation	Absent to rare	0
	Mild: scattered tubules have vacuoles in the epithelial cells (<2 tubules/field)	1
	Moderate: many tubules have vacuoles in the epithelial cells	2
	Severe: most tubules have vacuoles in the epithelial cells	3
Epithelial cell macrovacuolation	Absent to rare	0
	Mild: scattered tubules have vacuoles in the epithelial cells (<2 tubules/field)	1
	Moderate: many tubules have vacuoles in the epithelial cells	2
	Severe: most tubules have vacuoles in the epithelial cells	3
Tubular atrophy	Absent to rare	0
	Mild: scattered tubules are atrophied (<2 tubules/field)	1
	Moderate: many tubules are atrophied	2
	Severe: most tubules are atrophied	3
Tubular epithelial cell necrosis	Absent to rare	0
	Mild: one necrotic cell in 1 tubule	1
	Moderate : 1 necrotic cell in > 1 tubule	2
	Severe : > 1 necrotic cell in > 1 tubule	3
Fibrosis	Absent to rare	0
	Mild: fibrosis around tubules that does not result in separation of tubules	1
	Moderate: fibrosis which widely separates tubules but does not distort the overall architecture of the tubulointerstitium	2
	Severe: fibrosis around tubules that distorts the architecture of the tubulointerstitium (i.e. replaces tubules)	3
Inflammation	number of inflammatory cells	

Table 7. Primers

Gene	Gene bank ref	Forward	Reverse
BMP7	NC_006606.3	caacgtcgcagaaaacagc	gctgacgtacagttcgtgct
CLUST	NC_006607.3	agaagtggctcggggcta	gggagaactctggttcagga
CTGF	BQ839535.1	aaatgctgcgaggagtgg	aacgtgtcttccagtcggtaa
ECAD	NM_001287125.1	tttgaaaacaactaagggcttgg	cgttcaccacagtcacgtacaa
EGFR	XM_533073.4	agcgatgtgtggagctacg	ataccgtcgtaaggcttgga
HGF	NM_001002964.1	caagggaacagtgtctatcactaaga	gatagctcgaaggcaaaaagc
MMP14	XM_843664.1	gatctgaatgggaatgacatctt	gatggccgagggatcatt
MMP2	XM_535300.2	gggaccacggaagactatga	atagtggacatggcggtctc
MMP9	NM_001003219.1	tgagaactaatctcactgacaagca	gctcggccacttgagtgta
NCAD	XM_546371.4	gacttgatagagaaaaagtgcaaca	ggtgtttgaaaggccgtatg
PDGFB	NM_001003383.1	ccgagttggacctgaatttg	gtcttgcactcagcgatcat
PDGFD	XM_536595.4	tggctaaacctggattcaaga	tgactgactcccagttggtct
PDGFRα	AY525124.2	tttcccttggcggcacac	gtcaggcttggccatccg
PDGFRβ	NM_001003382.1	cacgcctctgacgagatttatg	ctcgagaagcagcaccagct
TBP	AY514773.1	ctgacccaccaacagtttagc	ttctgggtttgatcatcctgt
TGFR2	XM_005634331.1	ccaatatcctggtgaagaacg	catgtatcttgcagttcccactt
TGFβ	NC_006583.3	gcaagtagacattaacgggttcagt	ggtcggttcatgccatgaat
TIMP1	NM_001003182.1	cagggcctgtacctgtgc	cctgatgacgatttgggagt
TIMP2	NM_001003082.1	atgagatcaagcagataaagatgttc	ggaggaaggagccgtgtag
VEGF	AF133250.1	cgtgcccactgaggagtt	gccttgatgaggtttgatcc
VEGFR2	DQ269018.1	ccttaccaaccccatttcaa	cagggatttctcaccgatct
βCAT	NC_006605.3	cagcagcagtttgtggaggg	tgaacatcccgagctaggatatg

Table 8. Antibodies details

Antigen		Clone	Code	Dilution	Manufacturer
CLUSTERIN	mouse monoclonal	-	-	1:50	Novocastra
CTGF	rabbit polyclonal	H-55	sc-25440	1:50	Santa Cruz Biotechnology
EGFR	mouse monoclonal	111.6	AB-10	1:100	Neomarkers, Fremont,CA, USA
MMP2	rabbit polyclonal	AB-7	-	1:100	Neomarkers, Fremont,CA, USA
MMP9	mouse monoclonal	56-2A4	MAB 3309	1:200	Chemicon (Millipore)
TGFβ	rabbit polyclonal	H-112	sc-7892	1:50	Santa Cruz Biotechnology
TIMP1	mouse monoclonal	VT7	M7293	1:50	Dako

RESULTS

Dogs and samples

The study included 10 affected males and 5 controls. Among affected dogs, two subjects (2 and 5) reached their study end-point at 6 months of age; four dogs (7-10) at 7-9 months of age; and the remaining 4 dogs (1, 3, 4 and 6) greater than 10 months of age.

Morphological and clinicopathologic findings

Control dogs were characterized by absence of noteworthy renal lesions and clinico-pathological alterations throughout the course of the study.

Morphological changes were not observed in XLHN dogs at T0. Glomeruli focally displayed minimal segmental hypercellularity in association with small areas of mesangial matrix expansion classified as mild focal and segmental glomerulosclerosis. All XLHN dogs were proteinuric at T0 (UPC ratio, 1.84-18.66; urine albumin, 9.8-290 mg/dlL, despite the presence of negligible light microscopic morphological changes. Both UPC ratio and albuminuria were positively correlated with mesangial matrix expansion ($r=0.73$ and $r=0.76$, respectively; $P<0.01$).

At T1, a variable number of non-functional glomeruli (obsolescent and cystic atrophic glomeruli) were present (0-80%; mean, 40.1%) with equal distribution of obsolescent and cystic atrophic glomeruli (mean, 21% and 19.2%, respectively). The matrix expansion and mesangial hypercellularity were present in most glomeruli with a segmental to global distribution and occasional obliteration of capillaries. Additionally, the tubulointerstitium showed multifocal lesions mainly consisting of degeneration and occasional necrosis of TECs and mild interstitial fibrosis. The latter frequently consisted of small multifocal areas associated with non-functional glomeruli, often associated with atrophy of adjacent tubules.

Along with the increased severity of morphological changes, the impairment of renal function as manifested by increased albuminuria, UPC and decreased serum albumin concentration was more prominent at T1 in affected dogs compared with controls and with XLHN dogs at T0 ($P<0.05$). A not significant increase was also noted in the concentration of SCr in affected dogs. In addition, albuminuria and SCr concentration were both positively correlated with the percentage of non-functional, obsolescent and cystic glomeruli as well as with tubular atrophy and dilation, necrosis and interstitial fibrosis ($0.64<r<0.92$; $P<0.05$).

Glomerular and TI lesions were overall more severe at T2 compared with T1. The percentage of non-functional glomeruli ranged from 67.1-100% (mean, 85.2%) with a greater prevalence of cystic atrophic glomeruli (mean, 48%), and lesser proportion of obsolescent glomeruli (mean, 36.5%) (Fig. 14). Residual glomeruli had severe global expansion of mesangium and moderate to severe mesangial hypercellularity. Large bands of fibrotic tissue replaced the renal parenchyma and compressed the tubules that were either atrophic or ectatic. Compared with T1 samples, the inflammatory infiltrate (mostly lymphocytes, plasma cells and macrophages) was more severe at T2.

Serum creatinine concentration and magnitude of proteinuria (UPC and albuminuria) were significantly greater at T2 (mean 3.58 mg/dl; 15.63 and 272.38 mg/dl respectively, $P<0.01$) in affected dogs compared with T1 and were positively correlated with the percentage of non-functional, obsolescent and cystic glomeruli as well as with tubular atrophy and dilation, necrosis, fibrosis and the number of inflammatory cells ($0.62<r<0.96$; $P<0.05$).

Significant morphological and clinicopathologic findings in XLHN dogs compared with age-matched controls are shown in Figures 15 and 16. The percentage of obsolescent and cystic atrophic glomeruli was positively correlated with each other at each time-point ($0.60<r<0.97$; $P<0.05$).

Considering both morphological and clinicopathologic results, a CDA was performed to identify the parameters that were most strongly associated with presence of renal disease at each time-point. Proteinuria was strongly associated with renal disease at each time-point and was the only parameter discriminating between affected dogs and controls at T0. At T1, two morphological parameters (number of non-functional glomeruli and presence of fibrosis) were most strongly associated with renal disease. At T2 cystic glomerular atrophy, and tubular atrophy were the two morphological parameters most strongly associated with renal disease ($P<0.01$).

Gene expression

RNA extracted from frozen tissue that was stored at -80°C but not conserved in RNA-later was severely degraded, and the samples were excluded from the study. Therefore, gene expression analysis was performed in 21 samples from affected dogs (7 dogs at T0; 8 at T1 and 6 at T2) and in all controls.

The gene expression analysis dataset was analyzed by HCL and PCA as a preliminary analysis to determine whether control and pathologic samples could be differentiated based on gene expression. Using gene expression data from all time points, both the HCL tree and PCA differentiated XHLN from control dogs (Fig. 17). Even when using gene expression data from only the earliest time point (T0, 4 months of age), both the HCL tree and PCA differentiated XHLN from controls dogs (Fig. 18). The first three components of the PCA analysis accounted for a substantial fraction of the total variance in both instances (85.91% and 82%, respectively). Using data from all time points, three cases were located borderline between the two groups in PCA. Of these, one was a control dog that clustered with affected dogs and two were affected dogs that clustered with controls in the HCL tree.

Among 21 candidate genes, mRNA levels of 8 genes were significantly higher in XLHN dogs compared with controls: TGFβ, CTGF, PDGFD, N-CADHERIN, CLUST, MMP2, MMP9 and TIMP1 ($P<0.05$). In contrast, EGFR expression was higher in controls compared with XLHN dogs ($P<0.01$). Subsequently, genes were analyzed individually according to the different time points: TGFβ, CTGF and PDGFRα were significantly overexpressed in T0 affected dogs compared with controls. TGFβ, TIMP1 and CLUST were significantly overexpressed in affected dogs at T1 and CLUST in T2 affected dogs compared. Figure 19 shows the trends of genes differentially expressed in XLHN dogs compared to controls. Significant correlations among genes at different time-points are shown in Table 9.

Gene expression data, morphological, and clinicopathologic findings showing differences in XLHN dogs compared with controls were analyzed together in order to associate the expression of gene(s) with renal lesions and function at the different time-points. Relevant correlations between gene expression and morphological and clinicopathologic findings are provided in Table 10.

Protein expression

The protein expression of selected molecules was investigated by immunohistochemistry in controls and XLHN dogs. TGFβ and CTGF immunostaining was detected diffusely in the cytoplasm of podocytes at all time-points (Fig. 20a and 20b), with no differences between controls and affected dogs. However, in cystic and obsolescent glomeruli, positive-staining podocytes were rarely seen lining the glomerular tuft but were commonly seen sloughed in the urinary space. In the tubular compartment, TGFβ and CTGF

were multifocally detected in the cytoplasm of TECs both in affected and control kidneys at all time-points.

Protein expression was similar for CLUST and TIMP1. The two molecules were absent in normal dogs at all time-points and at T0 in XLHN dogs. However, at T1 and T2 affected dog kidneys were characterized by diffuse mild positive cytoplasmic staining in TECs (Fig 20c and 20d).

MMP9 was diffusely detected in the cytoplasm of podocytes, parietal epithelium and TECs both in controls and in XLHN dogs. However, in XLHN dogs at T1 and T2, the atrophic tubules often showed less intense staining, and infiltrating plasma cells were strongly and diffusely positive. MMP2 was not detected in controls or XLHN dogs at T0. In contrast, occasional tubules in XLHN dogs showed positive MMP2 immunostaining at T1 and T2 in association with the thickening and splitting of the tubular basement membrane.

EGFR was detected only in affected kidneys at T2. The protein was evident in podocytes, parietal epithelium and TECs both in controls and in affected dogs. The immunostaining was detected on the cellular membrane of the glomerular epithelium and at the basolateral surface of TECs.

Figure 14. Renal lesions in 9 months old XLHN dogs

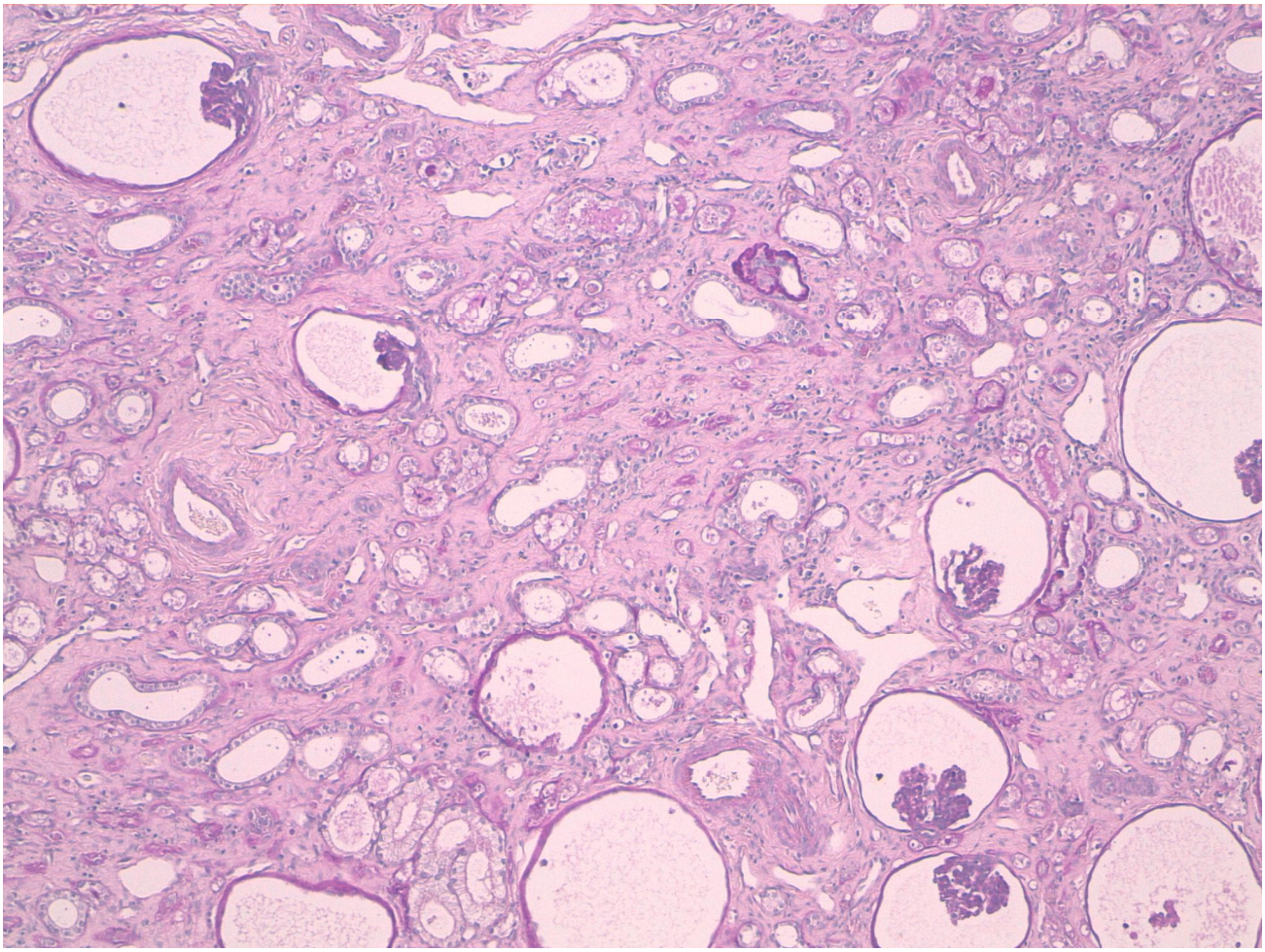

Severe histological lesions are evident both the glomerular and tubulointerstitial compartments. Most glomeruli are cystic and atrophic or obsolescent. The interstitium is severely expanded by fibrosis and marked lymphoplasmacytic infiltrate associated with multifocal atrophic tubules. PAS 200x

Figure 15. Relevant morphological and clinical parameters

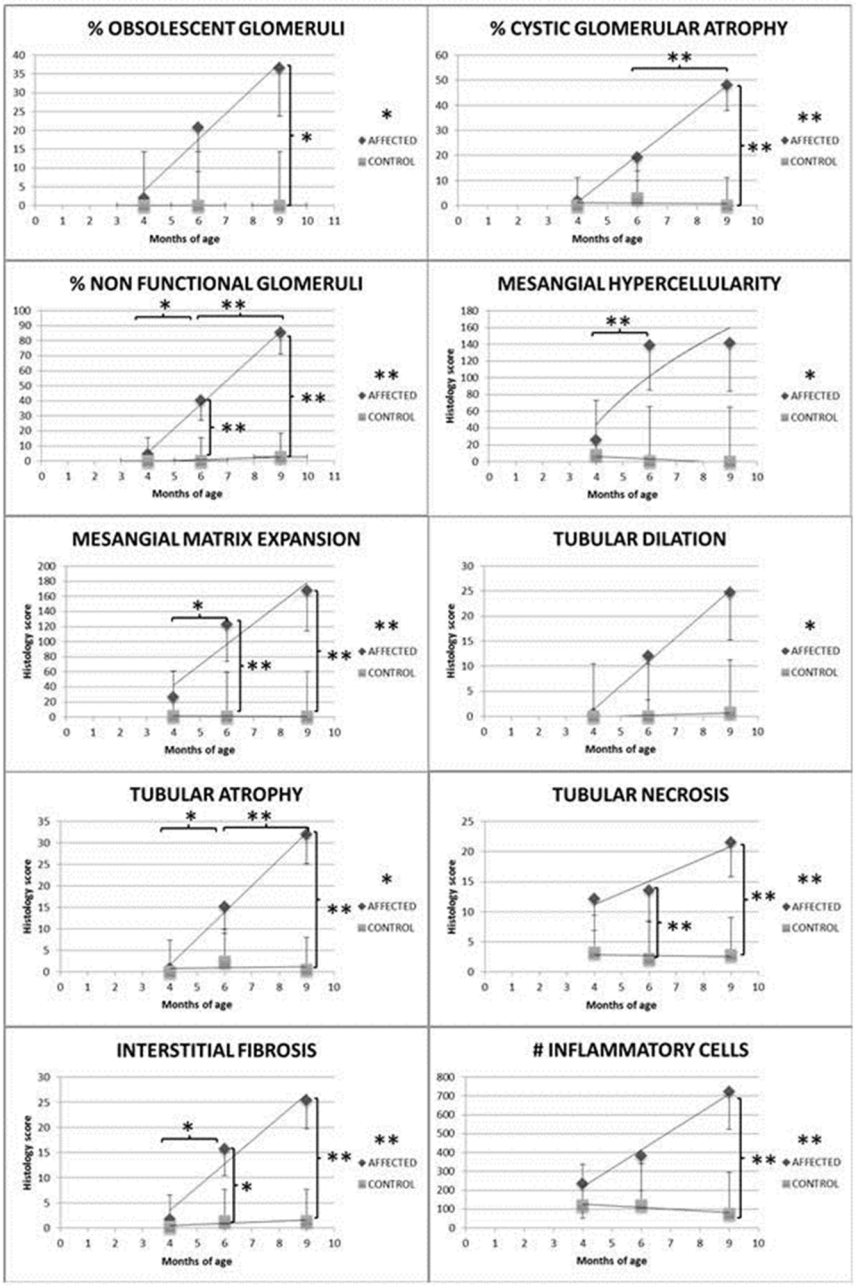

Affected dogs (dark grey), controls (light grey). Bonferroni adjusted. *: $P < 0.05$; **: $P < 0.01$

Figure 16. Relevant morphological and clinical parameters

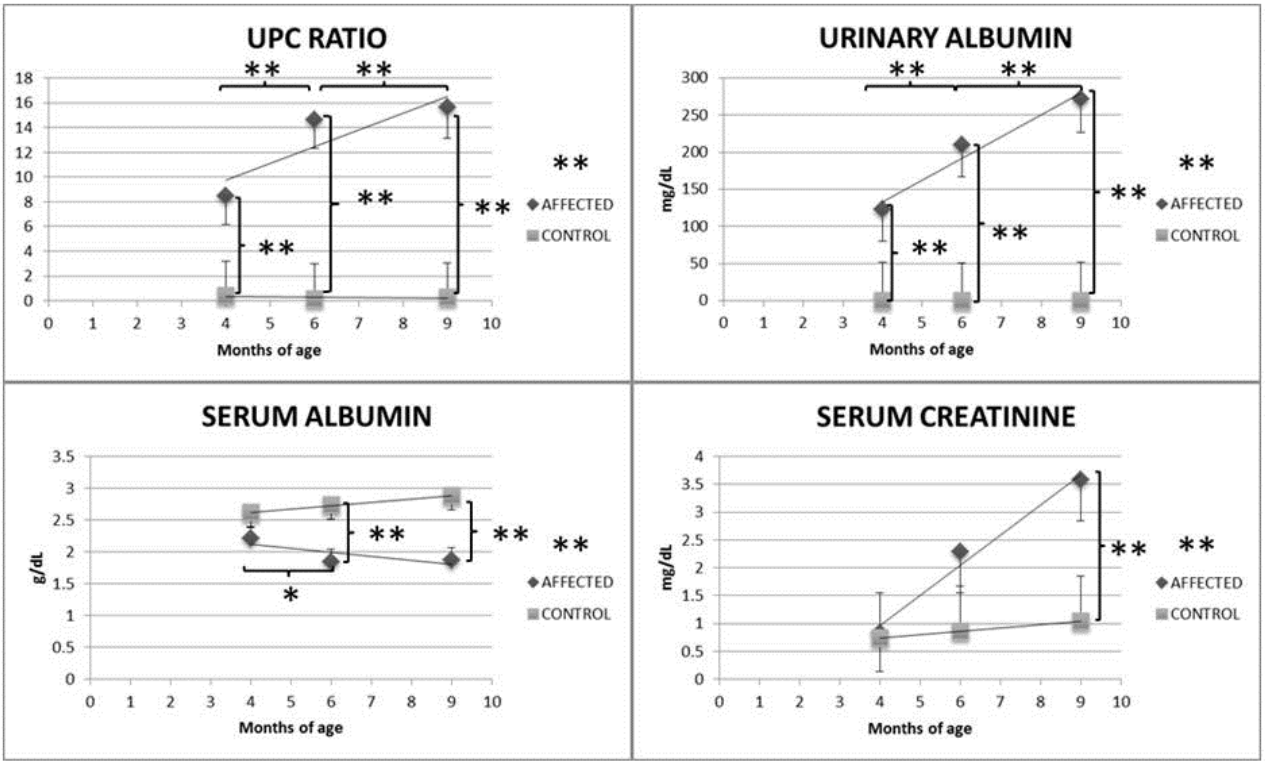

Affected dogs (dark grey), controls (light grey). Bonferroni adjusted. *: $P < 0.05$; **: $P < 0.01$

Figure 17. Hierarchical Clustering (HCL) and (B) Principal Component Analysis (PCA)

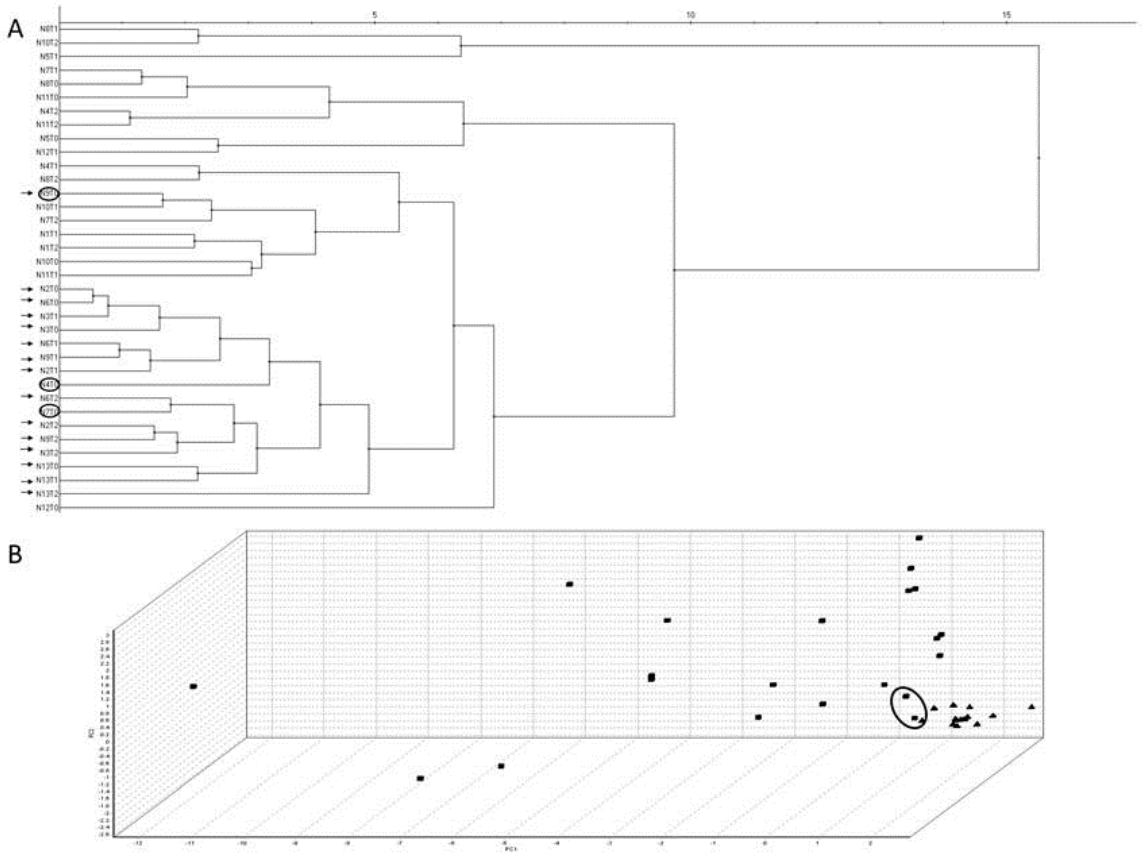

(A) HCLand (B) PCA were performed using all gene expression data with MultiD-Genex software for qPCR data, using the following settings: mean center scaling, complete linkage and Euclidean. Both HCL tree and PCA identified, two main groups, attributable to XHLN (indicated by ▲ in PCA) and controls (indicated by arrows in HCL and by ■ in PCA) dogs. Three cases were located borderline between the groups in PCA (black circle). These three were all T0 samples one from a control and two from affected dogs.

Figure 18 Hierarchical Clustering (HCL) and (B) Principal Component Analysis (PCA) only of T0 samples

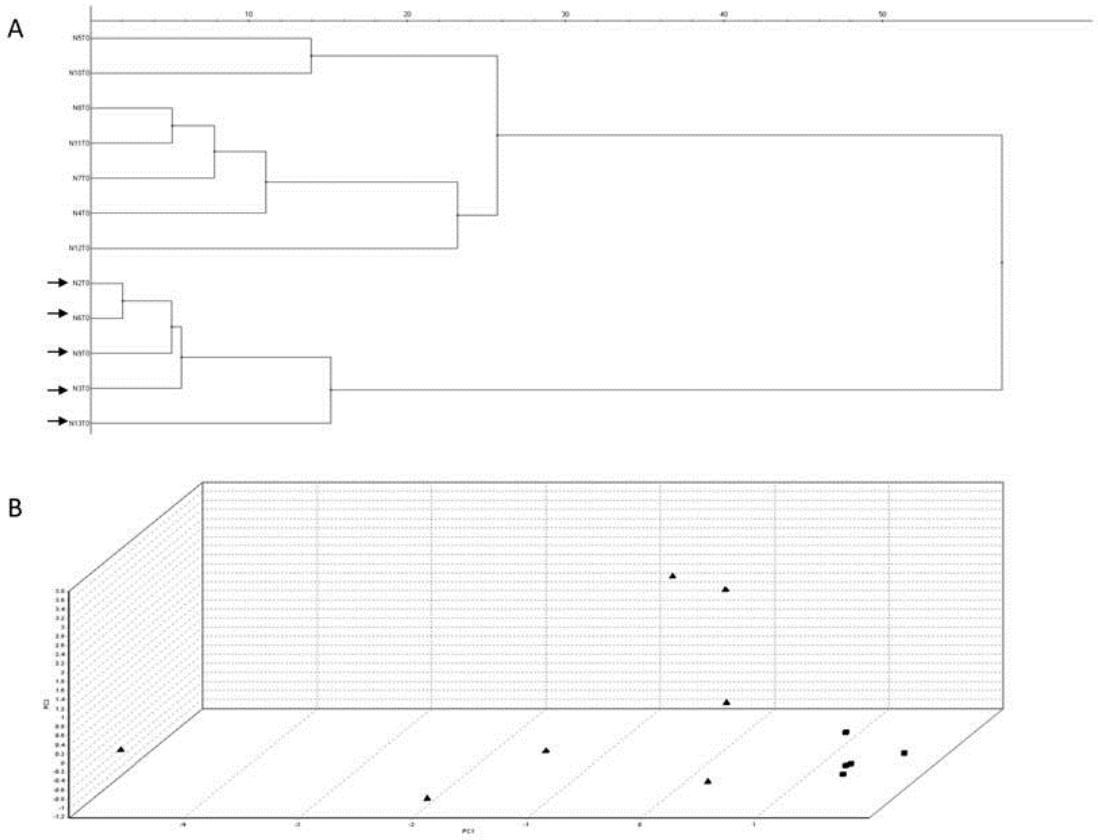

(A) HCL and (B) PCA were performed using gene expression data from T0 samples with MultiD-Genex software for qPCR data, using the following settings: mean center scaling, Ward's algorithm, Manhattan distance. Both HCL tree and PCA separate two main groups identifying XHLN (indicated by ▲ in PCA) and controls (indicated by arrows in HCL and by ■ in PCA) dogs.

Figure 19. Gene expression analysis

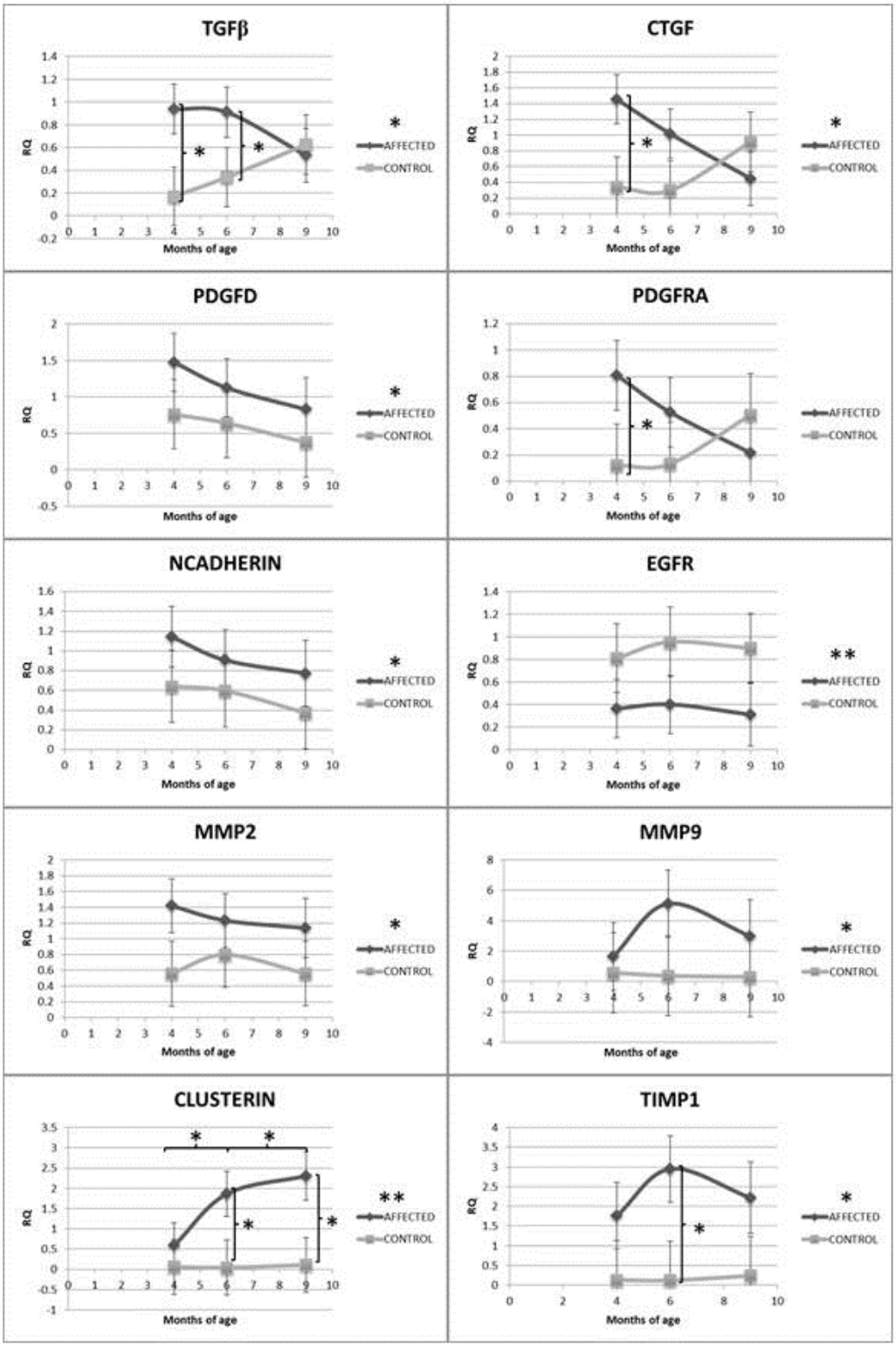

Affected dogs (dark grey), controls (light grey). RQ: Relative Quantification Bonferroni adjusted. *: P < 0.05; **: P < 0.01

Figure 20. Immunohistochemistry for Transforming Growth Factor beta (TGFβ), Connective Tissue Growth Factor (CTGF), Clusterin (CLUST) and Tissue Inhibitor of Matrix Metalloproteinases-1 (TIMP-1) in renal tissue from XLHN affected dogs.

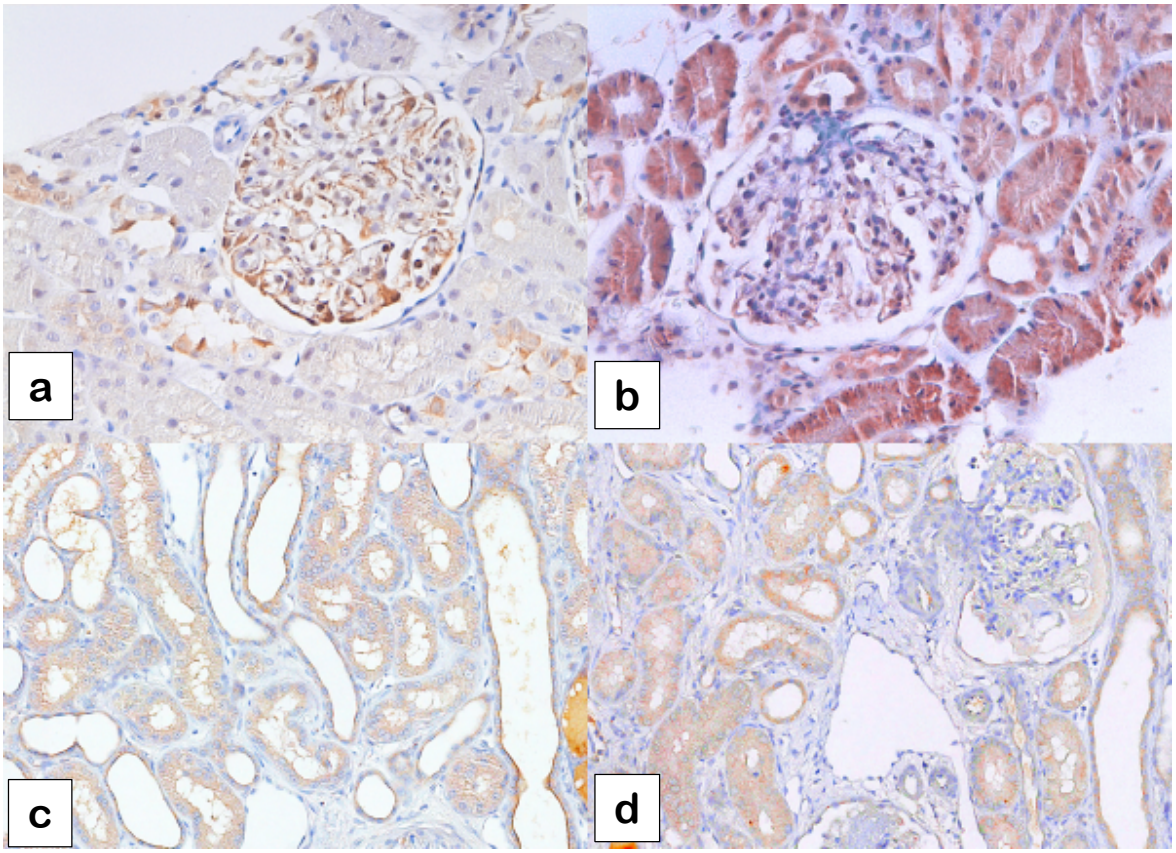

Representative micrographs are presented. (a) TGFβ positive immunolabelling is diffusely present in the cytoplasm of podocytes and multifocally in the cytoplasm of tubular epithelial cells. Immunohistochemical staining for TGFβ, haematoxylin counterstain (400x); (b) CTGF positive immunolabelling is diffusely present in the cytoplasm of podocytes and of tubular epithelial cells. Immunohistochemical staining for CTGF, haematoxylin counterstain (400x); (c) CLUST and (d) TIMP1 positive immunolabelling is diffusely evident within the cytoplasm of tubular epithelial cells only in T2 (9 months of age) samples. Immunohistochemical staining for CLUST and TIMP1, haematoxylin counterstain (400x)

Table 9. Significant correlation (P <0.05) among genes according to time-points.

GENE	T0	T1	T2
TGFβ- CTGF	r = 0.78	-	r = 0.78
TGFβ - PDGFD	r = 0.77	r = 0.61	-
TGFβ - PDGFRα	r = 0.80	r = 0.82	-
TGFβ - MMP2	r = 0.74	-	-
TGFβ - TIMP1	r = 0.77	r = 0.75	-
CTGF -PDGFRα	r = 0.76	r = 0.66	r = 0.63
CTGF - TIMP1	r = 0.64	r = 0.61	-
PDGFD - PDGFRα	r = 0.74	-	-
PDGFD - MMP2	r = 0.86	-	-
PDGFD - TIMP1	r = 0.65	r = 0.78	-
MMP2 - PDGFRα	r = 0.67	-	-
MMP2 - TIMP1	r = 0.81	r = 0.62	r = 0.76
TIMP1 - CLUST	r = 0.66	r = 0.80	r = 0.97
TIMP1 - MMP14	r = 0.59	r = 0.89	-
CLUST - TGFβ	-	r = 0.69	-
CLUST - CTGF	-	r = 0.65	-
CLUST - PDGFRα	-	r = 0.64	-
CLUST - MMP9	-	r = 0.70	-
CLUST - MMP2	-	-	r = 0.79
CLUST - NCAD	r = 0.73	-	r = 0.76
EGFR- TGFβ	r = - 0.78	-	r = 0.79
EGFR- CTGF	r = - 0.60	r = - 0.69	r = 0.81
EGFR - TIMP1	r = -0.75	r = - 0.63	-
EGFR - PDGFRα	-	-	r = 0.84

T0= 4 months of age; T1= 6 months of age; T2 = 9 months of age

Table 10a. Significant correlations (P < 0.05) among genes, morphological and clinical-pathological findings at T0 (4 months of age)

GENE	T0	
	Parameter	r (range)
CLUST	MESANGIAL HYPERCELLULARITY MESANGIAL MATRIX EXPANSION CAPILLARY THICKENING TUBULAR ATROPHY TUBULAR NECROSIS INFLAMMATORY CELLS COUNT UPC RATIO URINARY ALBUMIN	0.65 < r < 0. 88
TIMP 1	MESANGIAL HYPERCELLULARITY MESANGIAL MATRIX EXPANSION TUBULAR DILATION TUBULAR ATROPHY INTERSTITIAL FIBROSIS UPC RATIO URINARY ALBUMIN	0.58 < r < 0.74
NCAD	MESANGIAL HYPERCELLULARITY MESANGIAL MATRIX EXPANSION TUBULAR NECROSIS UPC RATIO URINARY ALBUMIN	0.72 < r < 0.84
TGFB CTGF	UPC RATIO URINARY ALBUMIN	0.65 < r < 0.77

Table 10b. Significant correlations (P < 0.05) among genes, morphological and clinical-pathological findings at T1 (6 months of age)

GENE	T1	
	Parameter	r (range)
CLUST	MESANGIAL HYPERCELLULARITY MESANGIAL MATRIX EXPANSION TUBULAR NECROSIS INTERSTITIAL NECROSIS UPC RATIO URINARY ALBUMIN SERUM CREATININE	0.60 < r < 0.76
TIMP 1	% CYSTIC GLOMERULAR ATROPHY % NON FUNCTIONAL GLOMERULI TUBULAR DILATION TUBULAR ATROPHY TUBULAR NECROSIS INTERSTITIAL FIBROSIS UPC RATIO URINARY ALBUMIN	0.58 < r < 0.80
TGFβ	% NON FUNCTIONAL GLOMERULI UPC RATIO URINARY ALBUMIN INTERSTITIAL FIBROSIS	0.58 < r < 0.70
MMP2	TUBULAR DILATION	r = 0.79
EGFR	% OBSOLESCENT GLOMERULI TUBULAR NECROSIS INTERSTITIAL FIBROSIS UPC RATIO URINARY ALBUMIN SERUM CREATININE	- 0.69 < r < - 0.62

Table 10c. Significant correlations (P < 0.05) among genes, morphological and clinical-pathological findings at T2 (9 months of age)

GENE	T2	
	Parameter	r (range)
CLUST	% OBSOLESCENT GLOMERULI % CYSTIC GLOMERULAR ATROPHY % NON FUNCTIONAL GLOMERULI MESANGIAL HYPERCELLULARITY MESANGIAL MATRIX EXPANSION CAPILLARY THICKENING TUBULAR DILATION TUBULAR ATROPHY TUBULAR NECROSIS INTERSTITIAL FIBROSIS INFLAMMATORY CELLS COUNT UPC RATIO URINARY ALBUMIN SERUM CREATININE	$0.65 < r < 0.85$
TIMP 1	% OBSOLESCENT GLOMERULI % CYSTIC GLOMERULAR ATROPHY % NON FUNCTIONAL GLOMERULI MESANGIAL HYPERCELLULARITY CAPILLARY THICKENING TUBULAR DILATION TUBULAR ATROPHY TUBULAR NECROSIS INTERSTITIAL FIBROSIS INFLAMMATORY CELLS COUNT UPC RATIO URINARY ALBUMIN SERUM CREATININE	$0.67 < r < 0.79$
NCAD	% OBSOLESCENT GLOMERULI % NON FUNCTIONAL GLOMERULI TUBULAR DILATION TUBULAR ATROPHY INTERSTITIAL FIBROSIS INFLAMMATORY CELLS COUNT SERUM CREATINE	$0.61 < r < 0.76$

GENE	T2	
	Parameter	**r (range)**
MMP2	% OBSOLESCENT GLOMERULI % NON FUNCTIONAL GLOMERULI MESANGIAL HYPERCELLULARITY MESANGIAL MATRIX EXPANSION CAPILLARY THICKENING TUBULAR DILATION TUBULAR ATROPHY INTERSTITIAL FIBROSIS INFLAMMATORY CELLS COUNT UPC RATIO URINARY ALBUMIN SERUM CREATINE	$0.64 < r < 0.89$
CTGF	% NON FUNCTIONAL GLOMERULI % CISTIC GLOMERULAR ATROPHY TUBULAR DILATION TUBULAR NECROSIS INTERSTITIAL FIBROSIS INFLAMMATORY CELLS COUNT UPC RATIO	$-0.76 < r < -0.66$
EGFR	% CYSTIC GLOMERULAR ATROPHY TUBULAR DILATION TUBULAR NECROSIS INTERSTITIAL FIBROSIS UPC RATIO	$-0.80 < r < -0.61$

DISCUSSION

Naturally occurring inherited type IV collagen defects that cause progressive renal injury leading to ESRD have been described in humans and several canine families (Lees, 2013). The Navasota dogs used in this study belong to a mixed-breed family of dogs with XLHN, a good model in which to study the progression of CKD in dogs (Lees 1999). In the present study, the availability of serial samples obtained in the early stages of the disease permitted the visualization of the sequence of events occurring in progressive hereditary nephropathy.

Based on our findings proteinuria is the earliest detectable change in XLHN and it is the only parameter discriminating affected dogs from controls at 4 months of age. In contrast, compare with proteinuria, the development of evident histological lesions seems to be delayed. XLHN dogs develop during their lifetime a mesangioproliferative glomerulopathy characterized by progressive loss of glomeruli, mostly undergoing cystic glomerular atrophy. The primary and persistent glomerular injury is associated with a secondary and progressive tubular loss, interstitial fibrosis and inflammation. With respect to the clinicopathologic data, the UPC as well as the urinary albumin and SCr concentrations increased in parallel with severity of tissue injury, confirming their utility in monitoring changes in renal structure and function in this disease.

Cystic glomerular atrophy is frequently observed in canine juvenile nephropathies (Lavuè et al., 2010; Wakamatsu et al., 2007; Chandler et al., 2007; Hood et al. 2002) and emerged as a peculiar feature of XLHN in this study. The cystic dilation of glomeruli is the consequence of tubular obstruction followed by increased intratubular and intraglomerular pressure, and progressive compression of the glomerular tuft. However which factor is primarily responsible for the tubular obstruction in XLHN is not presently understood. The interstitial fibrosis surely represents a potential main actor contributing to this phenomenon, but the cystic glomerular atrophy is not seen exclusively in association with renal fibrosis. Recent studies have demonstrated that many renal disorders are characterized by the formation of atubular glomeruli (Gallareta et al., 2013; Forbes et al., 2011). According to these studies, the formation of atubular glomeruli would be a consequence of damage occurring at the glomerulo-tubular junction and might represent an essential step in the progression of pediatric nephropathies (Chevalier et al, 2014; Gallareta et al., 2013; Forbes et al., 2011). It

was beyond the purposes of this study to examine the possible role of atubular glomeruli in canine XHLN, but the large number of cystic and atrophic glomeruli could indicate the presence of atubular glomeruli and thus identify a potential key feature in the pathogenesis of hereditary nephropathies in general that should be further investigated.

The expression of a number of molecules potentially involved in the pathogenesis and progression of XLHN was investigated in this study. The entire dataset obtained by gene expression analysis was used for preliminary HCL and PCA procedures that identified two separate well-defined groups: controls and affected dogs.

In three instances, both involving biopsies obtained at T0, the PCA procedure resulted in incorrect grouping, albeit adjacent to the borderline between the two groups in both instances. One control dog clustered with affected dogs, and two affected dogs clustered with controls. In an attempt to explain the “incorrect clustering” of the two samples, we reviewed the histopathology of the two cases: the first one, although from a control animal, was characterized by mild multifocal tubulointerstitial changes including epithelial cells degeneration, fibrosis and inflammatory cell infiltration. In the other two cases tubulointerstitial lesions were absent resembling normal renal tissue. Moreover, those same dogs subsequently exhibited relatively slow progression of their renal disease reaching the study endpoint at 10 months of age.

Progression of renal disease in NAV dogs is variable, with the standardized study end-point occurring between 6 and 15 months of age. It would be of great interest to identify factors predisposing to or predicting faster progression of XLHN. The number of dogs examined in the present study was too small to statistically explore an association between the mRNA expression profile and progression rate of XLHN; however no difference was observed upon cursory examination of the gene expression data related to dog survival. Interestingly by the examination only of sample at T0 by PCA and HCL, controls and affected dogs were separated into two well-defined groups. This observation illustrates and emphasizes that, well before renal lesions become evident by light microscopy.

In the gene expression analysis, an unexpected observation was the variable expression in control dogs of some genes that were initially expected to be constant over time. However post-natal renal maturation must be considered, especially in as much as many of the studied molecules (i.e. TGFβ, CTGF, EGFR) are reported to be involved in renal

development in several animal species (Ito et al.,2010; Hammerman, 1995; Hyink and Abrahamson, 1995; Goodyer et al., 1993).

In the present study, increased expression of TGFβ and CTGF was detected by 4 months of age in dogs affected with XLHN and preceded evident light microscopic damage. TGFβ and CTGF protein expression was detected in podocytes and parietal epithelium of their kidney as well as in TECs. Recently podocytes have been reported as the first cellular elements that detect altered ultrafiltration and react with conformational changes and produce pro-inflammatory factors with autocrine and paracrine effects (Fuchshofer et al., 2011). A previous study in a mouse model of Alport syndrome, have described an increased expression of TGFβ in podocytes of affected kidneys (Sayers et al., 1999). In their study Sayers and colleagues hypothesized an effect of TGFβ in the development of glomerular changes by stimulating mesangial cell proliferation and matrix deposition. In the present study the overexpression of TGFβ possibly by podocytes and the presence of proliferation of mesangial cells and matrix expansion occurring in initial stages of XLHN, gives support to this hypothesis. Both TGFβ and CTGF are known as pro-fibrotic factors and, surprisingly the present study showed a decrease of their expression in parallel with increasing fibrosis, although the lack of significant overexpression of TGFβ in late stages of XHLN is consistent with previous data of Greer et al. (2006). In late stages of XLHN the marked loss of glomeruli and prominent tubular atrophy are responsible for an overall reduction in the number of viable cells (ie, glomerular visceral and parietal epithelial cells and TECs present in the kidney). This great reduction in the number of viable cells might explain the reduction in TGFβ and CTGF expression observed in this study.

MMP2 and MMP9 expression was increased in XLHN dogs compared with controls, in this study. This finding is consistent with previous studies that explored the possible role of MMP2 and MMP9 in dogs with XLHN and in chronic TID (Rao et al. 2003; Aresu et al., 2011). The activity of MMPs and their inhibitors is essential in the remodeling and turnover of the extracellular matrix and an imbalance in MMPs and TIMPs expression was demonstrated in several fibrotic diseases (Cheng and Lovett, 2003; Guo and Friedman, 2007). MMP2 especially was reported to be involved in renal injury at both the glomerular and the tubulointerstitial level: in glomeruli it represents a pro-inflammatory factor produced by mesangial cells in response to injury; in the tubulointerstitium its increased activity is associated with a progression of renal fibrosis (Martin et al., 2001; Rao et al., 2003; Aresu et

al., 2011). Furthermore several lines of evidence support a role for MMP2 in promoting the process of EMT of TECs (Cheng et al., 2004; Cheng et al., 2006; Aresu et al., 2011). In the present study the identification of a positive correlation between MMP2 gene expression and the degree of fibrosis in T2 samples is consistent with a pro-fibrotic role of the enzyme. MMP9 expression showed a peculiar trend in XLHN: it was increased at 6 months of age but showed a decreased at 9 months. At the protein level MMP9 was diffusely expressed by tubular and glomerular epithelial cells in both control and affected dogs. A similar trend for MMP9 expression has been described in a study on nephrectomized mice reporting an initial increase of MMP9 followed by moderate decreased (Johnson et al., 2002). The peak of MMP-9 expression in 6-months samples can be attributed to the expression of the enzyme also by the inflammatory cell population (e.g. plasmacells). The reduction in 9 months samples could reflect the reduction of the number of viable cells as previously hypothesized for CTGF and TGFβ.

An up-regulation of TIMP1 was observed in the present work in XLHN dogs and its expression was positively correlated with the progression of glomerular and tubulointerstitial changes. A pro-fibrotic activity has been proposed in the progression of renal fibrosis, since inhibitory activity on MMPs, would lead to the accumulation of ECM (Ahmed et al., 2007). In this study the positive correlation of TIMP1 expression at all time-points with the degree of fibrosis ($0.66<r<0.74$) and with MMP2 expression ($0.62<r<0.81$), is consistent with a pro-fibrotic role of this enzyme in the progression of chronic TID. Similarly, studies in humans and dogs liver chronic disease, associated TIMP1 overexpression with strong exacerbation of fibrosis (Wang et al. 2013; Kanemoto et al 2011). According to the study of Wang and colleagues the pro-fibrotic activity of TIMP-1 is not limited to MMPs inhibition but TIMP1 would promote extracellular matrix accumulation through an anti-apoptotic activity on hepatic stellate cells (Wang et al 2013). Translating that information into renal pathology, the mechanisms through which TIMP1 could enhance the fibrosis might include (i) inhibition of MMPs activity; and (ii) reduction of the apoptosis of interstitial (myo)fibroblasts.

In the present study, clusterin expression was higher in canine XLHN compared with controls in agreement with the results reported by Greer and colleagues (2006). The increased expression of clusterin in affected dogs was progressive (Fig. 6) and positively correlated with the worsening of renal damage. Clusterin is a glycoprotein constitutively expressed in almost all mammalian organs and capable of interacting with a wide range of

molecules (Jones and Jamari, 2002). Increased expression of clusterin was found in several renal disease models, suggesting that it might have an important role in the pathogenesis of renal injury. For this reason, several studies investigated and proposed clusterin as potential biomarker of renal injury (García-Martínez et al., 2012; Fuchs and Hewitt, 2011). The role of clusterin in the development and progression of renal fibrosis is still unclear. Some author's hypothesized a nephroprotective activity of clusterin since its absence is associated with a faster progression of chronic TID (Jung et al. 2012). According to Jung and colleagues, clusterin would attenuate the development of fibrosis through the inhibition of TGFβ signalling.

Among the examined PDGF and PDGFR isoforms, PDGFD and PDGFRα were found significantly overexpressed in renal tissue of XLHN dogs compared with controls. To the best of the authors' knowledge, there are no reports examining PDGFs and PDGFRs expression in canine renal diseases, but in human medicine their role in renal fibrosis have been recently reviewed by Ostendorf and colleagues (2011). In the glomeruli, PDGFB and PDGFD autocrine and paracrine effects, through PDGFRβ activation lead to mesangial cell proliferation and the development of glomerulosclerosis. In the present study, PDGFD was found overexpressed in XHLN compared with controls dogs. This possibly reflects its action on mesangial cells inducing cell proliferation and mesangium expansion (van Roeyen et al., 2005). On the other hand, no difference emerged in comparisons of PDGF expression in the two groups at the different time-points. This could be a consequence of the high variability in PDGFD expression among the subjects. Higher PDGFRα expression was detected in XLHN dogs compared with controls only at 4 months at age and a subsequent decrease gene expression was associated with time-progression. Furthermore, the positive correlation between PDGFRα and the pro-fibrotic CTGF ($0.63<r<0.76$), suggests cross-talk between the two molecules in the progression of interstitial fibrosis. Based on these findings we can speculate that the PDGFRα expression and activation have a prominent role in the very beginning of the fibrotic process recruiting fibrocytes as seen in pulmonary and hepatic fibrosis (Aono et al., 2014; Hayes et al., 2014), but more data are needed to explain the role of this receptor in renal fibrosis.

XLHN dogs showed reduced EGFR expression compared with controls. EGFR is a tyrosine kinase receptor located on the basolateral surface of epithelial cells and is an important mediator of cell proliferation in renal tissue. EGFR is particularly involved in proliferation of the TECs occurring in post-natal renal development and maturation (Stuart et

al., 2001) giving reason for the high expression detected in normal dogs. On the contrary in renal injury, the role of EGFR is controversial and two apparently discordant actions have been described: in acute injury it is associated with faster recovery; whereas in chronic lesions EGFR appears to promote renal disease progression (Tang et al., 2013). The reason for this dual role of the molecule might be due to different consequences of its proliferative activity in different renal structures: in tubules the epithelial cell proliferation might help the recovery from degenerative changes, whereas in the glomeruli its proliferative activity on mesangial cells and podocytes might promote progression of glomerular dysfunction and indirectly promote chronic renal injury. Taking into consideration the different possible consequences on renal tissue of EGFR activation it would be necessary to determine the expression and activity of this molecule in the different renal cell types to better understand the action of this receptor in XLHN.

Summarizing we characterized morphological and clinicopathologic changes occurring in XLHN of NAV dogs.

A number of molecules (TGFβ, CTGF and PDGFRα) were identified as potential key players in initial events of XLHN. Clusterin and TIMP1, in contrast, appear more involved in the progression of the chronic TID. Further studies are needed to explore if these results are attributable to the specific hereditary disease here studied or can be regarded as common events occurring in the progression of TID secondary to a primary glomerular disease.

A limitation in this study is that gene expression was performed on homogenized cortical renal tissue and thus including several cell types. The immunohistochemical staining was helpful in identifying the cells expressing the different genes but further investigations are needed to better clarify the role of these molecules in the pathogenesis of XLHN.

On the other hand the opportunity to study an established and reproducible animal model offers certain important advantages. One of these is the availability of samples from the early stages of the disease that are not possible to collect in routine diagnostic settings because patients with renal disease are biopsied only when they develop evident disease. Furthermore, the examination of serial samples permits analysis of the evolution of the renal disease over time.

CONCLUSIONS

In summary, this project examined different aspects of the progression of TID in various canine renal diseases.

The first study confirmed that the primary glomerular diseases are associated with a secondary involvement of the tubulointerstitium. The progression of TID appears to be independent of the persistence of the causative agent if the tubulointerstitial involvement is already present and severe. On the other hand, the elimination of the causative agent (i.e. the use of leishmanicidal drug) seems to be associated with an improvement of the renal function and damage if the tubulointerstitium is mild or not affected.

The second part of the study explored the role of TECs in the progression of TID. TECs appear to be capable of acting as non-professional antigen presenting cells in canine renal tissue and actively interacting with inflammatory cells. The study offered further evidences that proteinuria is co-responsible for the activation of this function. Moreover, the phase in which the TECs act as APCs precedes and partially overlaps with the phenomenon of EMT of TECs possible representing a specific phase in this transition. The active role of TECs in the progression of TID is further supported by the expression of several growth factors and others molecules in progressive renal failure as shown in the third part of the project.

The last part of the study describes the evolution of the renal damage and progressive impairment of renal function in a naturally occurring model of hereditary nephropathy. Moreover, some molecules (TGFβ, CTGF and PDGFRα) were identified as potential key players in initial events of renal damage whether others (Clusterin and TIMP1) seemed more involved in the progression of the chronic TID.

The obtained results significantly improved the understanding of the progression of chronic TID in canine renal diseases pointing out the importance of proteinuria and other molecular changes that precede the morphological changes. More data are needed to further understand the mechanisms responsible for the initiation ad promotion of the secondary TID, the role of TECs and other major cellular players as well as important molecules and factors involved. The ultimate goal is the identification of early and specific markers of renal damage,

improving the time of the diagnosis. Also, this new research will define new targets for therapy and approaches for the management of dog with renal diseases.

REFERENCES

Abbate M., Zoia C., Corna D., Capitanio M., Bertani T., and Remuzzi, G. (1998). In Progressive Overload of Tubular Cells with Filtered Proteins Translates Glomerular Permeability Dysfunction into Cellular Signals of Interstitial Inflammation. JASN. 9, 1213–1224.

Abbate M., Zoja C., and Remuzzi, G. (2006). How does proteinuria cause progressive renal damage? JASN. 17(11), 2974–84.

Ahmed A, Haylor J, Nahas A El, Johnson T. Localization of matrix metalloproteinases and their inhibitors in experimental progressive kidney scarring. Kidney Int. 2007;755–63.

Aono Y, Kishi M, Yokota Y, Azuma M, Kinoshita K, Takezaki A, et al. Role of PDGF/PDGFR Axis in the Trafficking of Circulating Fibrocytes in Pulmonary Fibrosis. Am. J. Respir. Cell Mol. Biol. 2014

Aresu L, Pregel P, Bollo E, Palmerini D, Sereno A, Valenza F. 2008a. Immunofluorescence staining for the detection of immunoglobulins and complement (C3) in dogs with renal disease . The Veterinary Record 163:679–682.

Aresu L, Valenza F, Ferroglio E, et al. Membranoproliferative glomerulonephritis type III in a simultaneous infection of *Leishmania infantum* and *Dirofilaria immitis* in a dog. *J Vet Diagn Invest*. 2007a;19(5):569-72.

Aresu L., Benali S., Ferro S., Vittone V., Gallo E., Brovida C., and Castagnaro, M. (2012). Light and Electron Microscopic Analysis of Consecutive Renal Biopsy Specimens From Leishmania-Seropositive Dogs. Vet. Path. 50, 753–60.

Aresu L., Benali S., Garbisa S., Gallo E., and Castagnaro M. (2011). Matrix metalloproteinases and their role in the renal epithelial mesenchymal transition. Histol. Histopath. 26, 307–13.

Aresu L., Rastaldi M., Pregel P., Valenza F., Radaelli E., Scanziani E., and Castagnaro M. (2008b). Dog as model for down-expression of E-cadherin and b-catenin in tubular epithelial cells in renal fibrosis. Virchows Archiv. 453, 617–625.

Aresu L., Rastaldi M.P., Scanziani E., Baily J., Radaelli E., Pregel P., and Valenza, F. (2007b). Epithelial-mesenchymal transition (EMT) of renal tubular cells in canine glomerulonephritis. Virchows Archiv. 451, 937–42.

Benali SL, Lees GE, Castagnaro M, Aresu L.. 2014 “Epithelial mesenchymal transition in the progression of renal disease in dogs”. Histol Histopathol. May 28. [Epub ahead of print] Review

Benali SL, Lees GE, Nabity MB, Mantovani R, Bonsembiante F, Aresu L.. 2013 “De novo expression of human leukocyte antigen-DR (HLA-DR) and loss of beta-catenin expression in tubular epithelial cells: a possible event in epithelial-mesenchymal transition in canine renal diseases”. Vet J. Oct;198(1):229-34

Bergkvist A, Rusnakova V, Sindelka R, Garda JMA, Sjögreen B, Lindh D, et al. Gene expression profiling--Clusters of possibilities. Methods. 2010;50:323–35.

Binhazim AA, Chapman WL Jr, Latimer KS, Styles M, Comer K. Canine leishmaniasis caused by Leishmania leishmania infantum in two Labrador retrievers. *J Vet Diagn Invest*. 1992;4(3):299-305.

Bonner JC. *Regulation of PDGF and its receptors in fibrotic diseases*. Cytokine Growth Factor Rev. 2004 Aug;15(4):255-73

Brinkhof B, Spee B, Rothuizen J, Penning LC. Development and evaluation of canine reference genes for accurate quantification of gene expression. Anal. Biochem. 2006;356:36–43.

Cheng HF, Nolasco F, Cameron JS, Hildreth G, Neild GH, Hartley B. HLA-DR display by renal tubular epithelium and phenotype of infiltrate in interstitial nephritis.Nephrol Dial Transplant. 1989;4(3):205-15.

Cheng S., and Lovett D. H. (2003). Gelatinase A (MMP-2) Is Necessary and Sufficient for Renal Tubular Cell Epithelial-Mesenchymal Transformation. Am. J Pathol.162, 1937–1949.

Cheng S., Pollock A., and Mahimkar R. (2006). Matrix metalloproteinase 2 and basement membrane integrity: a unifying mechanism for progressive renal injury. FASEB J. 20, 1898-900.

Chevalier RL, Forbes MS, Galarreta CI, Thornhill BA. *Responses of proximal tubular cells to injury in congenital renal disease: fight or flight.* Pediatr Nephrol. 2014 Apr;29(4):537-41.

Christensen E. I., and Verroust P. J. (2008). Interstitial fibrosis: tubular hypothesis versus glomerular hypothesis. Kidney Int. 74, 1233–6.

Cianciolo RE, Brown CA, Mohr FC, Spangler WL, Aresu L, van der Lugt JJ, Jansen JH, James C, Clubb FJ, Lees GE. *Pathologic evaluation of canine renal biopsies: methods for identifying features that differentiate immune-mediated glomerulonephritides from other categories of glomerular diseases.* J Vet Intern Med. 2013 Nov-Dec;27 Suppl 1:S10-8.

Costa FA, Goto H, Saldanha LC, et al. Histopathologic patterns of nephropathy in naturally acquired canine visceral leishmaniasis. *Vet Pathol*. 2003;40(6):677-84.

Costa FA, Guerra JL, Silva SM, Klein RP, Mendonça IL, Goto H. CD4(+) T cells participate in the nephropathy of canine visceral leishmaniasis. *Braz J Med Biol Res*. 2000;33(12):1455-8.

Costa FA, Prianti MG, Silva TC, Silva SM, Guerra JL, Goto H. T cells, adhesion molecules and modulation of apoptosis in visceral leishmaniasis glomerulonephritis. *BMC Infect Dis*. 2010;11;10:112.

Cox ML, Lees GE, Kashtan CE, Murphy KE. Genetic cause of X-linked Alport syndrome in a family of domestic dogs. Mamm. Genome 2003 14:396–403.

Darbès J1, Majzoub M, Hermanns W. *Evaluation of the cross-reactivity between human and feline or canine leucocyte antigens using commercially available antibodies.*J Vet Diagn Invest. 1997 Jan;9(1):94-7.

Eddy A.A. (2000). Molecular basis of renal fibrosis. Pediatr. Nephrol. 15, 290–301.

Eddy AA. (2005) Can renal fibrosis be reversed? Pediatr. Nephrol. 20,1369–75.

Eddy, A.A. (2005). Progression in chronic kidney disease. Adv. Chronic Kidney D. 12, 353–65.

Erkan E. (2013). Proteinuria and progression of glomerular diseases. Pediatric Nephrol. 28, 1049–58.

Finco DR, Brown S a, Brown C a, Crowell W a, Cooper T a, Barsanti J. 1999. Progression of chronic renal disease in the dog. Journal of veterinary internal medicine 13:516–528

Forbes MS, Thornhill BA, Galarreta CI, Minor JJ, Gordon KA, Chevalier RL. *Chronic unilateral ureteral obstruction in the neonatal mouse delays maturation of both kidneys and leads to late formation of atubular glomeruli.* Am J Physiol Renal Physiol. 2013 Dec 15;305(12):F1736-46.

Frei, R. et al., 2010. MHC Class II Molecules Enhance Toll-Like Receptor Mediated Innate Immune Responses. Cytokine, 5(1), 1-6.

Fuchs TC, Hewitt P. *Biomarkers for drug-induced renal damage and nephrotoxicity-an overview for applied toxicology.* AAPS J. 2011 Dec;13(4):615-31.

Fuchshofer R, Ullmann S, Zeilbeck LF, Baumann M, Junglas B, Tamm ER. Connective tissue growth factor modulates podocyte actin cytoskeleton and extracellular matrix synthesis and is induced in podocytes upon injury. Histochem. Cell Biol. 2011;136:301–19.

Galarreta CI, Thornhill BA, Forbes MS, Simpkins LN, Kim DK, Chevalier RL. Transforming growth factor-β1 receptor inhibition preserves glomerulotubular integrity during ureteral obstruction in adults but worsens injury in neonatal mice. Am J Physiol Renal Physiol. 2013 Mar 1;304(5):F481-90.

García-Martínez JD1, Tvarijonaviciute A, Cerón JJ, Caldin M, Martínez-Subiela S. *Urinary clusterin as a renal marker in dogs.* J Vet Diagn Invest. 2012 Mar;24(2):301-6.

German J, Bland PW, Hall EJ, Day MJ. 1998 Expression of major histocompatibility complex class II antigens in the canine intestine. Veterinary immunology and immunopathology 61:171–180

Goodyer PR, Cybulsky A, Goodyer C. Expression of the epidermal growth factor receptor in fetal kidney. Pediatr. Nephrol. 1993;7:612–5.

Greer KK a, Higgins M a, Cox MMLM, Ryan TTP, Berridge BR, Kashtan CE, et al. Gene expression analysis in a canine model of X-linked Alport syndrome. Mammalian. 2006;17:976–90.

Groman RP, Bahr A, Berridge BR, Lees GE. Effects of serial ultrasound-guided renal biopsies on kidneys of healthy adolescent dogs. Vet. Radiol. Ultrasound 2004;45:62–9.

Guo J, Friedman SL. *Hepatic fibrogenesis* Semin Liver Dis. 2007 Nov;27(4):413-26. Review.

Hagerty DT, Allen PM. *Processing and presentation of self and foreign antigens by the renal proximal tubule*. J Immunol. 1992 Apr 15;148(8):2324-30

Hammerman MR. Growth factors in renal development. Semin. Nephrol. 1995;15:291–9.

Hayes BJ, Riehle KJ, Shimizu-Albergine M, Bauer RL, Hudkins KL, Johansson F, et al. Activation of platelet-derived growth factor receptor alpha contributes to liver fibrosis. PLoS One. 2014;9:92925.

Hood JC, Dowling J, Bertram JF, Young RJ, Huxtable C, Robinson W, Savige J. *Correlation of histopathological features and renal impairment in autosomal dominant Alport syndrome in Bull terriers.* Nephrol Dial Transplant. 2002 Nov;17(11):1897-908

Hyink DP, Abrahamson DR. Origin of the glomerular vasculature in the developing kidney. Semin. Nephrol. 1995;15:300–14.

Ito Y, Goldschmeding R, Kasuga H, Claessen N, Nakayama M, Yuzawa Y, et al. Expression patterns of connective tissue growth factor and of TGF-beta isoforms during

glomerular injury recapitulate glomerulogenesis. Am. J. Physiol. Renal Physiol. 2010;299:F545–58.

James C., Clubb F.J., Lees G.E. (2013). Pathological evaluation of canine renal biopsies: methods for identifying features that differentiate immune-mediated glomerulonephritides from other categories of glomerular diseases. J. Vet. Int. Med.. 27, 10–18.

Johnson TS, Haylor JL, Thomas GL, Fisher M, El Nahas AM. *Matrix metalloproteinases and their inhibitions in experimental renal scarring.* Exp Nephrol. 2002;10(3):182-95.

Jones SE, Jomary C. *Clusterin*. Int. J. Biochem. Cell Biol. 2002;34:427–31.

Jung G-S, Kim M-K, Jung Y-A, Kim H-S, Park I-S, Min B-H, et al. Clusterin attenuates the development of renal fibrosis. J. Am. Soc. Nephrol. 2012;23:73–85.

Kalluri R., and Weinberg R.A. (2009). The basics of epithelial-mesenchymal transition, J Clin Invest. 2009 119 1420-8.

Kanemoto H, Ohno K, Sakai M, Nakashima K, Takahashi M, Fujino Y, et al. Expression of fibrosis-related genes in canine chronic hepatitis. Vet. Pathol. 2011;48:839–45.

Kashtan C. Animal models of Alport syndrome. Nephrol. Dial. Transplant 2002 1359–61.

Kelley VR, Singer GG. 1993. The antigen presentation function of renal tubular epithelial cells. Experimental Nephrology 1:102–111.

Koutinas AF, Kontos V, Kaldrimidou H, Lekkas S. Canine leishmaniasis-associated nephropathy: a clinical, clinicopathologic and pathologic study in 14 spontaneous cases with proteinuria. *Europ. J. Comp. Anim. Pract*. 1995;5:31–38.

Kurts C, Heymann F, Lukacs-Kornek V, Boor P, Floege J. Role of T cells and dendritic cells in glomerular immunopathology. *Semin Immunopathol*. 2007;29(4):317-35. Review.

Lavoué R, van der Lugt JJ, Day MJ, Georges M, Busoni V, Merveille AC, Poujade A, Peeters D. Progressive juvenile glomerulonephropathy in 16 related French Mastiff (Bordeaux) dogs. J Vet Intern Med. 2010 Mar-Apr;24(2):314-22

Lees GE, Cianciolo RE, Clubb FJ Jr. Renal biopsy and pathologic evaluation of glomerular disease. Top Companion Anim Med. 2011 Aug;26(3):143-53.

Lees GE, Helman RG, Kashtan CE, et al. New form of X-linked dominant hereditary nephritis in dogs. Am. J. Vet. Res. 1999. 373–83.

Lees GE. Kidney diseases caused by glomerular basament membrane type IV collagen defects in dogs. J. Vet. Emerg. Crit. care 2013 1–10.

Liu Y. (2004). Epithelial to mesenchymal transition in renal fibrogenesis: pathologic significance, molecular mechanism, and therapeutic intervention. JASN. 15, 1–12.

Liu Y. (2010). New Insights into Epithelial-Mesenchymal Transition in Kidney Fibrosis. JASN. 21, 212–222.

Livak KJ, Schmittgen TD. Analysis of relative gene expression data using real-time quantitative PCR and the 2(-Delta Delta C(T)) Method. Methods. 2001;25:402–8.

López-Hernández FJ, López-Novoa JM. Role of TGF-β in chronic kidney disease: an integration of tubular, glomerular and vascular effects. Cell Tissue Res. 2012;347:141–54.

Maia C, Campino L. Methods for diagnosis of canine leishmaniasis and immune response to infection. *Vet Parasitol*. 2008 20;158(4):274-87. Review.

Martin J, Eynstone L, Davies M, Steadman R. Induction of metalloproteinases by glomerular mesangial cells stimulated by proteins of the extracellular matrix. J Am Soc Nephrol. 2001 Jan;12(1):88-96.

Meyer, E., Duchateau, L. & Daminet, S., 2010. Urinary Markers in Healthy Young and Aged Dogs and Dogs with Chronic Kidney Disease. Journal of Veterinary Internal Medicine, pp.65-72.

Meyrier A, Hill GS, Simon P. Ischemic renal diseases: new insights into old entities. Kidney Int. 1998 Jul;54(1):2-13. Review.

Nabity M.B., Lees G.E., Cianciolo R., Boggess M.M., Steiner J.M., and Suchodolski J.S. (2012). Urinary biomarkers of renal disease in dogs with X-linked hereditary nephropathy. J. Vet. Int. Med. 26, 282–93.

Nahas A.El. (2003). Plasticity of kidney cells: role in kidney remodeling and scarring. Kidney Int. 64, 1553–1563.

Nishinakamura R1, Sakaguchi M. *BMP signaling and its modifiers in kidney development.* Pediatr Nephrol. 2014 Apr;29(4):681-6. doi: 10.1007/s00467-013-2671-9. Epub 2013 Nov 12.

Ostendorf T, Eitner F, Floege J. *The PDGF family in renal fibrosis*. Pediatr Nephrol. 2012 Jul;27(7):1041-50.

Peters IR, Peeters D, Helps CR, Day MJ. Development and application of multiple internal reference (housekeeper) gene assays for accurate normalisation of canine gene expression studies. Vet. Immunol. Immunopathol. 2007;117:55–66.

Poli A, Abramo F, Mancianti F, Nigro M, Pieri S, Bionda A. Renal involvement in canine leishmaniasis: a light-microscopic, immunohistochemical and electron-microscopic study. *Nephron* 1991;57:444–452.

Polzin D, Osborne CA, Ross S. Chronic kidney disease. In: Ettinger SJ, Feldman EC, eds. *Textbook of Veterinary Internal Medicine*. St Louis, MO: Elsevier Saunders; 2005:1756–1785.

Polzin D.J. and Cowgill L.D. (2013). Development of Clinical Guidelines for Management of Glomerular Disease in Dogs. J. Vet. Int. Med. 27, 2–4.

Rao V, Lees G, Kashtan C, Nemori R. Increased expression of MMP-2, MMP-9 (type IV collagenases/gelatinases), and MT1-MMP in canine X-linked Alport syndrome (XLAS). Kidney Int. 2003;63:1736–48.

Roda, G., 2010. Intestinal epithelial cells in inflammatory bowel diseases. World Journal of Gastroenterology, 16(34), p.4264.

Roura X., Fondati A., Lubas G., Gradoni L., Maroli M., Oliva G., Paltrinieri S., Zatelli A. and Zini E. (2013). Prognosis and monitoring of leishmaniasis in dogs: a working group report. Vet. J. 198, 43–7.

Ruggenenti P, Remuzzi G. The role of protein traffic in the progression of renal diseases. *Annu Rev Med*. 2000;51:315-27.

Sayers, Robinlyn, Kalluri R, Rodgers KD, Shield CF, Meehan DT, Cosgrove D. Role for transforming growth factor-bold beta1 in Alport renal disease progression. Kidney Int 1999;56:1662–73.

Schlondorff DO. Overview of factors contributing to the pathophysiology of progressive renal disease. Kidney Int. 2008;74(7):860-6.

Schneider S.M., Cianciolo R.E., Nabity M.B., Clubb F.J. Jr., Brown C.A., and Lees G.E. (2013). Biopsied for Suspected Glomerular Disease : 501 Cases (2007 – 2012) J. Vet. Intern. Med. 27, 67–75.

Slocum J.L., Heung M., and Pennathur S. (2012). Marking renal injury: can we move beyond serum creatinine? J. Lab. Clin. Med. 159, 277–89.

Smets P., Meyer E., Maddens B.E.J., Duchateau L., and Daminet S. (2010). Urinary markers in healthy young and aged dogs and dogs with chronic kidney disease. J. Vet. Intern. Med. 24, 65–72.

Strutz F, Neilson EG. New insights into mechanisms of fibrosis in immune renal injury. Springer Semin Immunopathol. 2003;24(4):459-76.

Strutz F., Okada H., Lo C.W., Danoff T., Carone R.L., Tomaszewski J.E., and Neilson E.G. (1995). Identification and characterization of a fibroblast marker: FSP1. J. Cell Biol. 130, 393–405.

Strutz F.M. (2009). EMT and proteinuria as progression factors. Kidney Int. 75, 475–81.

Stuart RO, Bush KT, Nigam SK. *Changes in global gene expression patterns during development and maturation of the rat kidney.* Proc Natl Acad Sci U S A. 2001 May 8;98(10):5649-54.

Tang J, Liu N, Zhuang S. *Role of epidermal growth factor receptor in acute and chronic kidney injury.* Kidney Int. 2013 May;83(5):804-10. doi: 10.1038/ki.2012.435.

van Roeyen CR, Eitner F, Boor P, Moeller MJ, Raffetseder U, Hanssen L, Bücher E, Villa L, Banas MC, Hudkins KL, Alpers CE, Ostendorf T, Floege J. *Induction of progressive glomerulonephritis by podocyte-specific overexpression of platelet-derived growth factor-D.* Kidney Int. 2011 Dec;80(12):1292-305.

Vilafranca M., Wolhsein P., and Trautwein G. (1995). Expression of class II major histocompatibility complex molecules in renal tubular epithelial cells of canine kidneys affected with tubulointerstitial nephritis. Res. Vet. Sci. 59, 114–117.

Wang K, Lin B, Brems JJ, Gamelli RL. Hepatic apoptosis can modulate liver fibrosis through TIMP1 pathway. Apoptosis. 2013;18:566–77.

Wang Q, Usinger W, Nichols B, Gray J, Xu L, Seeley TW, et al. Cooperative interaction of CTGF and TGF-β in animal models of fibrotic disease. Fibrogenesis Tissue Repair [Internet]. BioMed Central Ltd; 2011;4:4.

Weier Qi et al., Transforming growth factor-b/connective tissue growth factor axis in the kidney. The international journal of biochemistry & cell biology 2008

Wuthrich, R., Yui, M. & Mazoujian, G., 1989. Enhanced MHC class II expression in renal proximal tubules precedes loss of renal function in MRL/lpr mice with lupus nephritis. The American journal of pathology, 134(1) 45-51.

Yamate J., Kuribayashi M., Kuwamura M., Kotani T., and Ogihara K. (2005). Differential immunoexpressions of cytoskeletons in renal epithelial and interstitial cells in rat and canine fibrotic kidneys, and in kidney-related cell lines under fibrogenic stimuli. Exp. Toxicol. Pathol. 57, 135–47.

Yukhi N., Beck, T., Stephens, R., Neelam, B., O'Brien, S.J., 2007. Comparative genomic structure of human, dog, and cat MHC: HLA, DLA, and FLA. Journal of Heredity 98, 390–399 .

Zatelli A, Borgarelli M, Santilli R, et al. Glomerular lesions in dogs infected with Leishmania organisms. *Am J Vet Res*. 2003;64(5):558-61.

Zeisberg Bone morphogenic protein-7 and the kidney: current concepts and open questions. Nephrol Dial Transplant (2006)

Zeisberg M. and Duffield J.S., 2010. Resolved: EMT produces fibroblasts in the kidney. J Am Soc Nephrol;21:1247–1253.

Zeng F, Singh AB, Harris RC. *The role of the EGF family of ligands and receptors in renal development, physiology and pathophysiology*. Exp Cell Res. 2009 Feb 15;315(4):602-10

LIST OF ORIGINAL PUBLICATIONS

1. Zini E, **Benali S**, Coppola L, Guscetti F, Ackermann M, Lutz TA, Reusch CE, Aresu L.. 2014 “Renal Morphology in Cats With Diabetes Mellitus”. Vet Pathol. Feb 24. [Epub ahead of print]
2. Aresu L, **Benali S,** Ferro S, Vittone V, Gallo E, Brovida C, and Castagnaro M. 2013 “Ligh and Electron Microscopic Analysis of Consecutive Renal Biopsy Specimens From Leishmania-Seropositive Dogs”. Vet Pathol. Sep;50(5):753-60
3. **Benali SL**, Lees GE, Castagnaro M, Aresu L.. 2014 “Epithelial mesenchymal transition in the progression of renal disease in dogs”. Histol Histopathol. May 28. [Epub ahead of print] Review
4. **Benali SL**, Lees GE, Nabity MB, Mantovani R, Bonsembiante F, Aresu L.. 2013 “De novo expression of human leukocyte antigen-DR (HLA-DR) and loss of beta-catenin expression in tubular epithelial cells: a possible event in epithelial-mesenchymal transition in canine renal diseases”. Vet J. Oct;198(1):229-34
5. Ferro S, Palmieri C, Cavicchioli L, De Zan G, Aresu L, **Benali SL..** 2013 “Leishmania amastigotes in neoplastic cells of 3 nonhistiocytic canine tumors”. Vet Pathol. Sep;50(5):749-52.
6. Giantin M, Aresu L, **Benali S**, Aricò A, Morello EM, Martano M, et al. 2012 “Expression of Matrix Metalloproteinases, Tissue Inhibitors of Metalloproteinases and Vascular Endothelial Growth Factor in Canine Mast Cell Tumours”. J Comp Pathol. Vol. 147 419-429
7. Aresu L, **Benali S**, Giannuzzi D, Mantovani R, Castagnaro M, Falomo ME. 2012 “The role of inflammation and matrix metalloproteinases in equine endometriosis”. J Vet Sci. Jun;13(2):171-7.

SCIENTIFIC CONTRIBUTIONS TO CONGRESSES

ORAL COMMUNICATIONS

1. **Benali S.L.,** Lees G.E., Nabity M.N., Aricò A., Drigo M., Gallo E., Giantin M., Aresu L. "Integrated analysis of renal morphology and gene expression during progression of canine x-linked hereditary nephropathy" Annual meeting of American College of Veterinary Pathology and American Society of Veterinary Pathology (Atlanta, 2014).
2. **Benali S.L**., Lees G.E., Nabity M.N., Aricò A., Drigo M., Gallo E., Giantin M., Aresu L. "The role of growth factors in canine x-linked hereditary nephropathy: an animal model of progressive renal failure" LXVIII Convegno SISVET, XI Convegno AIPVET e XII Convegno SIRA (Pisa, 2014).
3. Bonsembiante F., **Benali S.L.,** Trez D., Aresu L., Gelain M. "Hystological and immunohistochemical characterization of feline renal cell carcinoma: a case series". LXVIII Convegno SISVET, XI Convegno AIPVET e XII Convegno SIRA (Pisa, 2014).
4. **Benali S.L**., Lees G.E., Nabity M.N., Bonsembiante F., Aresu L. "De novo HLA-DR expression in canine renal tubular epithelium: a possible event in epithelial-mesenchymal-transition" XXXI meeting of the European Society and College of Veterinary Pathology (Londra, 2013).

POSTERS

1. Ferro S., **Benali S.L**., Palmieri C. "Leishmania intracellulare in tre differenti neoplasie canine". IX Congresso nazionale AIPVET (Perugia, 2012).